THE UNIVERSITY OF OKLAHOMA

GRADUATE COLLEGE

THE STRUCTURE AND CIRCULATION OF THE ATMOSPHERE OF VENUS

A DISSERTATION

SUBMITTED TO THE GRADUATE FACULTY

in partial fulfillment of the requirements for

the degree of

DOCTOR OF ENGINEERING

BY

DAVID EUGENE PITTS

Norman, Oklahoma

1971

THE STRUCTURE AND CIRCULATION OF THE

ATMOSPHERE OF VENUS

APPROVED BY

DISSERTATION COMMITTEE

ACKNOWLEDGMENTS

The author wishes to express his appreciation for the encouragement and technical guidance of Professor Yoshikazu Sasaki. Appreciation is also extended to my wife, Paula, for her moral support, encouragement and assistance in making time available to complete this research and to Donna Lennard who assisted by typing this manuscript. Thanks are also due to my parents, Mr. and Mrs. Sidney Pitts, and my friend, Mr. Dallas Evans who encouraged the undertaking of this research.

This research has been sponsored by the National Aeronautics and Space Administration under the full-time study program of the Employee Development Branch, Manned Spacecraft Center.

ABSTRACT

The physical properties of Venus are reviewed and upon these data, two models of the basic state vertical structure of the atmosphere are developed. One of these models assumes non-condensing "dust" clouds and the other assumes ice (H_2O) clouds. The purpose of these choices is to investigate the impact of these two cloud types on the derived circulation of the atmosphere.

A steady state two-dimensional compressible circulation model is developed which describes the response of a basic state atmosphere which is at rest, to sunlight falling on an opaque cloud layer. By virtue of this model, the phase effect of temperature in the lower atmosphere is determined to be non-existent.

The results of this model indicate that a shallow circulation cell develops near the cloud tops extending from the subsolar to the antisolar point. Making the Boussinesq approximation does not change this essential feature, but only decreases the wind speed to half the value of the compressible model. The choice of cloud type is determined to be important to the speed of the circulation due to the different temperature structures in the two cloud types studied.

TABLE OF CONTENTS

LIST OF TABLES

LIST OF ILLUSTRATIONS

LIST OF MATHEMATICAL SYMBOLS

v	wind velocity
t	time
ρ	density
P or p	pressure
g	acceleration due to gravity
Ω	angular velocity vector for Venus
R	universal gas constant
m or m_d	molecular weight of atmosphere
c_p	specific heat at constant pressure
T	temperature
β	coefficient of expansion
Q	net radiative flux
K	conductivity
k	diffusivity
μ	viscosity
ν	kinematic viscosity
τ	stress tensor
H_ρ	density scale height
u	wind along x
x	distance from subsolar point to antisolar point along great circle
w	wind along z

z	distance up from the surface of Venus along a radius vector
a_1	vertical basic state temperature gradient
c	basic state wind constant
b	basic state wind constant where $\bar{u} = c + bz$
θ	potential temperature
r	mixing ratio of water vapor
ρ_w	density of water vapor in atmosphere
m_w or m_v	molecular weight of water
L	latent heat of sublimation
e_s	saturation vapor pressure of water
U	unreduced path length (cm-atm)
U_r^*	reduced path length
γ_r	constants for strong line curve fit
m_r	constants for strong line curve fit
n_r	constants for strong line curve fit
σ	Stefan Boltzman constant
τ	transmission
τ_ω	transmission for ω
ω	wavenumber (cm^{-1})
Φ	viscous dissipation term
R_1	residual for 1st equation
γ	phase angle of sun (local noon is zero)
α	phase angle from subsolar point
G	Newton's gravitational constant
T_{BB}	equivalent blackbody temperature

$M_{♀}$	mass of Venus
%	parts per hundred
$^{o}/_{oo}$	parts per thousand
v	meridional velocity along y
y	distance from equator toward the North Pole
μ	microns wavelength
λ	wavelength
T_{rot}	rotational temperature
kg_f	kilograms force
μ precipitable	depth in microns of water above 1 cm^2 area, reduced to STP
R	solar flux at the orbit of Venus
⊙	sun
ε	emissivity

THE STRUCTURE AND CIRCULATION OF THE ATMOSPHERE OF VENUS

CHAPTER I

INTRODUCTION

The planet Venus, twin sister to Earth, has intrigued the imagination of man for many centuries. Much of the importance given to Venus in human history and mythology is no doubt due to the planet's extreme brightness, exceeded only by the Moon and Sun, and to its long endurance in the sky for several months at a time. Venus is often referred to as Earth's twin because of their similar mass, size, and close proximity in the solar system. However, this is where the similarity ends, as the atmospheric structure, composition and circulation are quite different from Earth.

Venus is a member of the terrestrial planets: Mercury, Venus, Earth, and Mars. These planets differ from the outer or Jovian planets in that the density of a terrestrial planet is high, indicating that thermal escape has driven off the lighter elements of the primordial atmosphere. This is due to the close proximity of the Sun, dissociating many molecules, and imparting higher thermal velocities to the upper atmosphere; and to the lower mass of the planet causing it to have a lower escape velocity. Thus, the atmosphere remaining on a terrestrial planet is generally: heavy (e.g., Carbon Dioxide and Nitrogen), inert (e.g., Argon, Neon, Krypton), or is a secondary atmosphere of recent chemical, biological and/or volcanic

origin (e.g., the atmosphere of Earth). In contrast, the Jovian planets are cool enough and massive enough to have retained an almost Sun-like composition ($\approx$60% Hydrogen, $\approx$36% Helium), according to Spinrad and Trafton (1963). Venus has long been thought to have an atmosphere, since the planet exhibits a halo of scattered light during inferior conjunction, most probably as a result of scattering by "cloud particles" in that atmosphere.

Until recently, less was known of the atmosphere of Venus than of almost any planet in the solar system. The planet's ubiquitous cloud cover has caused much of the controversy which has existed, since it prevents implementation of most experiments which would determine the structure and composition. When experiments are performed, the cloud cover usually makes the interpretation of these data difficult, since the origin of the detected signal is difficult to pinpoint. This lack of data, dealing with surface conditions and atmospheric structure below the clouds has lead to a wide variety of equally plausible model atmospheres being proposed.

Because Venus has the approximate radius and mass of Earth, it has historically been assumed that the atmospheres of the two planets were alike, except where evidence indicated different. Most early models, therefore, assumed surface pressures of a few atm (atmospheres pressure), an atmosphere with mostly Nitrogen and some Oxygen, and a negative temperature gradient in the troposphere. Sadly, only the latter of these has proven to be true.

According to Keldysh (1967) and Deirmendjian (1968), estimates of surface pressure of the atmosphere of Venus have ranged from 1 to 1000 atm or greater, with best estimates by Evans et al (1967) lying in the

range of 5 to 40 atm, Spinrad (1962) deriving a lower and upper limit of surface pressure of 10 and 30 atm, respectively, Cameron (1965) giving 100 atm, and with Kaplan (1962) predicting a nominal surface pressure of 10 atm. The knowledge of composition has also been very uncertain. It was generally assumed that only a small part of the atmosphere was carbon dioxide, and that the remainder was principally nitrogen (e.g., Spinrad (1962)). Opik (1961), however, did consider models in which 20, 40, and 80% by mass of the atmosphere was carbon dioxide.

Much controversy has existed about the temperature at the surface of the planet. Two factors contributed to this problem: the atmospheric models with relatively low surface pressures, regardless of the percentage of CO_2, were not able to reproduce the hot temperatures detected by the passive microwave instruments and the surface temperature measured with microwave radiometers from Earth depends upon the wavelength used. According to Koenig (1967), at millimeter wavelengths the measured temperature is about 380°K, at centimeter wavelengths - 550°K, and at about ten centimeter wavelengths - 680°K. There was some question as to whether these emissions were all of thermal origin, or if a hot dense ionosphere (Walker and Sagan, 1966), lightning emissions or chemical reactions could produce a non-thermal component, and it has been argued that the radiative equilibrium temperature of Venus should be 250 to 350°K depending upon its rotational speed. A strong greenhouse effect or dust cloud would tend to raise the temperatures, but with low pressures and low wind speeds being considered, temperatures of 700°K were not thought to be possible. Similarly, very little was known about the surface characteristics, the rotational speed, the magnetic field and the atmospheric circulation of the planet Venus.

The Mariner II, Venera 4, Mariner V, Venera 5, and Venera 6 have increased our knowledge of Venus many orders of magnitude over studies conducted from Earth. By virtue of these new data, it has become possible to reject many of the early proposed atmospheric models. Each probe accomplished much in unravelling the mysteries of Venus; however, each has made a particularly important contribution:

Mariner II - disproved the hot ionosphere theory and favored hot-surface models (Pollack and Sagan (1967)), Venera 4 - showed the surface pressure to be at least 20 atmospheres and the atmosphere to be composed of predominantly carbon dioxide, Mariner V showed most of atmosphere was CO_2, sounded the structure in and above the clouds, and indicated that Venera 4 stopped transmitting about 26 km above the surface. Venera 5 and 6 - reconfirmed that extremely high pressures near 100 atm exist near the surface and improved our knowledge of the atmospheric composition to the extent that uncertainties were reduced by 50%. By virtue of these new data, man's knowledge of the vertical structure of the Venus atmosphere is probably greater than for any planet except Earth. Circulation models of the atmosphere have been developed by Mintz (1961), Ohring et al (1965), Goody and Robinson (1966), Hess (1968), Stone (1968), and Bohachevsky and Yeh (1969), most of which were prior to the time that reasonably definitive data were available. Thus, significant improvements should be possible on these models. Furthermore, a new circulation model would extend our knowledge of the structure (e.g., vertical temperature, pressure, density, etc.) to other locales on Venus.

Since the surface is obscured from view by the clouds, the circulation of the lower regions of the atmosphere must be studied theoretically, or

measured in situ, while the circulation at cloud top levels can be studied in detail by visual observations and astronomical photography.

In the following chapters, the physical properties of Venus are reviewed and upon these data two models of the basic state vertical structure are developed. One of these models assumes non-condensing "dust" clouds and the other assumes ice (H_2O) clouds. The purpose of these choices is to investigate the impact of the present scientific uncertainty of the nature of the clouds on the derived circulation of the atmosphere.

A steady state two-dimensional circulation model is developed which describes the response, of a basic state atmosphere which is at rest, to sunlight falling on an opaque cloud layer (with a dense, 100% CO_2 atmosphere below), causing a circulation that redistributes the energy over the planet. This Anelastic (sound excluded), compressible circulation model is implemented in finite difference form for numerical relaxation on digital computers. Results are obtained for various basic state model atmospheres, various eddy viscosity values, various Prandtl numbers, etc. for: comparison to known experimental data, evaluation of other circulation models, and hopefully impacting the direction of new experimental measurements.

CHAPTER II

PHYSICAL PROPERTIES OF THE PLANET VENUS

Atmospheric models of the lower Venus Atmosphere are usually based on the assumption of hydrostatic equilibrium and the equation of state, and evidence describing:

1) the gaseous components of the atmosphere

2) the surface pressure

3) the surface temperature

4) the temperature profile as a function of altitude

5) the gravitational field of the planet

In order to make a dynamic model of the circulation of the atmosphere, one must have information including the following:

6) observational or photographic evidence of cloud morphology, distribution, and temporal nature

7) the nature of suspended particles or clouds and changes of phase that occur on the surface or in the atmosphere

8) the nature of turbulent transfer of heat and momentum

9) the speed of rotation and revolution of the planet and the direction of pointing of the polar axis

10) some estimate or measurement of horizontal wind speeds

11) diurnal and latitudinal variations in surface temperature, cloud top temperature.

In order to give perspective to current circulation models and to the models developed herewith, a brief review of the physical properties of Venus and the evolution of current theories is appropriate. Data relating to the eleven data requirements just mentioned will be emphasized. Koenig et al (1967) has summarized the data, theories and scientific thought about Venus, current through December 1965. These data, together with more recent data pertaining to Venera 4, Mariner V, Venera 5, and Venera 6, and results thereof, are discussed as follows.

Mariner II

Mariner II was launched on August 27, 1962 and encounter began on December 14, 1962 as the 460 lb probe passed within 21,598 miles of the center of Venus as described by Koenig (1967). The spacecraft had an infrared radiometer on board with two band passes centered at 8.4 and 10.4μ, a beamwidth of $0.9 \times 0.9^{\circ}$, and equivalent blackbody temperature limits of 200°K to 600°K (Chase et al (1963)). According to Barath et al (1963), Mariner II carried a 22 pound microwave radiometer operating at wavelengths of 13.5 mm (H_2O band) and 19.0 mm (a window). Other instruments on board are not discussed here because of their relatively small importance to the structure and circulation of the lower atmosphere.

Venera 4

The Venera-4 probe entered the atmosphere of Venus on October 18, 1967, near the equator in the dark hemisphere about 1500 ± 500 km from the dawn terminator (see Figure 1). The entry probe has a mass of 383 kg and a diameter of $\approx$ 1m and entered the atmosphere at the speed of

10,700 m/sec (Tass (1967)). After aerodynamic deceleration down to the speed of 300 m/sec, a drogue chute was deployed; subsequently, the main chute was deployed (at 26 km above the "surface") and scientific measurements were initiated. The mechanical rigidity, thermal characteristics, and the power supply (design lifetime of 100 minutes) were designed for operation to a level of about 25 atm pressure. The velocity of descent after deployment of the main chute varied from 10 m/sec at 26 $\pm$ 1.3 km to 3 m/sec when it reached the "surface", after transmitting for 93 minutes (Avduevsky et al (1968)). At the time of "landing" the transmission was interrupted suddenly without preliminary attenuation.

According to Avduevsky et al (1968), the scientific instruments aboard the entry package included: two resistance thermometers (270-600°K and 210-730°K capability), rms error $\pm$ 4 and $\pm$ 7°, respectively, a barometric transducer (aneroid barometer with range 0.13 to 7.3 kilograms force (kg_f) cm^{-2}, 100 to 5200 Torr), rms error $\pm$ 0.2 kg_f cm^{-2}, a densitometer (5×10^{-4} to 1.5×10^{-2} gm/cc capability), and Vinogradov et al (1968) reported that eleven chemical gas analyzers for carbon dioxide, nitrogen, oxygen, and water vapor were also aboard. Directly after the parachute opened at 26 km (550 mm Hg pressure), samples were taken in five of the analyzers, with the remaining 6 analyzing cells receiving samples 347 seconds later which corresponds to a pressure of 1500 mm Hg and an altitude of 19 km (Vinogradov et al (1968)). Temperature was measured during the entire operating period of the entry probe, and the density measurements were started simultaneously with the temperature and were conducted until device overshooting (Mikhnevitch et al (1968)). The distance above the planetary surface was determined with a radar.

Mariner V

On October 19, 1967 the Mariner V spacecraft passed Venus at a distance of 10,151 kilometers from the center of the planet, as reported by Snyder (1967). Seven scientific experiments were planned and all were conducted successfully. Three of these experiments dealt with the plasma environment of the planet, and therefore will not be discussed here. The other four dealt more directly with the atmosphere of the planet. The ultraviolet photometer was designed to detect atomic hydrogen and oxygen in the upper atmosphere of Venus (Barth et al (1967)). The occultation experiments were designed to detect any ionosphere which was present by using signals at 49.8 to 423.3 MHz (Mariner Stanford Group (1967)), and to determine temperature, density and pressure in the neutral atmosphere by measuring the frequency, phase and amplitude of the S-band radio signal of Mariner V (Kliore et al (1967)). The range and doppler radio tracking data from Mariner V have also yielded a very precise measurement of the mass of Venus (Anderson et al (1967)).

Venera 5 and 6

Venera 5 and 6 were launched toward Venus on January 5 and 10, 1969, respectively (Pravda (1969)). The entry capsules weighed 405 kg_f, and were similar to that of Venera 4, except that improvements in construction were hoped to produce an operating range of 0.5 to 25-27 atm pressure. Venera 5 and 6 entered the atmosphere of Venus at 11.8 km/sec at 62-65° inclination on May 16 at 0901 h and May 17 at 0905 h local Moscow time, respectively (Brichant (1969)). After decelerating to 210 m/sec, the parachute systems and the radio transmitters were activated. Chemical

gas analyzers, aneroid barometers, decimeter wavelength altimeters and resistance thermometers were employed which were similar to those on Venera 4. In addition a photoelectric sensor was installed to determine lighting conditions below the Venus clouds in the visible and near infrared.

Orbit

Venus is closer to the Sun than the Earth and thereby has a shorter period of revolution: 225 days (Koenig (1967)). The revolution of the Earth about the Sun gives Venus an apparent revolution period (ie., synodic period) of 584 days, which accounts for Venus serving as evening star for nearly 10 months, then passing through inferior conjunction to become the morning star for about the same length of time (Wyatt (1964)). Since Venus is an inferior planet (i.e., it lies inside the orbit of Earth), it goes through phases similar to the Moon and Mercury. The orbit of Venus is nearly circular, having an eccentricity close to zero: .0068206938, and its relatively high inclination to the ecliptic: 3.39363°, according to Koenig (1967), causes transits over the disk of the Sun to occur very infrequently, the most recent having occurred in 1882, and next to occur in 2004, as reported by Wyatt (1964).

Mass

The mass has been determined from the perturbations that Venus causes in the solar orbits of other bodies, principally the Earth, Mercury, Eros, and interplanetary probes from Earth. Thus determined, Venus has a mass only slightly less than that of Earth. Koenig (1967) calculates a best value of the absolute mass of Venus on the basis of several data to be $4.868\ (\pm\ 0.012) \times 10^{27}$ grams.

Density

Based on his value for the mass and a radius of 6085 ± 10 km for the solid surface of the planet, Koenig (1967) calculated a mean density of 5.158 ± 0.010 gm cm^{-3} which makes Venus the second most dense planet in the solar system, the Earth being most dense, at 5.52 gm cm^{-3} (Jones (1964)).

Rotation

The veil of clouds that eternally cover the surface of Venus (as seen from the Earth) has frustrated attempts to measure the rotational speed of the planet. Both a lack of detected doppler shift in the visible spectrum from one terminator to the other, and a lack of oblateness of the imaged disk indicates a very slow rotational speed (Wyatt (1964)). Radar results since 1961 have shown that the rotation rate is retrograde. The results of Goldstein (1964) indicate a rotation period of 248 days retrograde with a rotation axis nearly perpendicular to the orbit of Venus. Goldstein (1966) later revised this to 242.6 ± .6. Shapiro (1964) used the 1000 foot radio telescope at Arecibo, Puerto Rico to calculate a period of rotation of 247 ± 5 days, and a polar axis tilted at 84° from the plane of the orbit of Venus. The revolution period together with the rotation period indicate the length of the day on Venus is about 117 Earth days. Goldreich and Peale (1966) have suggested that the rotation period could be 243.16 days, thereby making Venus in a resonant condition, pointing the same point toward Earth each inferior conjunction.

Atmospheric Circulation

Wright (1927) and Ross (1928) in independent discoveries, found cloud patterns were visible in the Venus atmosphere when viewed in ultraviolet

light (3500-3700 Å is best (Hartman (1969)). These photos often show a banded structure or a cellular structure, and are usually attributed to high clouds analogous to the terrestrial noctilucent clouds, since they are transparent to visible light.

Figure 2 shows 25 such ultraviolet images taken by Slipher (1964) during the period 1928 to 1948, reprinted here with permission of Lowell Observatory. At times pairs of clouds are visible with symmetry along the equator. Banded structures are also seen which are reminiscent of, but less distinct than, those on Jupiter. These same bands also remind one of jet stream cirrus seen in Gemini photographs over the Sahara. Recently, Boyer and Carmichel (1961, 1965), Boyer (1965), Boyer and Guérin (1966), Smith (1967), Anon (1968), Kuiper et al (1969), Hartman (1969), and Fountain and Larson (1969) have reported a retrograde motion of 4-5 day period in the ultraviolet clouds. The lower permanent clouds occasionally show faint structure according to Kuiper et al (1969).

As Shapiro (1968) points out: to some, the widely different rotation periods of Smith (1967): 5 days, and the radar rotation period of 247 days, Shapiro (1964), may seem in conflict, whereas the first of these pertains to a "cloud feature" visible in ultraviolet light and the latter to the solid surface of Venus. Mintz (1961) treated several cases prior to the time when reasonably accurate information about the rotation rate and depth of the atmosphere was available. One of these cases treats a very slow rotating planet with a deep atmosphere in a 2-layer Boussinesq model. His calculations show that the main circulation is from sub-solar to anti-solar points at the lower levels changing into a symmetric zonal flow about the poles at higher levels, thus reproducing some features observed in the ultraviolet clouds. In the visible region of the spectrum,

Dollfus (1955) has compiled observations which show quasi-permanent markings suggesting a cellular pattern centered on the sub-solar point which are similar to the ultraviolet cloud data. In Goody and Robinson's (1966) non-linear Boussinesq model of the circulation, the equations were scaled using values that produced order of magnitude for the wind speeds of 18-34 m/sec. They found that Coriolis force is strong enough to exert a secondary influence on the flow despite the slow rotation rate and also a zonal thermal structure of the observed magnitude is expected from their other results. Ohring et al (1965) calculated wind speeds of 2-30 m/sec using a linear Boussinesq model. Bohachevsky and Yeh (1969) derived a linear Boussinesq model which is equivalent to the classical Rayleigh convection problem. They concluded that the circulation was mainly meridional with u = 4 m/sec, v = 10 m/sec, and w = 4 cm/sec.

Stone (1968) derived a non-linear rotating Boussinesq model which produced velocities of 1.5 m/sec horizontal velocity magnitude and 1.5 cm/sec vertical velocity. These models have many weaknesses, most assume the Boussinesq approximation which is a poor assumption in a deep atmosphere, many are linear and therefore fail to account for momentum advection, several are based on the (surface) microwave phase effect as a driving force for a classical Rayleigh convection, and none of the models reproduce the motions of 100 m/sec in the high ultraviolet clouds. Smith, Pope, Murrel and Reese were quoted in Sky and Telescope, Anon (1968) as having interpreted their ultraviolet photographs of high clouds as showing that it is possible to recognize similar cloud patterns in 3 to 5 days (giving wind speeds of about 100 m/sec). Guinot was quoted in the same article as having used a Fabry-Perot interferometer to detect an atmospheric equatorial

velocity of 100 ± 8 m/sec, which corresponds to 4.1 days ± 0.7 days.

Smith (1967) reports observing the west terminator of Venus and seeing the clouds move toward the subsolar point. On the east terminator, the wind appeared to move the clouds away from the subsolar point. This type of motion was observed in several instances, giving a retrograde period of somewhat less than 5 days.

Reproducing these cloud motions is a most critical test of any circulation model.

Surface

Evans et al (1965) have concluded that the surface of Venus is considerably smoother than the Moon, with slopes of about 8° over a horizontal distance of 5 to 50 cm based on radar observations made at 68 cm with the Millstone Hill Radar Observatory. Ash et al (1968) conclude that the equatorial region of Venus is remarkably free from large topographical variations on a horizontal scale of 100 km.

Photographs of Venus and Earth have been compared at 600 km resolution by Keene (1968) who concluded that few details on Earth are visible under viewing conditions similar to those under which we view Venus. Thus an orbiting satellite or fly-by of Venus could reveal openings in the clouds through which the surface can be seen. Imagery with 1 km resolution appears feasible for the Mariner Venus/Mercury 1973 fly-by (Eckman and Cole (1969)), which will investigate this possibility.

According to Sagan and Pollack (1965) fused quartz, powered oxides, carbonates and silicates may be possible surface materials on Venus, whereas magnetic materials, granite and hydrocarbons are excluded. On a

bulk basis the electrical properties appear similar to those of the Moon.

Light Levels Below the Clouds

The sensors on board Venera 5 and 6 failed to record light levels above the threshold of 0.5 watts m^{-2}, except one reading of 25 watts m^{-2} recorded 4 minutes prior to Venera 6 probe failure (Brichant (1969)). It is therefore highly likely that the surface of Venus has light levels less than Earth twilight.

Atmospheric Composition

The results of Venera 4 as reported by Vinogradov (1967) are given in Table 1 and show that 90 $\pm$ 10% of the atmosphere of Venus is carbon dioxide, that the nitrogen abundance is less than 7%, that water vapor occurs in quantities greater than 0.1% and less than 0.7% (i.e., 1-8 mg/liter), and that oxygen is present in quantities greater than 0.4% and less than 1.6%.

The Mariner V data indicates a scale height of 5.4 $\pm$ .2 km at 6150 $\pm$ 7 km from the center of Venus. If these data are interpreted as lying above the cloud tops and therefore at a temperature near 230°K, then the mean molecular weight is between 39 and 42, or about 75% and 90% carbon dioxide, respectively (Kliore et al (1967)). Barth et al (1967) analysis of the Mariner V ultraviolet photometer data indicates relatively large atomic hydrogen densities and a lack of atomic oxygen in the Venus exosphere.

Carbon dioxide is the only major component gas positively identified by spectroscopic study of the Venus atmosphere using terrestrial based telescopes (Spinrad (1962, 1966)). Many trace constituents, however, have

been detected by such means. Connes et al (1967) have detected hydrogen fluoride and hydrogen chloride using high resolution interferometric techniques. Earth based spectroscopic measurements by Bottema et al (1961); Spinrad and Shawl (1966); Belton and Hunten (1966); and Kuiper (1969) have detected water vapor and an upper limit on oxygen has been determined by Belton (1968). Table 2 summarizes the estimated mole fractions of the minor constituent gases of the Venus atmosphere. The oxygen upper limits reported by Belton et al (1968) and the UV data of Barth et al (1967) and the water vapor amounts detected from Earth are all in conflict with the data from the Venera 4 probe.

Brichant (1969) reports of the successful composition measurements conducted by Venera 5 and 6. These data were obtained over a range of 0.6 atm to 10 atm. Table 3 presents the detailed results showing an improvement in the Venera 4 uncertainty by 50%. Based on these data, the atmosphere is almost completely composed of carbon dioxide, molecular nitrogen, and inert gases (x) at about 95%, 5%-x, x, respectively. Therefore, for the purpose of calculating the structure and circulation of the atmosphere a 100% carbon dioxide model will not cause great error in analysis and will simplify considerably the calculation of gas properties.

Earth based microwave measurements near 1.35 cm were made by Pollack et al (1968), who report an upper limit of 0.8% for the water vapor amount in the Venus atmosphere. This upper limit was calculated using a model of 91.2 atm surface pressure, 747°K surface temperature, and 85% carbon dioxide atmosphere. This conclusion on the upper limit for water vapor is consistent with that detected by Venera 4, 5, and 6, and more importantly, with the existence of water-ice clouds. Moreover, Pollack and

Wood (1968) find a best fit to the microwave data using .5% water vapor and Strelkov (1968) confirms that measurements at 1.75 cm can be reproduced by a model atmosphere based on Venera 4 measurements. The polarization of scientific opinion on the amount of water vapor in the atmosphere of Venus is one of the most serious disagreements dealing with the properties of Venus. Furthermore, it is a problem that is not likely to be solved in the near future.

Libby (1968) reports that if Venus possessed an amount of water equal to that on Earth and if it were in vapor stage, the surface pressure on Venus would be 500 atm pressure. His solution to this apparent absence of large amounts of water vapor is the formation of polar ice caps. This theory, however, is based on early results of Venera 4 and is, I believe, no longer viable in light of the Venera 5 and 6 data, since the surface temperature now expected is above the critical temperature for steam: 374°C (Libby (1968)). Dayhoff et al (1967) and Palm (1969) theorize that mechanisms other than the formation of a polar cap could account for the lack of vast amounts of water on Venus. Their theories are very similar and suggest that the terrestrial planets may have formed at the same time and by the same mechanism, but have evolved differently due to different Sun-planet distances. Thus, their theories explain the present state of the atmosphere of Venus as a result of:

1) degassing of the planet's interior (mostly CO_2 and H_2O)

2) chemical reaction of this atmosphere with the surface

3) most water remains in the atmosphere and becomes unshielded from the solar ultraviolet when the carbon dioxide reacts with the crust, thus dissociating the water and allowing hydrogen to escape, while the oxygen reacts with the crust

4) after most of the water has escaped the planet in this fashion, the crust outgasses to produce a dense carbon dioxide atmosphere.

Cameron (1963) reports that the primitive solar nebula should have relative abundances of carbon, nitrogen, and oxygen of 16.6, 3.0, 29 respectively and the constituents of this proto atmosphere would form CH_4, NH_3, H_2O in the early phases which would eventually form CO_2, and N_2 atmosphere with abundance of 5:1. Thus, the theories only differ in emphases of the origin of the gases.

Clouds

The lack of visible surface details has long been attributed to a permanent veil of clouds. These clouds observed in the visible or in the near infrared sometimes, show some faint structure occasionally (Kuiper et al (1969a)). According to Kuiper (1969) this cloud layer is a yellow optically deep layer probably representing the upper levels of the troposphere. Pollack and Sagan (1967) have tested several atmosphere models using the 19mm Mariner II data, and find an absorbing cloud layer of water could exist or a scattering layer of particles 0.5mm in size, which together with the CO_2, N_2,and H_2O would produce correct microwave opacities.

There is currently much controversy over the nature of the cloud composition. Hunten (1968) reports that the clouds have extremely long scattering mean free path (> 1 km) and that they may be very small particles of NaCl or $NaCO_3$ since Earth based spectroscopy doesn't detect sufficient H_2O for ice clouds. Kuiper et al (1969b) report a mixing ratio of 10^{-6} for water vapor. If this corresponds to the interior of

the lower clouds, then neither layer of clouds can be due to water ice (Kuiper (1969), Chamberlain (1965)). Kuiper (1969) goes further to identify the meteorology of Venus as one involving Halide chemistry with the lower clouds being composed of $FeCl_2 \cdot 2H_2O$ and the upper clouds, NH_4Cl. Luming (1968) interprets the Venera 4 density anomaly at 41 km (T = 400°K) as a possible chemical reaction, perhaps the reaction that Kuiper proposed

$$2FeCl_3 + CO + H_2O = 2FeCl_2 + 2\,HCl + CO_2$$

Pollack and Sagan (1968), Sagan and Pollack (1967), Strong (1965), Anderson and Evans (1962), Zander (1965), and Bottema et al (1964) identify the clouds as due to ice crystals, a few microns in diameter on the basis of the reflectance 1-4 microns. Pollack (1968) reports microwave measurements near 1.35 cm that give an upper limit of 0.8% for water vapor, an amount in agreement with the Venera 4, 5 and 6 data and in agreement with the formation of ice clouds for both upper and lower clouds (Ginzburg and Feigelson (1969)). Water clouds are not consistent with observed cloud top temperatures and as Welch and Rea (1967) point out, the discovery of HCl by Connes et al (1967) eliminate their existence on the basis of the necessity of reproducing the microwave spectrum. A most important point in this controvery is the level of penetration of 1.4 and 1.9 micron radiation that Kuiper used. He maintains that the source is deep in the clouds. If so, his argument against water ice clouds is a good one. On the other hand, Owen (1969) calculates the depth of penetration of CO_2 bands:

λ	CO_2	T_{rot}
1.75 μ	3.75 km atm	240 $\pm$ 10°K
.87 μ	5 $\pm$ 1 km atm	298°K

where T_{rot} is the rotational temperature.

These data indicate that Kuiper's source is probably not much below the cloud tops. Furthermore, such measurements above terrestrial cloud cover at tropopause altitudes would detect very low water vapor concentrations that would not be indicative of concentrations below the cloud bases. Also, arguments against adequate water existing for ice clouds usually interpret spectra as coming from a layer of constant mixing ratio. Ohring (1966) has pointed out the error of this approach. Upon reanalysis using variable mixing ratios, Ohring (1966) found that some of the observed amounts were compatible with ice clouds on Venus, taking into account the uncertainty in our knowledge of the temperature of the cloud tops.

The science of remote sensing (reflectance spectroscopy) of surfaces is not as advanced as is gaseous spectroscopy. Matching of spectra is a necessary but not sufficient condition for identification; i.e., unique solutions are not obtained. Thus, the identification of cloud composition from a remote distance is not assured and the clouds may yet be found to be water (ice).

On the other hand, outgassing of the entry probe heat shield of the Venera 4, 5, and 6 at 11,000°C would probably produce vast quantities of water. Whether this water was still present during sampling is not known, but could conceivably account for the high water vapor amount detected.

Atmospheric Surface Pressure and Planetary Radius

The size of Venus has been determined to be slightly less than that of Earth by measuring the optical diameter of the planet's disk as seen through a telescope. Koenig (1967) gives a mean optical diameter of 12,240 $\pm$ 15 km, which corresponds to the top of the opaque cloud layer.

The atmospheric surface pressure as determined by a best fit to the temperature, pressure, and density data obtained by Avduevsky et al (1968) using data from Venera 4 is given as 17.2 to 20.8 $kg_f\ cm^{-2}$ with the best value being 18.5 $kg_f\ cm^{-2}$. Miknevitch and Sokolov report the results of fitting models to these data to be: surface pressures of 18.8 $kg_f\ cm^{-2}$ for the adiabatic model, 17.7 $kg_f\ cm^{-2}$ using smoothed density values and measured temperature values with an extrapolation using a polynomial curve, and 17.8 $kg_f\ cm^{-2}$ using measured temperature values with density boundary conditions at 8.47×10^{-3} gm cm^{-3} at 9.0 km and 3.23×10^{-3} gm cm^{-3} at 19.5 km. The extrapolations mentioned here were necessary because the densitometer became saturated at densities greater than 1.7×10^{-2} gm cm^{-3} (i.e., about 30 km above the radar surface). During descent the altitude was referenced at 26 km by a marking doppler altimeter. However, the planetary surface radius at the landing location was not measured, thus causing some uncertainty to whether these surface pressures correspond to that at a "mean planetary radius" or to some altitude above that.

The S-band occultation experiment conducted with Mariner V indicated density scale height data starting from 6140 $\pm$ 7 km ($\approx$1 mb) down to about 6085 km from the center of Venus (about 7 atm) (Kliore et al (1967 and 1969)), where critical refraction occurred. The experimental technique was not able to measure the refraction all the way to the surface due to excessive bending of the radio waves at pressures greater than 5 atm, but is important in verifying the Venera 4 results and in providing a reference of the distance to the center of the planet. The only common link between Mariner V and Venera 4 is atmospheric pressure. If the data from the two spacecraft are compared on this basis (Figure 3), then the point of cessation of transmission

of Venera 4 is determined to lie near 6074 km, which differs from radar values of the radius of Venus of 6056 ± 1.5 km reported by Ash et al (1967) and 6050 ± .5 km (Ash et al (1968)). Data obtained by Melbourne et al (1968) using the Goldstone radar indicate 6053.7 ± 2.2 km. Mariner V ranging data combined with simultaneous radar data reported by Anderson et al (1968) gives a planetary radius of 6052.8 ± 2 km. The value of 6053 km will be adopted for calculations in later chapters.

The Regulus occultation results reported by de Vaucouleurs et al (1960) have been interpreted to obtain independent information on the radius of Venus and on upper atmosphere structure. During this experiment the bright star Regulus was occulted by Venus on July 9, 1959, with de Vaucouleurs and Menzel (1960) making measurements of the decrease/increase of the light density from Regulus during immersion/emersion. The results of this experiment give a density scale height of 6.8 km and a density scale height logarithmic gradient (1/H dH/dZ) of 0.01 at 70 ± 8 km above the cloud layer using a model atmosphere consisting of 90% carbon dioxide. Hunten and McElroy (1968) have reanalyzed these data and believe the scale height is accurate to somewhat better than a factor of 2. Opik (1961) recalculated the height of the occultation level to be 86-96 km above the cloud by accounting for a scattering atmosphere causing the cloud tops to appear higher. Using the Regulus occultation data together with the upper atmosphere temperature structure calculated theoretically by McElroy (1968), Hunten and McElroy (1968) show that a downward extrapolation of only 15 km will join these data to the Venera 4 data. This approach gives a value of 6074 km for the point where Venera 4 stopped transmitting. My value of 6074 km obtained from the Mariner V and Venera 4 results by matching pressure

shows good agreement with their results.

Many investigations have been carried out trying to resolve this controversy on the radius of Venus and the associated problem of determining the surface pressure, among them: Eshleman et al (1968), Pitts (1968a), Reese and Swan (1968) and Ash et al (1968). The conclusion most often reached was that the Venera 4 doppler radar was quite likely in error by 21 to 26 km. Therefore, when the Venera 4 entry probe started transmitting it was at 52 km, not 26 km as was reported by the Russians. Thus, the 20 atm pressure reported by the Russians to be the surface pressure is low by a factor of 5. An interesting possibility proposed by Luming (1968) is that the radius controversy, and the difference in temperature gradient is due to a mean polarizability of aerosols or constituents in the atmosphere in addition to an error in the Venera 4 radar data. Since doppler radars are prone to errors involving multiples of the distance being measured, Luming's theory could perhaps explain why the error was not an exact multiple of 26 km.

As was mentioned earlier, the design criteria of Venera 5 and 6 were focused on deeper penetration capabilities and improved doppler radar so as to decide the controversy between Venera 4 and radar determinations of the Venus radius. Brichant (1969) reports that Venera 5 and 6 conducted measurements from 0.6 to 27 atm pressure, where the temperature varied from 25°C to 325°C. On Venera 5, 27 atm corresponded to 24-26 km altitude whereas on Venera 6, it corresponded to 10-12 km.. Thus, it is possible that substantial relief may exist on the surface, but in any event surface pressures higher than 20 atm do definitely exist. Brichant (1969) reports that 70 measurements of pressure and 50 measurements of

temperature were made on the two spacecraft.

Eshleman et al (1968) analysis of the radar, Venera 4, and Mariner V data predicted (through downward extrapolation), a surface pressure of about $100\ ^{+50}_{-33}$ atm and $700 \pm 100^{\circ}K$. Wood et al (1968) predicted $750 \pm 50^{\circ}K$ and $90\ ^{+90}_{-45}$ atm based on the same data together with the microwave and radar data. Their predictions seem to have been borne out by Venera 5 and 6.

In order to place reasonable bounds on the possible surface pressure, two choices seem reasonable: 1) If the Mariner V data at a radius of 6085 km is assumed correct (Table 1) and the mean surface lies at 6053 km, then the surface pressure can be obtained by an adiabatic extrapolation downward by 32 km, giving 87,370 mb; 2) Using the lowest radar value of the radius according to Ash et al (1968), 6048 km, defines the upper limit of surface, as 119,300 mb.

Atmospheric Temperature

The Venera 4 resistance thermometers measured temperature continually during descent. According to Mikhnevitch et al (1968), a temperature of $544^{\circ}K$ was measured at the last transmission. These data show that temperature is close to adiabatic the entire 26 km of measurement (it is assumed by the author to lie in the region 52 to 26 km). The Venera 5 and 6 data, shown in Table 3, corroborate the existence of a near adiabatic atmosphere in the troposphere of Venus. On the basis of the estimates of surface pressure made in the past paragraph, estimates may be made of surface temperature: 1) if the radius is 6053 km then a best estimate would be $735.19^{\circ}K$ and 2) the lowest probable radius of 6048 km would give the highest probable temperature of $772.26^{\circ}K$.

The Mariner V temperature profiles shown in Figure 3 correspond to the night side, and therefore warrant comparison to the Venera 4 results. The lapse rate for the "Mariner model" with 75% carbon dioxide is about 5°K/km and that for the 90% carbon dioxide case is about 5.5°K/km, up to 6120 km whereupon the structure becomes isothermal (Kliore et al (1967)). 5°K/km is about half the adiabatic value and is very close to pseudo-adiabatic. I have made calculations of the atmospheric structure assuming hydrostatic equilibrium and following the pseudo-adiabat upward from the condensation level up to the level where 125μ or less precipitable water lies above, thus meeting the requirements of Belton and Hunten (1966) on detectable water vapor. These models show that an average lapse rate near 5°K/km is not unreasonable, but that the rate does vary greatly over the calculated range of temperatures and pressures. Thus, the assumption does appear somewhat consistent with the observed profiles. Furthermore, in such calculations the temperature at the cloud tops is very near the measured temperature for the tops of the clouds: 205-245°K (Goody (1965), Westphal et al (1965), Murray et al (1963) and Koenig (1967)), and is within the best value for the optical diameter of Venus 12240 km.

Some geographical, diurnal, and hemispherical differences have been detected in the cloud top temperature (presumably the tropospheric clouds $\approx$60 km); however, they are small with the northern hemisphere appearing to have 1°K higher equivalent blackbody temperature (measured at 8-14μ) than the southern hemisphere. However, the data of Murray et al (1963) are heavily weighted by the equatorial regions, and Limb darkening is the principal feature seen in all the data. The bilateral symmetry indicated by the contours show the poles to be cooler than the equatorial regions.

Goody (1965) finds a small diurnal effect with the subsolar point being cooler than the antisolar point. This enhanced emission from the dark side could be due to: 1) the transparency increased by evaporation of cloud particles in subsiding air, or 2) a genuine atmospheric effect. Typical peak brightness temperatures range from 205°K-227°K according to Westphal et al (1965) and Murray et al (1963) up to 235°K which is a value Koenig et al (1967) summarized from several earlier papers.

The amplitude of the surface temperature variations with phase is currently without a recognized scientific consensus. Microwave observations of Venus show that the surface temperature is greatest just after zero phase angle (superior conjunction). The amplitude and phase of these variations is dependent upon the wavelength being used. At .8 cm, variations are apparently from the atmosphere (Pollack (1965)):

$$T_{BB} = 422 + 41 \cos (\alpha - 21^{\circ}) \qquad {}^{\circ}K$$

whereas wavelength at 3.15 cm appear to originate from the surface

$$T_{BB} = 621 + 73 \cos (\alpha - 11.7^{\circ}) \qquad {}^{\circ}K$$

while those at 10 cm also originate from the surface, although somewhat deeper

$$T_{BB} = 622 + 41 \cos (\alpha - 21^{\circ}) \qquad {}^{\circ}K$$

where α is the phase angle (zero at subsolar point and 180° at the antisolar point.

Differences of 78 to 146, or 150 to 200°K between the bright and dark side are suggested from such data (Koenig (1967)). Shapiro (1968) concludes that a slow rotation rate of 243 days would lead to larger temperature differences, day to night than exist on Earth. Sagan and Pollack's (1965) model for the microwave phase effect gives: mean disk

temperature - 700°K; mean darkside - 600°K; mean brightside - 800°K; subsolar - 1000°K; antisolar - 610°K; pole - 470°K. Their model incorporates a convective atmosphere topped with clouds that attenuate thermal emission short of 3 cm. According to Sagan and Pollack, this model successfully accounts for all phase effects, like those just described here. Seriously at odds with these theories, are more recent measurements at 4.52 cm by Dickel et al (1968) which show negligible phase effect at a blackbody temperature of 654 $\pm$ 35°K. Using a surface emissivity of .9, a mean surface temperature of 780°K can be derived from this data. Their data also indicates that the surface is reached at 6 cm wavelength, rather than at 3 cm as was thought earlier. Supporting these measurements are arguments by Thaddeus (1968) that the high thermal inertia of a deep atmosphere would not allow significant horizontal gradients in temperature (< 3°K) except perhaps in the boundary layer near the surface and near the upper regions of the atmosphere. Indeed, Mariner V failed to indicate significant differences in temperature structure from immersion to emersion which were night and day, respectively. Unfortunately, similar measurements have not been made in the lower atmosphere, so the question of phase effect and equator-pole temperature gradients remains open. Therefore, it now appears probable that the phase effects were a product of experimental error. If not, very unusual properties are required of the atmosphere. Unfortunately, this is a most important boundary condition for a circulation model, and the lack of a reasonably certain constraint will affect the certainty of the results of the circulation model.

Gravitational Field

Mariner V range and doppler radio tracking data has yielded a new value for the mass of Venus. It is expressed in terms of the universal gravitational constant G times the Mass of Venus M_{φ} (Anderson et al (1967)).

$$G\,M_{\varphi} = 324{,}859.61 \pm 0.49 \text{ km}^3/\text{sec}^2$$

Assuming a spherically symmetric planet, this value may be used to calculate surface values for gravity at any of the radii previously discussed. The value for a radius of 6053 km is 887 cm sec^{-2}.

Magnetic Field

Based on measurements of magnetic field strength and plasma properties made by Mariner V, Bridge et al (1967) estimate the magnetic dipole moment of Venus to be within 2×10^{-3} times that of Earth. Based on the absence of energetic electrons within 10,150 km from the center of the planet (i.e., no Van Allen Radiation Belts), Van Allen et al (1967) estimate the magnetic field at the equatorial surface to be almost certainly less than 350 gamma and probably below 35 gamma (1 gamma equals 10^{-5} Gauss). These values correspond to dipole moments of 0.01 and 0.001 times the dipole moment of the Earth.

Ionosphere

Kliore et al (1967) report peak electron densities at 6185 km from the center of Venus were measured at 5.5×10^{-5} cm^{-3} and the Mariner Stanford Group (1967) report nighttime peak concentration about two orders of magnitude below that of the daytime peak, with both layers being thin by terrestrial standards.

CHAPTER III

ATMOSPHERIC MODELS FOR VENUS

In order to make reasonable calculations dealing with the circulation of the atmosphere of Venus in later chapters, it is important to first make self consistent basic state models of the atmosphere.

Early model atmospheres were varied due to the extreme uncertainties and great controversy concerning the probable cause of the high carbon dioxide amounts, the ubiquitous clouds, the small quantities of water in the atmosphere, and the high surface temperatures detected by microwave techniques. The discovery of the impenetrable cloud cover (using visible wavelengths) prompted the proposal of a swamp model. In order to verify such a model, a detailed search for water resulted which caused the accidental discovery of large quantities of carbon dioxide in the atmosphere. According to Sagan (1961) this discovery caused the overthrow of the swamp model, since the carbon dioxide would react with the exposed surface materials in the presence of water. Menzel and Whipple (1955) proposed an ocean model in an attempt to account for a lack of this reaction and Sagan (1961) reports that Hoyle and Mintz suggested clouds composed of smog and oceans of oil to prevent such a reaction. However, the high surface temperatures now believed to exist at the surface make these models untenable.

Opik (1961) proposed a model atmosphere (aeolosphere) with a thick cloud of dust (aeolosphere) with surface wind friction as the best heat

source, when early theories made it appear that the greenhouse model could not have sufficient infrared opacities to produce the observed microwave temperatures. The key to this model is a near adiabatic temperature profile like that which has recently been confirmed by Venera 4, 5, and 6. In Opik's model, the low level clouds at .6 atm pressure and 340°K with upper clouds at .08 atm pressure, and 234°K. The atmosphere was assumed to be 20, 40, or 80% carbon dioxide with surface conditions of 4.3 to 7 atm and 570°K. In support of the aeolosphere model, Anderson (1969) reports that vertical wind velocities necessary to support dust in the Venus atmosphere are less than one half that necessary in the terrestrial atmosphere (because of the much higher Venus pressures). The main drawbacks of the concepts of this model are the difficulty in keeping the dust in the atmosphere and a lack of explaining the observed microwave phase effect. The aeolosphere model is almost certainly ruled out by the expected slow wind speeds at the surface where a high density produces an extremely high thermal heat capacity. However, a "dusty cloud" greenhouse model is not ruled out.

In the classical greenhouse model solar radiation, minus some reflection, penetrates to the surface, heating the surface. The atmosphere then traps the reemitted infrared energy by the high infrared opacity due to the pressure broadened lines of carbon dioxide and water vapor. The main objection to the model was that theoretical calculations could not reproduce high temperatures due to insufficient infrared opacity (it must be better than 99% opaque). Surface pressures for greenhouse models were much lower then; e.g., 4 atm (Owen (1965)), with current estimates near 100 atm. Furthermore, little if any data exists on the wings of water

vapor and carbon dioxide at high pressures and high temperatures so this effect and the effect of cloud cover were not taken into account in the early models. Ohring and Mariano (1963) calculated this cloud cover contribution and find it is significant. Applying recent results to their table for 99% cloudiness, I have calculated a required opacity of < 1 for a grey atmosphere. This is decreased by a factor of 6 over their original calculations due to data indicating increased depth of the atmosphere, since they made the original use of their nomograms. Water concentrations of .5% are required for an H_2O and CO_2 greenhouse effect, according to Pollack and Wood (1968), well within the Venera amounts. Overall, this model is probably the most widely accepted by the scientific community at the present. It is important to note dust clouds in the atmosphere alone do not make a model an aeolosphere model. A surface heating by wind friction is required for this. Therefore, dust clouds localized in a particular altitude regime, may comprise part of a greenhouse model. Unfortunately, "classical greenhouse" models have some serious drawbacks, given by Hunten and Goody (1969):

1) The atmosphere must be extremely opaque throughout the infrared; part, or even most, of the opacity is probably contributed by the clouds. Yet visible radiation must penetrate to great depths.
2) Heat transfer by convection, both free and forced, must be included in the model.
3) The clouds, if of dust must be supported by turbulent motions. If the material is condensable, the problem is less serious, but there are strong objections to the obvious possibility, water vapor.

4) Advection of heat by circulations of planetary scale must be considered.

In an alternative approach Hansen and Matsushima (1967) considered a dust insolation model with internal heat from the planet being the major heat source.

Strelkov et al (1969) calculated the greenhouse effect based on the Venera 4 pressure data and found temperatures equal to or greater than detected by Venera 4.

Kaplan (1962) proposed a greenhouse model of 10 $\pm$ 2.5 atm surface pressure and 700 $\pm$ 140°K surface temperature, using a composition of 10% carbon dioxide and 90% nitrogen. His models were keyed to satisfy conditions at three levels: the surface, the cloud tops, and the level of the Regulus occultation (discussed in Chapter II). While his boundary condition for the first of these is no longer thought to be correct, the latter two appear correct and are conditions that should be met by any self consistent model and will be met by the models to be developed later in this chapter. Sinton and Strong (1960) using the 8-12 micron band, have determined temperatures of the cloud top to be 225 - 235°K. Sagan and Pollack (1965) have developed a 50 atm greenhouse model with a mean disk temperature of 700°K and a convective atmosphere topped with clouds.

Thus, classical greenhouse models required visible penetration of solar energy to the surface, the aeolosphere model required surface heating by the wind, and both ignored dynamic effects (adiabatic warming/cooling of subsiding/rising air). Goody and Robinson's (1966) model induces planetary scale motion at the cloud tops by differences in insolation transporting energy downward from the cloud tops in the

process of distributing the energy globally, thus producing high surface temperature at great depth with no visible solar energy penetrating the clouds. This revolutionary model all but eliminates the need of surface heating by friction or from conduction from the interior.

Two recent engineering Venus model atmospheres: Schiffer (1968) and Martin (1969) and one scientific model: Hunten and Goody (1969) contain many of the essential boundary conditions for the models which will be developed here. However, since the intended use of these models is to construct circulation models, more attention must be given to the nature of the clouds, a parameter that does not affect the calculation of atmospheric structure enough to impact significantly the engineering design of an entry vehicle. In fact it will be shown that two models with similar temperature structures, one with ice clouds and the other with dust (or something else), appear consistent with the rather discordant dichotomy of observational data.

A computer program developed by Pitts (1968b) was used for calculating the model atmosphere using the temperature vs. altitude data of Avduevsky et al (1968) with an atmospheric composition of 100% carbon dioxide, which is very close to the composition given by Vinogradov et al (1968), Table 1, and Brichant (1968), Table 3. In addition, the envelope of temperature from Mariner V: 6120 $\pm$ 7 km, 215 - 245°K; 6095 $\pm$ 7, 400 - 450°K, reported by Kliore et al (1967) was used as a constraint. Spinrad's (1962) measurement of $\approx$440°K at 10 atm using a wavelength of 7820 Å, Belton's (1969) measurement of 240 - 270°K at .6 atm, and Gray's (1969) measurement of 244 $\pm$ 10°K for an average temperature above the cloud tops are assumed to hold. McElroy's (1968) upper atmosphere structure is adopted, the

structure is required to satisfy the Regulus occultation data, and cloud top temperatures are adopted as 205 - 245°K, Goody (1965), Westphal et al (1965), Murray et al (1963) and Koenig et al (1967). These data are shown with the temperature structure in Figure 3. From the best values of the radius of Venus as given in Chapter II, the radius for use in the model atmosphere is chosen as 6053 km. Using this value with the value of $G M_{\varphi}$ determined from Mariner V and Newton's law of gravitation gives a surface acceleration of gravity of 887 cm sec^{-2}. Vinogradov et al (1968) and Brichant (1969) describe the lower atmosphere of Venus as having an adiabatic structure down to 27 atm pressure. In order to calculate the pressure and temperature at the surface, it is assumed that the atmosphere continues as adiabatic ($\partial T/\partial Z = -g/c_p$) with c_p being a function of pressure and temperature as given by Hilsenrath et al (1955). It is further assumed that the atmosphere obeys the hydrostatic law and the gas is ideal. Using compressibility data from Hilsenrath et al (1955) it was determined that the perfect gas law is obeyed within 1% at temperatures and pressures that occur in the Venus atmosphere. Significant deviations from ideality only occur at high temperatures and low pressures which are extremely unlikely in the troposphere and stratosphere of Venus. By matching the Mariner V and Venera 4 data with a 6053 km radius, it is shown by these calculations in Table 4 that a downward adiabatic extrapolation (similar to Hunten (1968)) is necessary to find the surface conditions. In Table 4 the altitude (z) is given in km relative to the 6085 km level for which Mariner V gave 7170 mb pressure and 477°K (see Table 1), DTDZ is temperature lapse rate, HRHO is density scale height, ES is the saturation vapor pressure of ice, and E is the vapor pressure for ice for 2.4 $^{o}/_{oo}$.

This calculation results in a surface pressure of 8.737×10^4 mb and a temperature of 735.19°K, as shown in Table 4. After taking the curvature of the temperature structure in this extrapolation, a linear temperature gradient of -8.64°K/km was chosen to approximate closely the real situation, while at the same time permitting a necessary level of simplicity for the application to the circulation model. This simplification gives an average c_p of 1.03×10^7 ergs/(gm °K). It must be pointed out, however, that not all investigators agree that adiabatic extrapolations to the surface are reasonable. Liwshitz and Sinclair (1969) find a better fit to microwave data at wavelengths greater than 8 cm if the atmospheric models have an isothermal layer at 670 ± 20°K that extends from the surface to 7 ± 2 km. However, no physical reason for the existence of such a layer has been given as yet.

At high altitudes the adiabatic lapse rate gives way to pseudo-adiabatic when saturation is reached. In order to calculate the level of the cloud base for the "ice cloud" model the Venera 4, 5, and 6 data were converted from water vapor density to mixing ratio.

	Venera 4	Venera 5, 6
ρ_w	1-8 mg/liter	4-11 mg/liter
r	.35 - 2.7 °/oo	1.4 - 3.8 °/oo

Comparison of these mixing ratios to the adiabatic profile from the surface upward gives cloud bases of 55 - 60 km. Assuming the best optical radius (cloud tops) is 6120 km this gives cloud thicknesses of 7 - 12 km which is of sufficient thickness for the greenhouse model. In the clouds the lapse rate is calculated by

$$\frac{\partial T}{\partial z} = g \frac{1 + \frac{m_w L e_s}{PRT}}{c_p + \frac{m_w L^2 m_v e_s}{m_d PRT^2}} \qquad (1)$$

At higher altitudes radiative equilibrium very likely prevails with the temperature gradually falling until the thin ultraviolet clouds are formed at the mesopause, and at higher altitudes dissociation, recombination, and ultraviolet absorption occur. At these levels the models of McElroy (1968) and Whitten (1969) are used.

For the dust model the temperature is required to fall off less rapidly such that saturation mixing ratios do not drop below 3 gm/kg until the mesopause where ultraviolet clouds are again formed.

The model atmosphere for the ice cloud meets all these requirements and in addition has 97μ precipitable water vapor above the clouds, thus meeting Belton and Hunten's criteria as given in Table 2. The data for this model are tabulated in Table 5, giving fourteen variables up to 400 km altitude.

The dust cloud model is also consistent with described facts and will accept up to 2.7 $^{o}/_{oo}$ of water vapor with no condensation of ice until the mesopause is reached. These data are given in Table 6 up to 410 km.

CHAPTER IV

STEADY STATE TWO DIMENSIONAL CIRCULATION MODEL

In order to model the circulation of Venus, solutions will be sought for the fully coupled equations of motion, continuity, state, and thermodynamics. This set as given by Haltiner and Martin (1957), Hess (1959), Bird et al (1960), and Love (1968) are as follows.

$$\frac{\partial \vec{v}}{\partial t} + (\vec{v}\cdot\nabla)\vec{v} = -\frac{1}{\rho}\nabla p - \vec{g} + \frac{1}{\rho}(\nabla\cdot\overleftrightarrow{\tau}) - 2\vec{\Omega}\times\vec{v} - \vec{\Omega}\times\vec{\Omega}\times\vec{v} \qquad (2)$$

$$\frac{\partial \rho}{\partial t} + \nabla\cdot\rho\vec{v} = 0 \qquad (3)$$

$$p = \rho\frac{R}{m}T \qquad (4)$$

$$\rho c_p\left(\frac{\partial T}{\partial t} + (\vec{v}\cdot\nabla)T\right) = \beta T\left(\frac{\partial p}{\partial t} + (\vec{v}\cdot\nabla)p\right) + \nabla\cdot(K\nabla\vec{T}) + \mu\Phi - \nabla\cdot Q \qquad (5)$$

In these equations $\vec{v}$ is vector velocity, t is time, ρ is density, p is pressure, g is acceleration due to gravity, K is eddy conductivity, $\vec{\Omega}$ is the rotation vector of Venus, R is the universal gas constant, m is molecular weight, c_p is specific heat, β is the coefficient of thermal expansion, Q is the net radiative flux, and $\overleftrightarrow{\tau}$ is the eddy stress tensor.

It is the purpose here to model the steady state circulation in two dimensions, x and z (x being horizontal distance, and z being vertical)

around half the planet from the subsolar point to the antisolar point along a great circle.

Since Venus has a very slow sidereal rotation rate of about 243 days retrograde the $\vec{\Omega}$ is about 3×10^{-7} rad/sec, so it will be assumed that accelerations due to this rotation are negligible. It is also assumed that these equations written in coordinate form have solutions such that they can be described in terms of a basic state (barred terms) and small perturbations (primed terms).

$$u = \bar{u}(z) + u'(z,x) \tag{6}$$

$$w = w'(z,x) \tag{7}$$

$$p = \bar{p}(z) + p'(z,x) \tag{8}$$

$$\rho = \bar{\rho}(z) + \rho'(z,x) \tag{9}$$

$$T = \bar{T}(z) + T'(z,x) \tag{10}$$

The basic state solution being an average of the best known data of Venus as described in the previous two chapters and the perturbation represents the change in this basic state of the atmosphere in response to sunlight falling on the top of the cloud layer. The equations that we found to satisfy the basic state; i.e., $u' = o$, $w' = o$, $p' = o$, $\rho' = o$, $T' = o$ is the hydrostatic equation

$$\frac{\partial \bar{p}}{\partial z} = -\bar{\rho} g \tag{11}$$

the equation of state

$$\bar{p} = \bar{\rho} \bar{T} \frac{R}{m} \tag{12}$$

and the requirement that temperature be linear with height in the thermodynamics equation

$$\frac{\partial^2 \bar{T}}{\partial z^2} = 0 \tag{13}$$

Due to high opacity of the Venus atmosphere, radiative transfer is very inefficient relative to molecular conductivity permitting the radiative terms to be neglected in equation (13). The complete justification for ignoring radiation in the basic state thermodynamics equation is given in Appendix A.

These three basic state conditions (equations 11, 12, and 13) are, fortunately, those that are normally used in constructing static model planetary atmospheres and are the assumptions used in Chapter III in deriving the basic state dust model and ice cloud model atmospheres for Venus. Thus, these model atmospheres may now be employed toward solving the hydrodynamic equations describing the response of the atmosphere to sunlight falling on and being absorbed in the clouds. By writing equations 2 through 5 in coordinate form, and making reasonable and valid assumptions (such as eliminating products of primed terms) as described in Appendix B, these equations can be written in terms of 5 equations in 5 unknowns (u', v', p', ρ', T'), with two independent variables x and z. The barred terms (e.g., $\bar{\rho}$) are those which satisfy the basic state.

$$\bar{\rho}\,\bar{u}\,\frac{\partial w'}{\partial x} + \frac{\partial p'}{\partial z} + \rho' g - \bar{\rho}\,\nu_z \frac{\partial^2 w'}{\partial z^2} - \bar{\rho}\,\nu_x \frac{\partial^2 w'}{\partial x^2} = 0 \tag{14}$$

$$\bar{\rho}\left[\bar{u}\,\frac{\partial u'}{\partial x} + w'\frac{\partial \bar{u}}{\partial z}\right] + \frac{\partial p'}{\partial x} - \bar{\rho}\,\nu_z \frac{\partial^2 u'}{\partial z^2} - \bar{\rho}\,\nu_x \frac{\partial^2 u'}{\partial x^2} = 0 \tag{15}$$

$$\frac{\bar{u}}{\bar{\rho}}\frac{\partial \rho'}{\partial x} + \frac{\partial u'}{\partial x} + \frac{\partial w'}{\partial z} - \frac{w'}{H_\rho} = 0 \tag{16}$$

$$p' = \frac{R}{m}\left(\bar{\rho}\,T' + \bar{T}\,\rho'\right) \tag{17}$$

In equation (17), p' must be required to be zero in order to prevent the solutions from including compressional waves (i.e., this is the Anelastic assumption).

$$\bar{u}\left[\frac{\partial T'}{\partial x} - \frac{1}{\rho c_p}\frac{\partial p'}{\partial x}\right] + w'\left[\frac{\partial \bar{T}}{\partial z} + \frac{g}{c_p}\right] - k_z\frac{\partial^2 T'}{\partial z^2} - k_x\frac{\partial^2 T'}{\partial x^2} = 0 \tag{18}$$

Employing the linear function $\bar{u}(Z)$ is a method by which a linearized set of differential equations can be made to act like a non-linear set. Thus, this set of equations accounts for both horizontal momentum advection and compressibility in the continuity equation due to the extremely deep (60 km) troposphere of Venus. No other circulation models to date are this general. Equations (14) through (18) and a point iterative relaxation scheme (Appendix B) were programmed in finite difference form in fortran V using the Univac 1108 computers at the Manned Spacecraft Center, Houston, Texas. The computer program using this scheme is presented in Table 7. The model atmosphere subroutine and other needed subroutines are described by Pitts (1969).

Circulation Models

The circulation models to be discussed here are based on the basic state model atmospheres developed in Chapter III. Also, each model atmosphere is based on assumptions of: the depth of the model, eddy viscosity in vertical and horizontal, Prandtl number, basic state horizontal wind, and whether the Boussinesq approximation $\frac{\partial \bar{\rho}}{\partial z} = 0$ is to be used or the full Anelastic solution is sought.

The first model to be described is 52 km deep, it is assumed that the clouds are composed of dust, that $\nu_z = 10^3$ cm^2/sec, that $\nu_x = 10^5$ cm^2/sec, that no horizontal advection occurs (i.e., linear $\bar{u}(Z) = o$), that the Prandtl number is unity, and that the atmosphere is Anelastic. This model assumes that Goody and Robinson's (1966) method is valid, in which the clouds are impenetrable by visible light with solar heating taking place in the top of the clouds on the day side of the planet with cooling occurring in this same layer on the night side (described in Appendix B). The large scale temperature gradient in the cloud tops causes motion which creates a large scale circulation, transferring energy to the dark side. Goody and Robinson required that the top level of these clouds be constant in temperature at 230°K, whereas temperature is allowed to vary on the top of this model. Furthermore, Goody and Robinson's model incorporated the Boussinesq assumption, whereas this model allows for the variation in $\bar{\rho}$ with altitude. The lower boundary condition of this model is similar to Goody and Robinson's and requires the atmosphere to receive zero heat flux from planetary surface, thus requiring an adiabatic temperature gradient

$$\frac{\partial(\bar{T} + T')}{\partial z} + g/c_p = o$$

This model took 18 iterations to converge, and since each term of each equation (14) through (18) is printed out upon convergence, the predominant terms are easily determined to be

$$\frac{\partial w'}{\partial z} + \rho' g = 0 \tag{19}$$

$$\frac{\partial w'}{\partial x} - \bar{\rho}\,\nu_z \frac{\partial^2 u'}{\partial z^2} = 0 \tag{20}$$

$$\frac{\partial u'}{\partial x} + \frac{\partial w'}{\partial z} - \frac{w'}{H_\rho} = 0 \tag{21}$$

$$w'\left(\frac{\partial \bar{T}}{\partial z} + \frac{g}{c_p}\right) - k_z \frac{\partial^2 T'}{\partial z^2} = 0 \tag{22}$$

$$\bar{p} T' + \bar{T} \rho' = 0 \tag{23}$$

In the top of the atmosphere where sunlight warms the cloud top $\frac{\partial^2 T'}{\partial z^2}$ is positive, thus requiring upward transfer of potentially warm air $w' \frac{\partial \theta}{\partial z}$, and since $\frac{\partial \theta}{\partial z}$ is positive, the w' is positive. The opposite effect occurs on the night side with $\partial^2 T'/\partial z^2$ being negative. Due to compressibility w' will increase/decrease as the parcel ascends/descends, until it gets near the top where this motion is translated into a horizontal velocity. The wind (u') increases with height such that $\frac{\partial^2 u'}{\partial z^2}$ is positive, requiring a balance by $\frac{\partial p}{\partial x}$ being positive.

The solution as given in Figure 4 indicates a circulation extending downward from the cloud tops about 20 km with the maximum speed at the top being about 28 m/sec, and vertical speeds in this cell being of the order of one cm/sec. Horizontal speeds below this cell fall off by 2 orders of magnitude in the next 5 km and by 2 more the 5 km below that. Thus, the lower atmosphere is almost completely at rest. Cloud top temperatures at the subsolar point are calculated to be 329°K at subsolar point and are 213°K at the antisolar point and are approximately constant at this latter value over the night portion of the planet. The region of the highest temperature gradient occurs on the sunny side near the terminator. No perceptible horizontal temperature gradients occur below this cell (no phase effect), thus confirming the measurements of Dickel (1968)

and supporting the thesis of high thermal heat capacity of Thaddeus (1968). Moreover, this model predicts a thermal phase effect in the clouds that may have gone undetected to date because of the difficulty of observing Venus at superior and inferior conjunctions due to the proximity of the solar image and the high atmospheric noise that is present at 8-14μ. The shallow circulation doesn't agree with any of the models that assume that a variation of surface heating is the driving force: Ohring (1965), Bohachevsky and Yeh (1968), and also doesn't agree with Goody and Robinson's (1966) or Stone's (1968) top heated Boussinesq model in terms of the depth of the circulation. Moreover, the region of ascent is narrow in this model, whereas Goody and Robinson's (1966) and Stone's (1968) models have narrow regions of subsidence. This difference may be due to the fact that this model accounts for compressibility and Goody and Robinson (1966) and Stone (1968) assumed the Boussinesq approximation to hold. The velocities in the upper boundary layer predicted by this model compare favorably to Goody and Robinson's 34 m/sec. Making the Boussinesq assumption halves the cloud top horizontal velocity and the vertical velocities, with the lower atmosphere remaining almost at rest. This model is in good agreement with the recent model by Hess (1968), the details of which are not available in the literature. The principal features of his model are a 52 km deep atmosphere, with a circulation about 15 km deep from the cloud tops.

Kerzhanovich et al (1969) have made calculations of the vertical and horizontal velocities in the Venus atmosphere based upon doppler measurements from Venera 4. These results were taken from about 52 km down to 26 km and the approximate trajectory is superimposed on Figure 4. Upward velocities $\approx$3m/sec were deduced until 7:53 a.m. Moscow time which is

approximately 47 km on model in Figure 4 and from that point down, downward velocities almost constant at ≈3 m/sec were recorded. These measurements are claimed to have an accuracy of ± 0.6 m/sec with an uncertainty in the zero point of ± 6 m/sec. Due to unfavorable conditions of measurements, Kerzhanovich et al (1969) could make no horizontal velocity calculations but could set an upper limit of 32 m/sec. These Venera 4 data agree fairly well with the model in Figure 4, which predicts 23 m/sec at the Venera entry corridor. The Venera 4 vertical velocities are the same order of magnitude, but are a little too large to agree well with the circulation model.

The second model (see Figure 5) to be discussed is identical to the first (the same equations predominate) except $\nu_z = 10^4$ cm^2/sec, thus causing an increase in viscous mixing which requires an increase in horizontal pressure gradient to balance it. Since the Prandtl number is still unity, the eddy diffusivity term also increased, since the heat in and out of the top layer specifies a Neumann (slope) condition on temperature, this to a great extent determines $\frac{\partial^2 \dot{T}'}{\partial z^2}$ so that an increase in k_z causes a proportional increase in vertical velocity. Through the continuity equation this causes an increase in horizontal velocity in the top layer, up to 288 m/sec, thus exceeding the speed of sound and making this model untenable. In this model, temperature at the subsolar point is 328°K and the temperature of the night side cloud tops is 216°K.

The third model to be discussed is the same as the second, except the Prandtl number is 10.0, making eddy viscous process predominant over eddy diffusion. Thus, at the cloud top a thin thermal mixing region develops, and a thick turbulent layer develops. This model produces a circulation

almost identical to that of model one, thus indicating that the value of eddy viscosity is not as critical in determining the circulation as is the value of eddy diffusivity. No figure is given for this model.

The fourth model (Figure 6) to be discussed has the same basic state structure as the previous three models, and is similar to model 2 except the Prandtl number is .1, making the cloud top have a thick thermal mixing region and a thin turbulent layer. The higher eddy diffusivity causes an increase by 2 orders of magnitude in the vertical velocity resulting in horizontal speeds (1640 m/sec) much in excess of the speed of sound, thus making this model untenable. Temperature effects of $1^{\circ}K$ or more propagate downward to ≈ 25 km, in response to the higher diffusivity.

Another model was run which was identical to the first except that Pr = .1, thus causing $k_z = 10^{+4}$ cm^2/sec. Since the diffusivity term is of greater importance than the viscous term, the resulting model is almost identical to model 2 and Figure 5 may be referred to for the derived circulation.

Model 5 (Figure 7) is a 60 km deep dust model with $\nu_z = 10^{+3}$ cm^2/sec, and a Prandtl number of unity. This model is typical of the other dust models discussed previously, showing one cell with vertical velocities of 10^{-3} cm/sec and horizontal velocities on the order of .1 m/sec. The basic state model is so stable in the upper atmosphere that little vertical velocity is required to replace the heat diffused downward. The small vertical velocity produces a small horizontal velocity (at the top boundary through the equation of continuity), whose mixing balances the pressure gradient. The cloud top temperature ranges from $340^{\circ}K$ at the solar point

to 203°K on the night side. Increasing ν_z in another model to 10^4 increased the velocities by a factor of 10, but didn't affect the cloud top temperatures significantly.

Model 6 (Figure 6) is a 60 km deep ice cloud model; otherwise, it is similar in all characteristics to model 5. The basic state model is very close to adiabatic, thereby requiring a higher vertical velocity to vertically advect heat. At the same time, the vertical diffusion must slow down to balance the situation. Therefore, the cloud top temperatures at the subsolar point rise to 436°K and the temperature at night drops to 161°K. Clearly horizontal advection of heat must be very important in this layer.

A 52 km deep dust model was run to determine the importance of the non-linear advection terms to the heat transfer process. This model has $\nu_z = 10^3$ cm^2/sec and Prandtl number equal to 1.0, thus making it similar to model 1, which was a linear model.

The $\bar{u}(Z)$ was chosen so as to simulate the shallow circulation seen in model 1. The choice of the constants c and b was made so that $\bar{u}$ = -18 m/sec at 41.6 km and +18 m/sec at 46.8 km. At all other levels $\bar{u}$ is zero. This model took 38 iterations to converge, and since each term of the equations is printed out upon convergence, the predominant terms are easily determined to be

$$\frac{\partial p'}{\partial z} + \rho' g = 0 \tag{24}$$

$$\bar{\rho}\left[\bar{u}\frac{\partial u'}{\partial x} + w'\frac{\partial \bar{u}}{\partial z}\right] + \frac{\partial p'}{\partial x} = 0 \tag{25}$$

$$\frac{\partial u'}{\partial x} + \frac{\partial w'}{\partial z} - \frac{w'}{H_\rho} = 0 \tag{26}$$

$$\bar{u}\left[\frac{\partial T'}{\partial x} - \frac{1}{\rho c_p}\frac{\partial p'}{\partial x}\right] + w'\left[\frac{\partial \bar{T}}{\partial z} + \frac{g}{c_p}\right] - k_z \frac{\partial^2 T'}{\partial z^2} = 0 \tag{27}$$

$$\bar{\rho} T' + \bar{T} \rho' = 0 \tag{28}$$

Again the atmosphere continues to remain hydrostatic as seen in equation (24). Equation (25) shows that both upward and horizontal momentum are balancing the horizontal pressure gradient. The horizontal perturbed velocities are much lower, reducing the magnitude of the eddy viscous mixing terms in this equation. The equation of continuity is not affected. In equation (27) the horizontal advection and the vertical diffusion tend to balance with the horizontal pressure advection and the vertical advection being respectively 1 and 2 orders of magnitude smaller. The resulting circulation is similar to that of model 1 except that the vertical and horizontal perturbation velocities are decreased by a factor of 100, and the circulation is deepened by about 5 km. The circulation speed is decreased because the horizontal transfer of heat tends to balance the downward diffusion, requiring less vertical advection, and a slower vertical velocity creates (by continuity) a slower horizontal at the top boundary. Because of the arbitrary nature of the u(Z) circulation, it would be advantageous to construct a full non-linear model. The cloud top temperatures are within one degree of model one, and no temperature phase effect is evident below the cloud top.

CHAPTER V

CONCLUSIONS

The current data on the static structure of the atmosphere of Venus can be adequately explained by hydrostatic models that assume either non-condensing "dust" clouds or ice (H_2O) clouds. What small difference exists between the two models occurs near the tropopause (52-62 km). The dust model avoids temperatures cold enough to condense 2.4 $^{o}/_{oo}$ water vapor until the mesopause ($\approx$120 km) is reached. The ice cloud model produces water clouds at both the tropopause and the mesopause. Both models will remain as candidates until more convincing data on the nature of the clouds is obtained. A consensus on the surface pressure and temperature is starting to emerge in the literature and the values derived in Chapter III, 87.4 atm and 735.2^{o}K, respectively, are in good agreement with the literature. However, enough relief may exist on the surface of Venus so as to prevent refinements beyond a certain point, until an arbitrary datum is defined.

The cloud models derived in Chapter IV show that a shallow circulation cell develops near the cloud tops, and that the horizontal velocities, vertical velocities, horizontal pressure gradients and horizontal temperature gradients decrease rapidly as the interior of the atmosphere is reached. Thus, by these models the phase effect of temperature in the lower atmosphere is determined to be non-existent and all circulation models based upon this as a driving mechanism are rejected. Moreover, the model developed by Hess (1968) is the only top heated model with which these

results agree. Boussinesq models were found to be similar in structure to compressible models but significantly lower in the velocity of the cloud tops. The ice cloud and dust cloud models were found to produce significantly different circulation speeds, with the former being fastest. Non-linear models were found to produce significantly slower circulation speeds, because of the transport of heat from the day to the night side, whereas the linear models transport downward.

The temperatures of the cloud tops in these models show a large phase effect. These temperatures would cause significant evaporation of the ice cloud tops down to temperatures where equilibrium prevails. Thus, if measurements of the cloud top temperatures by radiometry or spectrometry continue to show constant values and the day values are at higher pressures than at night, then the case for ice clouds will be strengthened. In this case, latent heat must be added to the circulation model. If a phase effect in cloud top temperature has been overlooked, the dust cloud is more probable.

The models have been run with eddy viscosities and diffusivities of 10^3 to 10^4 cm^2/sec in the vertical. Values higher than these were found to cause divergence of the iterative scheme. These values were chosen because they are used to describe some eddy processes on Earth.

Many earlier circulation models have been based on a classical Rayleigh convection assumption that requires penetration of sunlight to the surface. The light level measurements made below the clouds by Venera 5 and 6 cast doubts on the validity of this assumption. The visible imagery to be made by the Venus, Mercury Mariner, 1973 fly-by should help decide this uncertainty. If accurate cloud top temperatures

are measured by this spacecraft, then the circulation models for the Venus atmosphere can be further refined.

APPENDIX A

RADIATION

The unreduced path length (u) in a 100% carbon dioxide atmosphere can be calculated by:

$$u = \frac{P}{g\rho} \tag{A1}$$

where P is the surface pressure, g is the average acceleration of gravity and ρ is the density of CO_2 at STP (1.94×10^{-3} g/cm^3). Using this definition, a surface pressure of 8.737×10^4 mb gives 5×10^7 cm atm or a 500 km thick layer of CO_2 at STP. Data are not available for band models, line strength or widths for these large amounts nor for these high pressures. The best laboratory data that is available in the current literature is for 10^4 cm-atm. However, Bartko and Hanel (1968) have used the available laboratory data and theoretical calculations to derive a fit to a strong line absorption law. They used this model for temperature structure calculations above the Venus cloud tops and Ohring (1969) used it to investigate the greenhouse effect below the cloud tops. In this model the region between 0 and 8000 cm^{-1} is divided into seventeen regions in which the transmission (τ) for the band (r) is given as

$$\tau_r = \exp\left[-(m_r U_r^*)^{n_r}\right] \tag{A2}$$

where m_r and n_r are constants and U_r^* is the reduced path length as defined by

$$U_r^* = 1.66u\ (288.16/T)^{3/2}\ \exp\left[\gamma_r\ (1/288.16 - 1/T\right]^*\left[\frac{1013.25}{p}\right]^{2n_r} \quad (A3)$$

where γ_r is a constant

Using this approach the transmission of a finite layer τ can be calculated

$$\tau = \frac{\int_0^{8000} \tau_\omega\, d\omega}{8000} \quad (A4)$$

Having τ available enables calculations to be made as to the importance of radiation on the Venus atmosphere dynamics. For convenience the lowest 43km of the Venus atmosphere was divided into 10 layers. The transmission of these layers ranges from 2.2×10^{-4} near the surface to .5 near the tropopause. In such an optically thick medium, the Roseland Approximation (Love (1968)) offers an attractive way of simplifying the calculations of the basic state net flux ($\bar{Q}$)

$$\bar{Q} = \frac{-16}{3}\ \sigma\ \bar{T}^3\ \frac{d\bar{T}}{d\tau} \quad (A5)$$

Using this formulation, the basic state temperature structure can be calculated incorporating radiation. The thermodynamics equation for the basic state reduces to:

$$K_z\ \frac{\partial^2 \bar{T}}{\partial z^2} = \frac{\partial \bar{Q}}{\partial z} \quad (A6)$$

Assuming K_z is independent of height allows relatively straightforward calculations of the temperature lapse rate. This was accomplished by programming the Bartko and Hanel (1968) model and using the Roseland

Approximation to solve equation (A6). The minimum thermal conductivity (molecular thermal conductivity) that could be expected for a 100% CO_2 atmosphere at 560°K is about 10^4 ergs/(cm sec °K) (Brokaw (1961)). This will produce the maximum temperature lapse rate ($-\partial T/\partial z$). However, solving equation (A6) for the dust model case reveals that no significant superadiabatic temperature gradients are formed. It is apparent that molecular conductivity alone is sufficient to dissipate energy in the highly opaque atmosphere at a rate high enough so as to not produce instabilities. The fact that motions will likely produce eddy conductivities somewhat higher than 10^4 ergs/(cm sec °K) (10^{-1} cm^2/sec diffusivity) indicates that the lapse rates would be approximately zero. Since this is not observed, then dynamic effects must be predominant over radiation, thus justifying neglecting radiation in the basic state thermodynamic equation. This then requires that the temperature structure be linear (see equation 18) so that

$$\frac{\partial^2 \overline{T}}{\partial z^2} = 0 \qquad \text{(A7)}$$

which can fit the known data indicating an almost adiabatic temperature structure in the lower atmosphere.

APPENDIX B

GOVERNING EQUATIONS AND NUMERICAL METHOD FOR A STEADY STATE TWO DIMENSIONAL CIRCULATION MODEL

The state of an atmospheric circulation will be described in terms of solutions to a complete set of partial differential equations (B-1) through (B-4). This set consists of the equation of motion, continuity, and state, equations (B-1) through (B-3) (Haltiner and Martin (1957), Hess (1959), and Bird et al (1960)) are as follows:

$$\frac{\partial \vec{v}}{\partial t} + (\vec{v}\cdot\nabla)\vec{v} = -\frac{1}{\rho}\nabla p - \vec{g} + \frac{\nabla\cdot\overleftrightarrow{\tau}}{\rho} - 2\vec{\Omega}\times\vec{v} - \vec{\Omega}\times\vec{\Omega}\times\vec{v} \qquad \text{(B-1)}$$

$$\frac{\partial \rho}{\partial t} + \nabla\cdot\rho\vec{v} = 0 \qquad \text{(B-2)}$$

$$p = \frac{\rho R T}{m} \qquad \text{(B-3)}$$

The equation of thermodynamics (Love (1968)) is as follows

$$\rho c_p\left(\frac{\partial T}{\partial t} + (\vec{v}\cdot\nabla)T\right) = \beta T\left(\frac{\partial p}{\partial t} + (\vec{v}\cdot\nabla)p\right) + \nabla\cdot(k\nabla T) + \mu\Phi - \nabla\cdot Q \qquad \text{(B-4)}$$

In these equations, $\vec{v}$ is the vector velocity, t is time, ρ is density, p is pressure, $\vec{g}$ is acceleration due to gravity, $\vec{\Omega}$ is the rotation vector for Venus, $\overleftrightarrow{\tau}$ is the stress tensor, R is the universal gas constant, m is molecular

weight, K is conductivity, μ is viscosity, Φ is the viscous dissipation term, Q is the net radiative flux vector, β is the coefficient of expansion of the gas and c_p is the specific heat of the gas.

In order to solve the two dimensional equatorial circulation, these equations (B-1 through B-4) are written as five scalar equations with five unknowns and are simplified in that a steady state and no rotation (Ω = o) is assumed.

$$\rho u \frac{\partial w}{\partial x} + \rho w \frac{\partial w}{\partial z} = -\frac{\partial p}{\partial z} - g\rho + \frac{\partial}{\partial z}\left(2\mu \frac{\partial w}{\partial z} - \frac{2}{3}\mu \nabla \cdot \vec{u}\right) + \frac{\partial}{\partial x}\left(\mu\left(\frac{\partial u}{\partial z} + \frac{\partial w}{\partial x}\right)\right) \quad \text{(B-5)}$$

$$\rho u \frac{\partial u}{\partial x} + \rho w \frac{\partial u}{\partial z} = -\frac{\partial p}{\partial x} + \frac{\partial}{\partial x}\left(2\mu \frac{\partial u}{\partial x} - \frac{2}{3}\mu \nabla \cdot \vec{u}\right) + \frac{\partial}{\partial z}\left[\mu\left(\frac{\partial u}{\partial z} + \frac{\partial w}{\partial x}\right)\right] \quad \text{(B-6)}$$

$$\frac{\partial(\rho u)}{\partial x} + \frac{\partial(\rho w)}{\partial z} = 0 \quad \text{(B-7)}$$

$$p = \rho T \frac{R}{m} \quad \text{(B-8)}$$

Furthermore, ideal gases have a coefficient of expansion equal to 1/T so assuming the Venus atmosphere is ideal reduces the βT factor in the thermodynamics equation (B-4) to unity.

$$u \frac{\partial T}{\partial x} + w \frac{\partial T}{\partial z} = \frac{1}{\rho c_p}\left[\left(u \frac{\partial p}{\partial x} + w \frac{\partial p}{\partial z}\right) + \frac{\partial}{\partial z}\left(K \frac{\partial T}{\partial z}\right) + \frac{\partial}{\partial x}\left(K \frac{\partial T}{\partial x}\right) + \mu \Phi - \left(\frac{\partial Q}{\partial z} + \frac{\partial Q}{\partial x}\right)\right] \quad \text{(B-9)}$$

In these equations, u is the velocity in the x direction, x is the distance around the planet along a great circle, w is the velocity in the z direction, z is the distance perpendicular to the planet's surface, given as positive

away from the planet, μ and K are the coefficients of viscosity and conductivity, respectively.

Assuming that μ is constant in x and z simplifies the last two terms in each of equations (B-5) and (B-6) to

$$\mu \nabla^2 w + \frac{\mu}{3}\left[\frac{\partial}{\partial z}\left(\nabla \cdot \vec{u}\right)\right]$$

$$\mu \nabla^2 u + \frac{\mu}{3}\left[\frac{\partial}{\partial x}\left(\nabla \cdot \vec{u}\right)\right]$$

respectively

where $\nabla \cdot \vec{u}$ is often referred to as the dilatation or compressibility. The terms expressing the vertical and horizontal gradients of the compressibility are 3 to 4 orders of magnitude smaller than the smallest of other terms, and therefore are neglected. It is also necessary to assume that the variables p, ρ, u, and T are composed of two parts, a slowly varying basic state which is a function of z only, and a small perturbation that is superimposed on the basic field, which is a function of both x and z. The former quantities are denoted by bars over the variable, and the latter by primes. It is assumed that w consists only of a perturbation quantity. These assumptions are:

$$w = w'(x, z) \tag{B-10}$$

$$p = \bar{p}(z) + p'(x, z) \tag{B-11}$$

$$\rho = \bar{\rho}(z) + \rho'(x, z) \tag{B-12}$$

$$T = \bar{T}(z) + T'(x, z) \tag{B-13}$$

$$u = \bar{u}(z) + u'(x, z) \tag{B-14}$$

where $\bar{U}(Z)$ is assumed to be equal to c + bz, c and b being constants.

Since the basic state as determined by:

$$u' = o,\ w' = o,\ p' = o,\ \rho' = o,\ T' = o$$

and equations (B-10) - (B-14) should satisfy equations (B-5) to (B-9), and since w' is required to be zero in the basic state for all x and z, then $\frac{\partial w'}{\partial z}$ and $\frac{\partial w'}{\partial x}$ are also zero. Similar arguments apply to $\frac{\partial u'}{\partial x}$, $\frac{\partial T'}{\partial x}$, $\frac{\partial p'}{\partial x}$, $\frac{\partial \rho'}{\partial x}$, $\frac{\partial^2 w'}{\partial x^2}$, $\frac{\partial^2 w'}{\partial z^2}$, $\frac{\partial^2 T'}{\partial z^2}$, and $\frac{\partial^2 T'}{\partial x^2}$. The divergence of net radiation flux for the basic state in the x direction is zero since the basic state temperature is not a function of x. The divergence of net radiative flux for the basic state in the vertical direction has been calculated using the Bartko and Hanel (1968) non-grey model and the Roseland Approximation. Due to the high opacity of the very dense atmosphere the radiative transfer is extremely small and can be neglected. It is also assumed that the viscous dissipation is negligible.

These assumptions result in the following basic state equations which must hold at all locations throughout the x, z plane.

$$\frac{\partial \bar{p}}{\partial z} = -\bar{\rho}\, g \qquad \text{(B-15)}$$

$$\bar{p} = \bar{\rho}\frac{R}{m}\bar{T} \qquad \text{(B-16)}$$

$$\frac{\partial^2 \bar{T}}{\partial z^2} = 0 \qquad \text{(B-17)}$$

The last of the above equations (B-17) indicates that the basic state temperature profile must always be linear in form, e.g.

$$\bar{T} = a_1 z + T_{low}$$

where a_1 and T_{low} are constants.

Applying these requirements, together with (B-10) to (B-14) on equations (B-5) to (B-9), and neglecting products of primed terms gives the following simplified set of equations for perturbations superimposed on the prespecified basic state,

$$\bar{\rho}\,\bar{u}\frac{\partial w'}{\partial x} + \frac{\partial p'}{\partial z} + \rho' g - \bar{\rho}\,\nu_z \frac{\partial^2 w'}{\partial z^2} - \bar{\rho}\,\nu_x \frac{\partial^2 w'}{\partial x^2} = 0 \qquad \text{(B-18)}$$

$$\bar{\rho}\left[\bar{u}\frac{\partial u'}{\partial x} + w' c\right] + \frac{\partial p'}{\partial x} - \bar{\rho}\,\nu_z \frac{\partial^2 u'}{\partial z^2} - \bar{\rho}\,\nu_x \frac{\partial^2 u'}{\partial x^2} = 0 \qquad \text{(B-19)}$$

$$\frac{\bar{u}}{\bar{\rho}}\frac{\partial \rho'}{\partial x} + \frac{\partial u'}{\partial x} + \frac{\partial w'}{\partial z} - \frac{w'}{H_\rho} = 0 \qquad \text{(B-20)}$$

$$\frac{R}{m}\bar{\rho}\,T' + \frac{R}{m}\bar{T}\rho' = 0 \qquad \text{(B-21)}$$

In equation (B-21) p' is ignored to make the set Anelastic.

$$\bar{u}\left(\frac{\partial T'}{\partial x} - \frac{1}{\bar{\rho} c_p}\frac{\partial p'}{\partial x}\right) + w'\left(\frac{\partial \bar{T}}{\partial z} + \frac{g}{c_p}\right) - k_z \frac{\partial^2 T'}{\partial z^2} - k_x \frac{\partial^2 T'}{\partial x^2} = 0 \qquad \text{(B-22)}$$

ν_x, ν_z, k_x, k_z are the eddy kinematic viscosity and diffusivity, respectively.

Since radiation divergence was found to be small for the basic state, it is assumed to be even smaller for the perturbations.

The ratio of horizontal to vertical scale on Venus is about 900, whose square is 8.1×10^5. Thus, if values of eddy viscosity in the Venus atmosphere are representative of Earth's lower atmosphere ($\nu_z = 10^4$ cm^2/sec and $\nu_x = 10^{10}$ cm^2/sec) then the horizontal eddy terms may be of the same order of magnitude as the vertical terms.

In order to solve the above equations simultaneously, they were set

up in a finite difference form using centered differences for second derivatives and forward differences for gradients. From the author's experience, better convergence of the numerical solution is achieved by this choice of finite difference form, since the equations are more highly coupled about the ij terms. Furthermore, a centered difference scheme would not allow a comparison of the Anelastic and Boussinesq Cases.

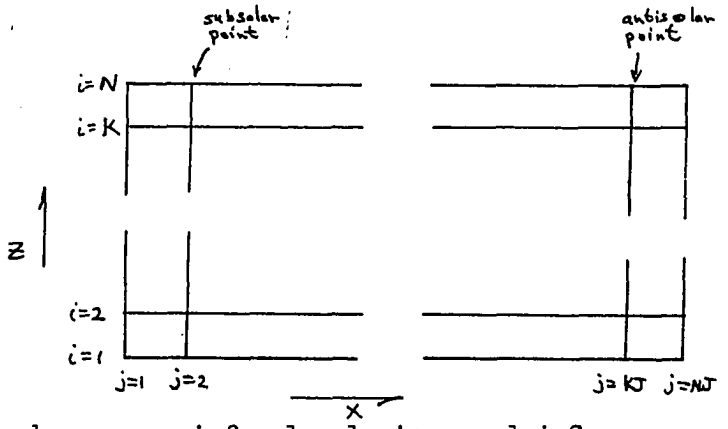

The scheme uses i for levels in z and j for x.

Each differential equation has a residual R which is required to be zero or smaller than an allowable prespecified limit for all i and j when solutions for ρ_{ij}, p_{ij}, u_{ij}, w_{ij}, and T_{ij} are found. The residual equations are

$$\overline{\rho_i}\,\overline{u_i}\left[\frac{w_{i,j+1}-w_{ij}}{\Delta x}\right]+\left(\frac{p_{i+1,j}-p_{ij}}{\Delta z}\right)+\rho_{ij}\,g-\overline{\rho_i}\,\nu_z\left[\frac{w_{i+1,j}-2w_{ij}+w_{i-1,j}}{\Delta z^2}\right] \quad \text{(B-23)}$$
$$-\overline{\rho}\,\nu_x\left[\frac{w_{i,j+1}-2w_{ij}+w_{i,j-1}}{\Delta x^2}\right]=R_1^{\nu}$$

$$\overline{\rho_i}\left[\overline{u_i}\left(\frac{u_{i,j+1}-u_{ij}}{\Delta x}\right)+w_{ij}\frac{\partial \overline{u_i}}{\partial z}\right]+\left(\frac{p_{i,j-1}-p_{ij}}{\Delta x}\right)-\overline{\rho_i}\,\nu_z\left[\frac{u_{i+1,j}-2u_{ij}+u_{i-1,j}}{\Delta z^2}\right] \quad \text{(B-24)}$$
$$-\overline{\rho}\,\nu_x\left[\frac{u_{i,j+1}-2u_{ij}+u_{i,j-1}}{\Delta x^2}\right]=R_2^{\nu}$$

$$\left(\frac{u_{i,j+1}-u_{ij}}{\Delta x}\right)+\left(\frac{w_{i+1,j}-w_{ij}}{\Delta z}\right)-\frac{w_{ij}}{\bar{H}_\rho}+\frac{\bar{u}_i}{\bar{\rho}_i}\left(\frac{\rho_{i,j+1}-\rho_{ij}}{\Delta x}\right)=R_3^{\nu} \qquad \text{(B-25)}$$

$$\bar{u}_i\left[\frac{T_{i,j+1}-T_{ij}}{\Delta x}-\frac{1}{\bar{\rho}_i c_p}\cdot\frac{P_{i,j+1}-P_{ij}}{\Delta x}\right]+w'\left(\frac{\partial\bar{T}_{\omega}}{\partial z}+\frac{g}{c_p}\right) \qquad \text{(B-26)}$$

$$-k_z\left[\frac{T_{i+1,j}-2T_{ij}+T_{i-1,j}}{\Delta z^2}\right]-k_x\left[\frac{T_{i,j+1}-2T_{ij}+T_{i,j-1}}{\Delta x^2}\right]=R_4^{\nu}$$

$$-\frac{R}{m}\bar{\rho}_i T_{ij}-\frac{R}{m}\bar{T}_i\rho_{ij}=R_5^{\nu} \qquad \text{(B-27)}$$

These five equations were programmed on the Univac 1108 at the NASA, Manned Spacecraft Center at Houston, Texas. The residuals are denoted as R_k^{ν} in the equations where the superscript ν indicates the number of the iteration; i.e., R_K^{ν} is the residue at the end of the νth iteration, and k denotes the equation as seen from (B-23) to (B-27). Each residual is expanded to first order in a Taylor series about the νth guess for the dependent variables (p_{ij}, ρ_{ij}, T_{ij}, u_{ij}, W_{ij}) in order to apply a point iterative method such as the Gauss-Seidel scheme (Todd, 1962).

$$R_1^{\nu}=\frac{\partial R_1^{\nu}}{\partial\rho_{ij}}\Delta\rho_{ij}+\frac{\partial R_1^{\nu}}{\partial p_{ij}}\Delta p+0+\frac{\partial R_1^{\nu}}{\partial w_{ij}}\Delta w+0 \qquad \text{(B-28)}$$

$$R_2^\nu = 0 + \frac{\partial R_2^\nu}{\partial p_{ij}} \Delta p_{ij} + \frac{\partial R_2^\nu}{\partial u_{ij}} \Delta u_{ij} + \frac{\partial R_2^\nu}{\partial w_{ij}} \Delta w_{ij} + 0 \qquad \text{(B-29)}$$

$$R_3^\nu = \frac{\partial R_3^\nu}{\partial \rho_{ij}} \Delta \rho_{ij} + 0 + \frac{\partial R_3^\nu}{\partial u_{ij}} \Delta u_{ij} + \frac{\partial R_3^\nu}{\partial w_{ij}} \Delta w_{ij} + 0 \qquad \text{(B-30)}$$

$$R_4^\nu = 0 + \frac{\partial R_4^\nu}{\partial p_{ij}} \Delta p_{ij} + 0 + \frac{\partial R_4^\nu}{\partial w_{ij}} \Delta w_{ij} + \frac{\partial R_4}{\partial T_{ij}} \Delta T_{ij} \qquad \text{(B-31)}$$

$$R_5^\nu = \frac{\partial R_5^\nu}{\partial \rho_{ij}} \Delta \rho_{ij} + 0 + 0 + 0 + \frac{\partial R_5^\nu}{\partial T_{ij}} \Delta T_{ij} \qquad \text{(B-32)}$$

By writing these equations in matrix form they may be solved by finding the inverse to a matrix.

$$\begin{bmatrix} \Delta \rho_{ij} \\ \Delta p_{ij} \\ \Delta u_{ij} \\ \Delta w_{ij} \\ \Delta T_{ij} \end{bmatrix} = \begin{bmatrix} \frac{\partial R_1^\nu}{\partial \rho_{ij}} & \frac{\partial R_1^\nu}{\partial p_{ij}} & 0 & \frac{\partial R_1^\nu}{\partial w_{ij}} & 0 \\ 0 & \frac{\partial R_2^\nu}{\partial p_{ij}} & \frac{\partial R_2^\nu}{\partial u_{ij}} & \frac{\partial R_2^\nu}{\partial w_{ij}} & 0 \\ \frac{\partial R_3^\nu}{\partial \rho_{ij}} & 0 & \frac{\partial R_3^\nu}{\partial u_{ij}} & \frac{\partial R_3^\nu}{\partial w_{ij}} & 0 \\ 0 & \frac{\partial R_4^\nu}{\partial p_{ij}} & 0 & \frac{\partial R_4^\nu}{\partial w_{ij}} & \frac{\partial R_4^\nu}{\partial T_{ij}} \\ \frac{\partial R_5^\nu}{\partial \rho_{ij}} & \frac{\partial R_5^\nu}{\partial p_{ij}} & 0 & 0 & \frac{\partial R_5^\nu}{\partial T_{ij}} \end{bmatrix}^{-1} \begin{bmatrix} R_1 \\ R_2 \\ R_3 \\ R_4 \\ R_5 \end{bmatrix} \qquad \text{(B-33)}$$

The $(\nu+1)$th guesses are obtained using the Gauss-Seidel method

$$\begin{aligned} \rho_{ij}^{\nu+1} &= \rho_{ij}^{\nu} - \Delta \rho_{ij} * c \\ p_{ij}^{\nu+1} &= p_{ij}^{\nu} - \Delta p_{ij} * c \\ u_{ij}^{\nu+1} &= u_{ij}^{\nu} - \Delta u_{ij} * c \\ w_{ij}^{\nu+1} &= w_{ij}^{\nu} - \Delta w_{ij} * c \\ T_{ij}^{\nu+1} &= T_{ij}^{\nu} - \Delta T_{ij} * c \end{aligned} \qquad \text{(B-34)}$$

where c is a convergence constant. The desired solution will be obtained at the limit

$$\lim_{\nu \to \infty} \left(R_k^{\nu} \right) \to 0 \qquad \text{or} \quad \left| R_k^{\nu} \right| \leq \epsilon \text{ (maximum allowable error)}$$

The derivates given in (B-26) are as follows

$$\frac{\partial R_1}{\partial \rho_{ij}} = g \tag{B-35}$$

$$\frac{\partial R_1}{\partial p_{ij}} = \frac{-1}{\Delta z} \tag{B-36}$$

$$\frac{\partial R_1}{\partial w_{ij}} = \frac{2\bar{\rho}_i \nu_z}{\Delta z^2} + \frac{2\bar{\rho}_i \nu_x}{\Delta x^2} - \frac{\bar{\rho}_i \bar{u}_i}{\Delta x} \tag{B-37}$$

$$\frac{\partial R_2}{\partial p_{ij}} = \frac{-1}{\Delta x} \tag{B-38}$$

$$\frac{\partial R_2}{\partial u_{ij}} = \frac{2\bar{\rho}_i \nu_z}{\Delta z^2} + \frac{2\bar{\rho}_i \nu_x}{\Delta x^2} - \frac{\bar{\rho}_i \bar{u}_i}{\Delta x} \tag{B-39}$$

$$\frac{\partial R_3}{\partial u_{ij}} = \frac{-1}{\Delta x} \tag{B-40}$$

$$\frac{\partial R_3}{\partial w_{ij}} = \frac{-1}{\Delta z} - \frac{1}{H_\rho} \tag{B-41}$$

$$\frac{\partial R_4}{\partial w_{ij}} = \frac{\partial \bar{T}_i}{\partial z} + \frac{g}{c_p} \tag{B-42}$$

$$\frac{\partial R_4}{\partial T_{ij}} = \frac{2k_z}{\Delta z^2} + \frac{2k_x}{\Delta x^2} - \frac{\bar{u}_i}{\Delta x} \tag{B-43}$$

$$\frac{\partial R_4}{\partial p_{ij}} = \frac{\bar{u}_i}{\bar{\rho}_i c_p \Delta x} \tag{B-44}$$

$$\frac{\partial R_5}{\partial \rho_{ij}} = -\frac{R}{m}\overline{T}_i \tag{B-45}$$

$$\frac{\partial R_5}{\partial p_{ij}} = 0 \tag{B-46}$$

$$\frac{\partial R_5}{\partial T_{ij}} = -\frac{R}{m}\overline{\rho}_i \tag{B-47}$$

$$\frac{\partial R_3}{\partial \rho_{ij}} = \text{———} \tag{B-48}$$

$$\frac{\partial R_2}{\partial w_{ij}} = \overline{\rho}_i \frac{\partial \overline{u}_i}{\partial z} \tag{B-49}$$

Due to the highly coupled nature of the differential equations, a very complex matrix equation (B-33), results for the new guess algorithm which makes an analytic solution for the convergence criteria extremely difficult. Because of this, a graphical illustration verifying convergence is given as follows, which is based on trial and error success at obtaining a workable convergence criteria.

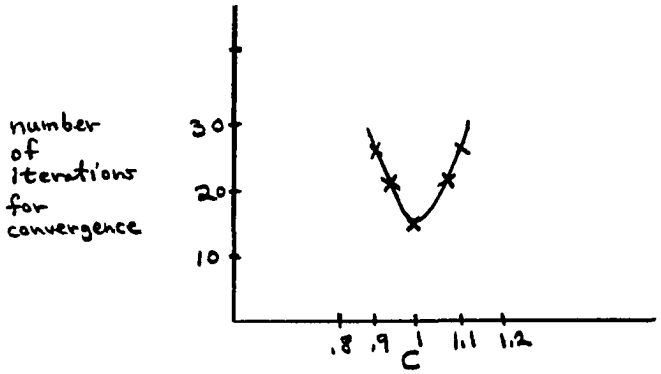

The circulation is assumed to be between j = 2 and j = KJ (please refer to page 59) and represent one half the circumference of the planet; i.e., from sub-solar point to the anti-solar point, respectively. The boundaries on each end are made one finite step away and are used so as to promote

numerical stability for the relaxation method. Thus, for all i

$$\begin{aligned} w'(i,1) &= 0 \\ u'(i,1) &= 0 \\ T'(i,1) &= 0 \end{aligned}$$

$$\begin{aligned} w'(i,KJ) &= 0 \\ u'(i,KJ) &= 0 \\ T'(i,KJ) &= 0 \\ p'(i,KJ) &= 0 \\ \rho'(i,KJ) &= 0 \end{aligned} \qquad \text{(B-50)}$$

Using these restrictions, the values at the boundaries j = 2 and j = KJ can be calculated using the same technique as for the rest of the interior.

The boundary conditions at the top and bottom depend on the case being studied; however, an example (the one used for convergence criteria determination) is included for completeness.

Surface Boundary Condition

It is assumed that no heat flux is lost or gained from the surface of the planet so that

$$g/c_P + \frac{\partial \overline{T}}{\partial z} + \frac{\partial T'}{\partial z} = 0 \qquad \text{(B-51)}$$

that a non slip condition exists

$$u' = 0 \qquad \text{(B-52)}$$

and no vertical wind can penetrate the solid surface

$$w' = 0 \qquad \text{(B-53)}$$

Top Boundary Condition

Likewise, the top boundary has the same assumptions except that a radiative-"conductive" boundary (Love (1968)) is assumed at the cloud top

$$-K\bar{\rho}C_p\left[\frac{g}{C_p}+\frac{\partial(\bar{T}+T')}{\partial z}\right]=\epsilon\sigma(\bar{T}+T')^4-R_\odot(1-A)\cos\gamma \qquad \text{(B-54)}$$

where k is the eddy diffusivity, ϵ is the emissivity of the cloud top, assumed unity for the thermal infrared, and $R_\odot$ is the solar incident flux at the orbit of Venus, 2.667×10^6 ergs/(cm^2 sec), A is the geometric albedo .77 (Irvine (1968)) for Venus, and γ is the phase angle from the sub-solar point. By approximating the diffuse emission from the cloud top by the first two terms of a binomial series

$$\sigma(\bar{T}+T')^4\approx\sigma\bar{T}^4+4\sigma\bar{T}^3T' \qquad \text{(B-55)}$$

and neglecting higher order terms since $\bar{T} \gg T'$

then the T' at the upper boundary can be calculated.

$$T'_{Nj}=\frac{-K\bar{\rho}C_p\left[\frac{\partial\bar{T}}{\partial z}+\frac{g}{C_p}-\frac{T'_{N-1,j}}{\Delta z}\right]-\sigma\bar{T}^4+\sigma(1-.77)R_\odot\cos\gamma}{\frac{K\bar{\rho}C_p}{\Delta z}+4\sigma\bar{T}^3} \qquad \text{(B-56)}$$

$$\gamma=\frac{j-2}{NJ-2}\,2\pi$$

and $\sigma=0$ if $\cos\gamma<0$, night

$\sigma=1$ if $\cos\gamma\geq 0$ day

The pressure at the top boundary is calculated by equation B-23 and the density is calculated employing equation B-27. A slip condition is allowed for U and it is assumed that no vertical velocity exists at the top boundary.

BIBLIOGRAPHY

Anderson, A. D., 1969: Dust in the Lower Atmosphere of Venus. Science, 163, 275-276.

Anderson, C. E. and D. C. Evans, 1962: The Nature of the Venus Cloud System. Institute of Aerospace Sciences, New York, presented at National Summer Meeting, Ambassador Hotel, Los Angeles, California, June 18-22.

Anderson, J. D., G. E. Pease, L. Efron, and R. C. Tausworthe, 1967: Celestial Mechanics Experiment. Science, 1958, 1689-1690.

Anderson, J. D., D. L. Cain, L. Efron, R. M. Goldstein, W.G. Melbourne, D. A. O'Handley, G. E. Pease, R. C. Tausworthe, 1968: The Radius of Venus as Determined by Planetary Radar and Mariner V Radio Tracking Data. J. Atmos. Sci., 25, 1171-1173.

Anon, 1968: Planetary and Lunar Notes from Prague. Sky and Telescope, 35, p. 7.

Ash, A., I. Shapiro, W. Smith, 1967: Astronomical Constants and Planetary Ephemerides Deduced from Radar and Optical Observations. Astron. J., 72, No. 3, April.

Ash, M., D. Campbell, R. Dyce, R. Ingalls, R. Jurgens, G. Pettengill, I. Shapiro, M. Slade, T. Thompson, 1968: The Case for the Radar Radius of Venus. Science, 160, 985-987.

Avduevsky, V. S., M. Ya. Marov, and M. K. Rozhdestvensky, 1968: Model of the Atmosphere of the Planet Venus Based on Results of Measurements made by the Soviet Automatic Interplanetary Station Venera 4. J. Atmos. Sci., 25, 537-545.

Barath, F. T., A. H. Barrett, J. Copeland, D. E. Jones, and A. E. Lilley, 1963: Mariner II: Preliminary Reports on Measurements of Venus, Microwave Radiometers. Science, 139, 905-910.

Barth, C. A., J. B. Pearce, and K. K. Kelly, 1967: Ultraviolet Emissions Observed Near Venus from Mariner V. Science, 158, 1675-1678.

Bartko, F., and R. A. Hanel, 1968: Non-Grey Equilibrium Temperature Distributions above the Clouds of Venus. Ap. J., 151, 365-378.

Belton, M., D. Hunten, 1966: Water Vapor in the Atmosphere of Venus. Ap. J. 146, 307-308.

Belton, M. J. S., A. Lyle Broadfoot, and D. M. Hunten, 1968: Upper Limit to O_2 on Venus. J. Atmos. Sci., 25, p. 582.

Belton, M. J. S., 1969: Theory of the Curve of Growth and Phase Effects in a Cloudy Atmosphere: Applications to Venus, The Venus Atmosphere, edited by R. Jastrow, and S. I. Rasool, Gordon and Breach, New York, p. 604.

Bird, R. B., W. E. Stewart, and E. N. Lightfoot, 1960: Transport Phenomena. John Wiley and Sons, Inc., New York, 780 pp.

Bottema, M., W. Plummer, and J. Strong, 1964: Water Vapor in the Atmosphere of Venus. Ap. J., 139, p. 1021.

Bottema, M., W. Plummer, and J. Strong, 1965: A Quantitative Measurement of Water Vapor in the Atmosphere of Venus. Annales d'Astrophysique, 28, 225-228.

Boyer, C. and H. Carmichel, 1961: Observations Photographiques de la Planete Vénus. Ann. Astroph., 24, 531-535.

Boyer, C. and H. Carmichel, 1965: Etude Photographique de la Rotation de Vénus. C. R. Acad. Sci., 260, 809-810.

Boyer, C., 1965: Recherches sur la Rotation de Vénus. L'Astronomie, 79, 223, 228.

Boyer, C. and P. Guérin, 1966: Mise en Evidence directe, par la Photographie, d'une Rotation Retrograde de Vénus en 4 Jours. C. R. Acad. Sci., 263, 253-255.

Bohachevsky, I. O. and T. T. J. Yeh, 1969: General Circulation in the Atmosphere of Venus Driven by Polar and Diurnal Variations of Surface Temperature. Bellcomm, Inc. Report, TR-69-103-7-2.

Brichant, A. L., 1969: Analysis of Pravda Editorial, 1969: Important Step in the Knowledge of Universe, Soviet Interplanetary Stations Venera 5 and Venera 6: Pravda, No. 155 (18568), June 4, Goddard Space Flight Center, NAS-5-12407.

Bridge, H. S., A. J. Lazarus, C. W. Snyder, E. J. Smith, L. Davis, Jr., P. J. Coleman, Jr., and D. E. Jones, 1967: Mariner V: Plasma and Magnetic Fields Observed Near Venus. Science, 158, 1669-1673.

Brokaw, R. S., 1961: Alignment Charts for Transport Properties Viscosity, Thermal Conductivity and Diffusion Coefficients for Non-Polar Gases and Gas Mixtures at Low Density, NASA TR R-81.

Cameron, A. G. W., 1963: The Origin of the Atmospheres of Venus and the Earth. Icarus, 2, 249-257.

Chamberlain, J. W., 1965: The Atmosphere of Venus Near Her Cloud Tops. Ap. J., 141, 1184-1205.

Chase, S. C., L. D. Kaplan, and G. Neugebauer, 1963: The Mariner 2 Infrared Radiometer Experiment. Jet Propulsion Laboratory Technical Report No. 32-484, 13 pp.

Connes, P., J. Connes, W. S. Benedict, L. D. Kaplan, 1967: Traces of HCl and HF in the Atmosphere of Venus. Ap. J. 147, 1230-1237.

Cruikshank, D. P., and G. P. Kuiper, 1967: Sulphur Compounds in the Atmosphere of Venus. Comm. of Lunar and Planetary Laboratory, 6, 195-200.

Dayhoff, M. O., R. V. Eck, E. R. Lippincott and C. Sagan, 1967: Venus: Atmospheric Evolution, Science 155, 556-558.

de Vaucouleurs, G. and D. H. Menzel, 1960: Results of the Occultation of Regulus by Venus, July 7, 1959. Nature, 188, 28-33.

Deirmendjian, D., 1968: Introductory Comments on Venus's Lower Atmosphere, The Atmospheres of Venus and Mars, ed. by J. C. Brandt and M. B. McElroy, Gordon and Breach, New York, 288 pp.

Dickel, J. R. and W. W. Warnock, 1968: Lack of Phase Variation on Venus. Nature, 220, 1183-1185.

Dollfus, A., 1955: Étude Visuelle et Photographique de l'Atmosphere de Venus. L'Astronomie, 69, 413-425.

Eckman, P. K. and C. W. Cole, 1969: Mariner Venus/Mercury 1973 Study. Jet Propulsion Laboratory Technical Memorandum 33-434.

Eshleman, V. R., G. Fjeldbo, J. D. Anderson, A. Kliore, and R. B. Dyce, 1968: Venus: Lower Atmosphere. Nat. Measured Science, 162, 661-665.

Evans, D. E., D. E. Pitts, and G. L. Kraus, 1967: Venus and Mars Nominal Natural Environment for Advanced Manned Planetary Mission Programs. National Aeronautics and Space Administration SP-3016, 52 pp.

Evans, J. V., R. A. Brockelman, J. C. Henry, G. M. Hyde, L. G. Kraft, W. A. Reid, 1965: Radio Echo Observations of Venus and Mercury at 23 cm Wavelength. Astron. J., 70, 486-501.

Fountain, J., and S. Larson, 1969: UV Photographs of Venus Taken with the 61-inch NASA Telescope, 1967. Comm. of the Lunar and Planetary Laboratory, 6, 264-274.

Ginzburg, A. S., and E. M. Feigelson, 1969: Some Optical Properties of the Atmosphere of Venus and the Condition of Radiative Equilibrium. Cosmic Research 7, 230-237.

Goldstein, R. M., 1964: Venus Characteristics by Earth-Based Radar. Astron. J., 69, 12-18.

Goldstein, R. M., 1966: Radar Studies of Venus. COSPAR, International Space Science Symposium, 7th, Vienna, Austria, May 10-19, 1966, available as A66-29955.

Goldreich, P. and S. J. Peale, 1966: Resonant Rotation for Venus. Nature, 209, 1117-1118.

Goody, R., 1965: The Structure of the Venus Cloud Veil. J. Geophys. Res., 70, 5471-5481.

Goody, R. M., and A. R. Robinson, 1966: A Discussion of the Deep Circulation of the Atmosphere of Venus. Ap. J., 146, 339-355.

Gray, L. D., R. A. Schorn, and E. Baker, 1969: High Dispersion Spectroscopic Observations of Venus IV: The Weak Carbon Dioxide Band at 7883 Å. Applied Optics, 8, 2087-2093.

Haltiner, G. J., and F. L. Martin, 1957: Dynamical and Physical Meteorology. McGraw-Hill Book Co., New York, 470 pp.

Hansen, J. E., and S. Matsushima, 1967: The Atmosphere and Surface Temperature of Venus A Dust Insolation Model. Ap. J., 150, 1139-1157.

Hartman, W. K., 1969: Multicolor Photography of Venus, 1962. Comm. of the Lunar and Planetary Laboratory, 6, 266-264.

Hess, S. L., 1959: Introduction to Theoretical Meteorology, Henry Haltand Co., New York, 362 pp.

Hess, S. L., 1968: The Hydrodynamics of Mars and Venus, The Atmospheres of Venus and Mars, ed. by J. C. Brandt and M. B. McElroy, Gordon and Breach, New York, 288 pp.

Hilsenrath, J., H. J. Hoge, C. W. Beckett, J. F.Masi, W. S. Benedict, R. L. Nattal, L. Fono, Y. S. Touloukian, H. W. Woolley, 1955: Tables of Thermal Properties of Gases. National Bureau Standards Circular 564.

Hunten, D. M., and M. B. McElroy, 1968: The Upper Atmosphere of Venus: The Regulus Occultation Reconsidered. J. Geophys. Res., 73, 4446-4448.

Hunten, D. M., 1968: The Structure of the Lower Atmosphere of Venus, J. Geophys. Res., 73, 1093-1095.

Hunten, D. M. and R. M. Goody, 1969: Venus: The Next Phase of Planetary Exploration, Science, 26, 1317-1323.

Irvine, W. M., 1968: Monochromatic Phase Curves and Albedos for Venus. J. Atm. Sci., 25, 610-616.

Jones, H. S., 1964: Dimension and Rotation. Appearing in Kuiper, G. P., 1964: The Earth as a Planet. Chicago, The Univ. of Chicago Press, 751 pp.

Kaplan, L. D., 1962: A Preliminary Model of the Venus Atmosphere. Jet Propulsion Laboratory Technical Report No. 32-379, 5 pp.

Keene, G. T., 1968: Venus: Uniformity of Clouds, and Photography. Science, 159, p. 305.

Keldysh, M. L., 1967: Press Conference of Soviet and Foreign Journalist anent "Venera-4", Izvestia, 257, 15651, 31 October.

Kerzhanovich, V. V., V. M. Gotlib, N. V. Chetyrkin, and B. N. Andreev, 1969: Results of Determining the Dynamics of the Atmosphere of Venus from Data of Measurements of the Radial Velocity of the Interplanetary Probe "Venera-4". Cosmic Research, 7, pp. 536-540.

Kliore, A., G. S. Levy, D. L. Cain, G. Fjeldbo, and S. I. Rasoal, 1967: Atmosphere and Ionosphere of Venus from the Mariner V S-Band Radio Occultation Measurement. Science, 158, 1683-1688.

Kliore, A., D. L. Cain, G. S. Levy, G. Fjeldbo, and S. I. Rasoal, 1969: Structure of the Atmosphere of Venus Derived from Mariner V S-Band Measurements. Space Research IX, North-Holland Publishing Company, Amsterdam, 1969.

Koenig, L. R., F. W. Murray, C. M. Michaux, and H. A. Hyatt, 1967: Handbook of the Physical Properties of the Planet Venus. National Aeronautics and Space Administration SP-3029, 132 pp.

Kuiper, G. P., J. W. Fountain, and S. M. Larson, 1969a: Photographs of Venus Taken with the 8-2 inch Telescope at McDonald Observatory, 1950-1956. Comm. of the Lunar and Planetary Laboratory, 6, 251-262.

Kuiper, G. P., F. F. Forbes, D. L. Steinmetz, R. I. Mitchell, 1969b: High Altitude Spectra from NASA CV-990 Jet, II Water Vapor on Venus. Comm. of Lunar and Planetary Laboratory, 6, 200-228.

Kuiper, G. P., 1969: Identification of the Venus Cloud Layers. Comm. of Lunar and Planetary Laboratory, 6, 229-250.

Libby, W. F., 1968: Ice Caps on Venus? Science, 159, 1097, 1098.

List, R. J., 1963: Smithsonian Meteorological Tables, Smithsonian Institution, Washington, D. C., 527 pp.

Love, T. J., 1968: Radiative Heat Transfer, Charles E. Merrill Publ. Co., Columbus, Ohio, 287 pp.

Luming, M., 1968: A Review of Interpretations of the Mariner V - Venera 4 Discrepancy on the Venus Neutral Atmosphere. Bellcomm, Inc. TM 68-1014-7.

Mariner Stanford Group, 1967: Venus: Ionosphere and Atmosphere as Measured by Dual-Frequency Radio Occultation of Mariner V. Science, 158, 1678-1683.

Martin, C. D., 1969: Venus Mean Model Atmospheres. North American Rockwell Corp. SD 69-707.

McElroy, M. B., 1968: The Upper Atmosphere of Venus. J. Geophys. Res., 73, 1513-1521.

Melbourne, W. G., D. O. Muhleman, and D. A. O'Handley, 1968: Radar Determination of the Radius of Venus. Science, 160, 987-989.

Menzel, D. H., and F. L. Whipple, 1955: The Case for H_2O Clouds on Venus. J. Astron. Soc. of Pacific, 67, 161-168.

Mikhnevitch, V. V., and V. A. Sokolov, 1968: Temperature and Density of the Venus According to Measurement Results Obtained on "Venera-4". The 9th session of COSPAR, Tokyo, Japan, 25 pp.

Mintz, Y., 1961: Temperature and Circulation of the Venus Atmosphere. Planetary and Space Science, 5, 141-152.

Murray, B. C., R. L. Wildey, and J. A. Westphal, 1963: Infrared Photographic Mapping of Venus through the 8-14 micron Atmospheric Window. J. Geophys. Res. 68, 4813-4818.

Ohring, G., 1966: Water-Vapor Mixing Ratios Near the Cloudtops of Venus. Icarus, 5, 329-333.

Ohring, G., 1969: High Surface Temperature on Venus: Evaluation of the Greenhouse Exploration. Icarus, 11, 171-179.

Ohring, G. and J. Mariano, 1963: The Effect of Cloudiness on a Greenhouse Model of the Venus Atmosphere. Geophysics Corp. of America Report 63-17-N.

Ohring, G., W. Tong, and J. Mariano, 1965. Planetary Meteorology, NASA CR-280.

Opik, E. J., 1961: The Aeolosphere and Atmosphere of Venus. J. Geoph. Res. 66, 2807-2819.

Owen, R. B., 1965: Theoretical Model Atmosphere of Venus. NASA, TND-2527, Jan., N65-14117.

Owen, T., 1969: Spectroscopic Observations of Venus. IITRI Final Report NAS R-65/26.

Palm, A., 1969: The Evolution of Venus' Atmosphere. Planet. Space Sci., 17, 1021-1028.

Pitts, D. E., 1968a: A Discussion of Environment for Manned Planetary Missions. Supplement to AIAA Technology for Manned Planetary Missions Meeting, New Orleans, March 4-6, 1968, 101-103.

Pitts, D. E., 1968b: A Computer Program for Calculating Model Planetary Atmospheres. NASA TND-4292.

Pitts, D. E., 1969: A Model Atmosphere for Earth Resources Applications. NASA TMX-58033.

Pollack, J. B., and C. Sagan, 1967: A Critical Test of the Electrical Discharge Model of the Venus Microwave Emission. Ap. J., 150, 699-706.

Pollack, J. B., and C. Sagan, 1967: An Analysis of the Mariner 2 Microwave Observations of Venus. Ap. J., 150, 327-344.

Pollack, J. B., and C. Sagan, 1968: The Case for Ice Clouds on Venus. J. Geophys. Res., 73, 5943-5949.

Pollack, J. B., and A. T. Wood, Jr., 1968: Venus: Implication from Microwave Spectroscopy of the Atmospheric Water Content. Science, 161, 1125-1127.

Reese, D. E., P. R. Swan, 1968: Venera 4 Probes Atmosphere of Venus. Science, 159, 1228-1230.

Ross, F. E., 1928: Photographs of Venus. (Contri. of Mt. Wilson, No. 363), Ap. J., 68, 57-92.

Sagan, C., 1961: The Planet Venus. Science, 133, 849-858.

Sagan, C., and J. B. Pollack, 1965: The Microwave Phase Effect of Venus. Icarus 4, 62-103.

Sagan, C., and B. Pollack, 1967: Anisotropic Nonconservative Scattering and the Clouds of Venus. J. Geophys. Res., 72, 469-477.

Schiffer, R. A., 1968: Models of Venus Atmosphere, 1968: NASA SP-8011.

Shapiro, I. I., 1964: Quoted in Astronomical Notes from Hamburg. Sky and Telescope, 28, December, p. 341.

Shapiro, I. I., 1968: Rotation of Venus. Science, 159, p. 1124.

Sinton, W. M., and J. Strong, 1960: Radiometric Observations of Venus. Ap. J., 131, 470-490.

Slipher, E. C., 1964: A Photographic Study of the Brighter Planets. Lowell Observatory, Flagstaff, Arizona.

Smith, B. A., 1967: Rotation of Venus: Continuing Contradictions. Science, 158, 114-116.

Snyder, C. W., 1967: Mariner V Flight Past Venus. Science, 158, 1665-1668.

Spinrad, H., 1962: A Search for Water Vapor and Trace Constituents in the Venus Atmosphere. JPL Report 32-256.

Spinrad, H., 1962: Spectroscopic Temperature and Pressure Measurements in the Venus Atmosphere. Publ. of the Astron. Soc. Pac., 74, 187-201.

Spinrad, H., 1966: Resolution of a CO_2 Hot Band in the Venus Spectrum, Ap. J., 145, p. 943.

Spinrad, H., E. Richardson, 1965: An Upper Limit to the Molecular Oxygen Content in the Venus Atmosphere. Ap. J., 141, p. 282.

Spinrad, H., and S. Shawl, 1966: Water Vapor on Venus - A Confirmation. Ap. J., 146, p. 328.

Spinrad, H., and L. Trafton, 1963: High Dispersion Spectra of the Outer Planets. I, Jupiter in the Visual and Red. Icarus, 2, 19-28.

Stone, P. H., 1968: Some Properties of Hadley Regimes on Rotating and Non-Rotating Planets. J. of Atm. Sci., 25, 644-657.

Strelkov, G. M., 1968: Venusian Emissions Near 1.35 cm. Astronomicheskii Vestnik, 2, 217-228.

Strelkov, G. M., and N. F. Kukharskaya, 1969: The Greenhouse Effect in the Atmosphere of Venus. Cosmic Research, 7, 221-229.

Strong, J., 1965: Infrared Astronomy by Balloon. Scientific American, 212, 28-37.

Tass, 1967: Soviet Interplanetary Station "Venus 4". Pravda, No. 295 (17977), 22 October.

Thaddeus, P., 1968: The Dry Massive Model of the Atmosphere of Venus and the Microwave Phase Effect, in The Atmospheres of Venus and Mars, ed. by J. C. Brandt and M. B. McElroy, Gordon and Breach Science Publishers, New York, 288 pp.

Todd, J. (editor), 1962: A Survey of Numerical Analysis. McGraw-Hill Book Co., New York, p. 589.

Van Allen, J. A., S. M. Krimgis, L. A. Frank, and T. P. Armstrong, 1967: Venus: An Upper Limit on Intrinsic Magnetic Dipole Moment Based on Absence of a Radiation Belt. Science, 158, 1673-1675.

Vinogradov, A. P., U. A. Surkov, and C. P. Florensky, 1968: The Chemical Composition of the Venus Atmosphere Based on the Data of the Interplanetary Station Venera 4. J. Atmos. Sci., 25, 535-536.

Walker, R. G., and C. Sagan, 1966: The Ionospheric Model of the Venus Microwave Emission: An Obituary. Icarus 5, 105-123.

Welch, W. J., and D. C. Rea, 1967: Upper Limits on Liquid Water in the Venus Atmosphere. Astron. J., 148, L151-L454.

Westphal, J. A., R. L. Wildey, and B. C. Murray, 1965: The 8-14 Micron Appearance of Venus Before the 1964 Conjunction. Ap. J., 142, 799-802.

Whitten, R. C., 1969: Thermal Structure of the Ionosphere of Venus. J. Geophy. Res., 74, 5623-5628.

Wood, A. T., Jr., R. B. Watson, and J. B. Pollack, 1968: Venus: Estimates of the Surface Temperature and Pressure from Radio and Radar Measurements. Science, 162, 114-116.

Wright, W. H., 1927: Photographs of Venus Made by Infrared and by Violet Light. Pub. A.S.P., 39, 220-221.

Wyatt, S. P., 1964: Principles of Astronomy. Boston, Allyn and Bacon, Inc., 561 pp.

Zander, R., 1965: Recents Resultats Spatiaux Par Ballons Stratospheriques. Ciel et Terre, 81, 155-156.

TABLE 1

Venus Atmosphere Composition and Structure from Venera 4, after Vinogradov et al (1968) and from Mariner V, after Kliore et al (1969) using a 90% CO_2 atmosphere

Venera 4

Altitude (km)	Temperature (°C)	Pressure (mm Hg)	Component	Results (volume %)
26 ± 1	25 ± 10	550	CO_2	> 1
			CO_2	90 ± 10
			N_2	< 7
			O_2	> 0.4
			H_2O	≥ 0.1
19 ± 1 km	90 ± 10	1550	CO_2	> 30
			CO_2	> 1
			N_2	≤ 2.5
			$O_2 + (H_2O)$	< 1.6
			H_2O	> 0.05
			H_2O	< 0.7

Mariner V

Radius from Center (km)	P (mb)	T (°K)
6140	1.0	241
6123	28.4	241
6101	1239	334
6088.5	5146	445
6085	7170	477

TABLE 2

Minor Constituents of the Venus Atmosphere
as Determined from Earth

Component	Mole Fraction	Source
NH_3	$< 3 \times 10^{-7}$	Kuiper (1969)
H_2O	< 125μ precipitable	Belton and Hunten (1966)
H_2O	10^{-6}	Kuiper (1969)
H_2O	2.5×10^{-4} (222μ precipitable)	Bottema et al (1965)
H_2O	60μ precipitable	Spinrad and Shawl (1966)
O_2	$< 4 \times 10^{-5}$	Belton (1968)
HCl	10^{-6}	Connes et al (1967)
HF	10^{-8}	"
CH_4	10^{-6}	"
COS	10^{-6}	"
SO_2	$< 2.5 \times 10^{-8}$	Cruikshank (1967)
H_2S	$< 2 \times 10^{-4}$	"

TABLE 3

Venus Atmosphere Composition and Structure
from Venera 5 & 6, after Brichant (1969)

Venera 5 Composition Measurements Occurred at:

Temperature	Pressure
25°C	0.6 atm
150°C	5 atm

Venera 6 Composition Measurements Occurred at:

60°C	1 atm
225°C	10 atm

Component	Volume Percent
CO_2	93 - 97
N_2 + inert	2 - 5
O_2	< 0.4
H_2O	4-11 mg/liter

TABLE 4

A Downward Adiabatic Extrapolation to Find the Surface Pressure and Temperature

RADIUS	Z	PRESSURE	TEMP	DTDZ	HRHO	ES	E
km	km	mb	K°	K°/km	km	mb	mb
	-49.	2.445+05	861.91	6.99	21.60		
	-49.	2.379+05	858.40	7.01	21.52		
	-48.	2.315+05	854.89	7.02	21.44		
	-48.	2.252+05	851.38	7.03	21.36		
	-47.	2.191+05	847.85	7.05	21.27		
	-47.	2.131+05	844.32	7.06	21.19		
	-46.	2.072+05	840.78	7.08	21.11		
	-46.	2.015+05	837.24	7.09	21.03		
	-45.	1.960+05	833.69	7.10	20.95		
	-45.	1.905+05	830.13	7.12	20.87		
	-44.	1.852+05	826.56	7.13	20.78		
	-44.	1.800+05	822.99	7.14	20.70		
	-43.	1.749+05	819.41	7.16	20.62		
	-43.	1.700+05	815.83	7.17	20.54		
	-42.	1.652+05	812.23	7.19	20.45		
	-42.	1.604+05	808.63	7.20	20.37		
	-41.	1.559+05	805.03	7.21	20.29		
	-41.	1.514+05	801.41	7.23	20.20		
	-40.	1.470+05	797.79	7.24	20.12		
	-40.	1.427+05	794.16	7.25	20.03		
	-39.	1.386+05	790.53	7.27	19.95		
	-39.	1.345+05	786.89	7.28	19.86		
	-38.	1.305+05	783.24	7.29	19.78		
	-38.	1.267+05	779.59	7.31	19.69		
	-38.	1.229+05	775.93	7.32	19.60		
6048	-37.	1.193+05	772.26	7.34	19.52		
	-36.	1.157+05	768.59	7.35	19.43		
	-36.	1.122+05	764.90	7.36	19.35		
	-35.	1.088+05	761.22	7.38	19.26		
	-35.	1.055+05	757.52	7.39	19.17		
	-34.	1.023+05	753.82	7.41	19.09		
	-34.	9.913+04	750.11	7.42	19.00		
	-33.	9.607+04	746.39	7.43	18.91		
	-33.	9.309+04	742.66	7.45	18.83		
	-32.	9.019+04	738.93	7.46	18.74		
6053	-32.	8.737+04	735.19	7.48	18.65		
	-31.	8.462+04	731.45	7.49	18.56		
	-31.	8.194+04	727.69	7.51	18.47		
	-30.	7.934+04	723.93	7.52	18.39		
	-30.	7.680+04	720.16	7.54	18.30		
	-29.	7.433+04	716.38	7.55	18.21		
6056	-29.	7.193+04	712.60	7.57	18.12		
	-28.	6.960+04	708.80	7.59	18.03		
	-28.	6.733+04	705.00	7.60	17.94		
	-27.	6.512+04	701.19	7.62	17.85		
	-27.	6.297+04	697.38	7.63	17.76		
	-26.	6.088+04	693.55	7.65	17.67		
	-26.	5.885+04	689.72	7.67	17.58		
	-25.	5.688+04	685.88	7.68	17.49		
	-25.	5.496+04	682.03	7.70	17.40		
	-24.	5.310+04	678.17	7.72	17.31		
	-24.	5.129+04	674.30	7.73	17.22		
	-23.	4.953+04	670.42	7.75	17.13		
	-23.	4.783+04	666.54	7.77	17.03		
	-22.	4.617+04	662.65	7.79	16.94		

-22.	4.456+04	658.74	7.80	16.85		
-21.	4.300+04	654.83	7.82	16.76		
-21.	4.148+04	650.91	7.84	16.66		
-20.	4.001+04	646.98	7.86	16.57		
-20.	3.858+04	643.04	7.88	16.48		
-19.	3.719+04	639.10	7.89	16.38		
-19.	3.585+04	635.14	7.91	16.29		
-18.	3.455+04	631.18	7.93	16.20		
-18.	3.328+04	627.20	7.95	16.10		
-17.	3.206+04	623.22	7.97	16.01		
-17.	3.087+04	619.22	7.99	15.91		
-16.	2.972+04	615.22	8.01	15.82		
-16.	2.860+04	611.21	8.02	15.72		
-15.	2.752+04	607.19	8.04	15.63		
-15.	2.648+04	603.15	8.06	15.53		
-14.	2.546+04	599.11	8.08	15.43		
-14.	2.448+04	595.06	8.10	15.34		
-13.	2.353+04	591.00	8.12	15.24		
-13.	2.262+04	586.93	8.14	15.14		
-13.	2.173+04	582.84	8.16	15.05		
-12.	2.087+04	578.75	8.19	14.95		
-11.	2.004+04	574.65	8.21	14.85		
-11.	1.923+04	570.53	8.23	14.75		
-10.	1.845+04	566.41	8.25	14.66		
-10.	1.770+04	562.27	8.27	14.56		
-9.	1.698+04	558.13	8.29	14.46		
-9.	1.628+04	553.97	8.32	14.36		
-8.	1.560+04	549.80	8.34	14.26		
-8.	1.495+04	545.62	8.36	14.16		
-8.	1.431+04	541.43	8.39	14.06		
-7.	1.371+04	537.22	8.41	13.96		
-6.	1.312+04	533.00	8.43	13.86		
-6.	1.255+04	528.77	8.46	13.76		
-5.	1.200+04	524.53	8.48	13.65		
-5.	1.148+04	520.28	8.51	13.55		
-4.	1.097+04	516.01	8.54	13.45		
-4.	1.048+04	511.73	8.56	13.35		
-3.	1.001+04	507.43	8.59	13.24		
-3.	9.555+03	503.13	8.61	13.14		
-3.	9.118+03	498.81	8.64	13.04		
-2.	8.697+03	494.48	8.67	12.93		
-1.	8.293+03	490.13	8.69	12.83		
-1.	7.904+03	485.77	8.72	12.72		
-1.	7.530+03	481.39	8.75	12.62		
.0	7.170+03	477.00	8.78	12.62	1.693+04	1.000+3n
.5	6.824+03	472.61	8.78	12.40	1.545+04	1.000+3n
1.0	6.493+03	468.20	8.81	12.29	1.406+04	1.000+3n
1.5	6.174+03	463.78	8.84	12.19	1.277+04	1.000+3n
2.0	5.868+03	459.35	8.87	12.08	1.157+04	1.000+3n
2.5	5.575+03	454.90	8.90	11.97	1.046+04	1.000+3n
3.0	5.293+03	450.43	8.93	11.86	9.434+03	1.000+3n
3.5	5.023+03	445.95	8.96	11.76	8.484+03	1.000+3n
4.0	4.765+03	441.45	9.00	11.65	7.610+03	1.000+3n
4.5	4.517+03	436.94	9.03	11.54	6.806+03	1.000+3n
5.0	4.280+03	432.40	9.07	11.43	6.068+03	1.000+3n
5.5	4.053+03	427.85	9.10	11.32	5.394+03	1.000+3n
6.0	3.836+03	423.28	9.14	11.21	4.778+03	1.000+3n
6.5	3.628+03	418.70	9.17	11.10	4.219+03	1.000+3n

7.0	3.429+03	414.09	9.21	10.99	3.711+03	1.000+3n
7.5	3.239+03	409.47	9.25	10.87	3.253+03	1.000+3n
8.0	3.058+03	404.83	9.28	10.76	2.839+03	5.316+0?
8.5	2.885+03	400.17	9.32	10.65	2.468+03	2.426+0?
9.0	2.720+03	395.49	9.36	10.54	2.136+03	1.499+0?
9.5	2.562+03	390.79	9.40	10.42	1.841+03	1.044+0?
10.0	2.412+03	386.07	9.44	10.31	1.578+03	7.749+0?
10.5	2.269+03	381.33	9.49	10.19	1.346+03	5.974+0?
11.0	2.133+03	376.56	9.53	10.08	1.143+03	4.722+0?
11.5	2.003+03	371.77	9.58	9.96	9.641+02	3.797+0?
12.0	1.880+03	366.96	9.62	9.84	8.087+02	3.089+0?
12.5	1.763+03	362.13	9.67	9.73	6.741+02	2.534+0?
13.0	1.652+03	357.27	9.71	9.61	5.582+02	2.090+0?
13.5	1.546+03	352.39	9.76	9.49	4.591+02	1.729+0?
14.0	1.446+03	347.48	9.81	9.37	3.748+02	1.432+0?
14.5	1.351+03	342.55	9.86	9.25	3.036+02	1.187+0?
15.0	1.261+03	337.59	9.92	9.13	2.439+02	9.817+01
15.5	1.176+03	332.61	9.97	9.01	1.942+02	8.101+01
16.0	1.095+03	327.59	10.03	8.88	1.532+02	6.661+01
16.5	1.019+03	322.55	10.08	8.76	1.197+02	5.451+01
17.0	9.468+02	317.48	10.14	8.64	9.256+01	4.435+01
17.5	8.789+02	312.38	10.20	8.51	7.076+01	3.584+01
18.0	8.148+02	307.25	10.26	8.39	5.346+01	2.874+01
18.5	7.545+02	302.08	10.33	8.26	3.988+01	2.285+01
19.0	6.976+02	296.89	10.39	8.13	2.935+01	1.798+01
19.5	6.442+02	291.66	10.45	8.00	2.129+01	1.399+01
20.0	5.940+02	286.40	10.52	7.87	1.521+01	1.076+01
20.5	5.469+02	281.11	10.58	7.74	1.069+01	8.159+0n
21.0	5.027+02	275.79	10.65	7.61	7.376+00	6.096+0n
21.5	4.613+02	270.42	10.73	7.48	4.995+00	4.480+0n
22.0	4.227+02	265.02	10.80	7.34	3.312+00	3.233+0n
22.5	3.865+02	259.58	10.88	7.21	2.148+00	2.288+0n
			CONDENSATION AT PREVIOUS LEVEL			
23.0	3.529+02	255.99	7.18	6.44	1.596+00	1.840+0n
23.5	3.218+02	252.21	7.57	6.41	1.155+00	1.474+0n
24.0	2.930+02	248.20	8.01	6.38	8.098-01	1.135+0n
24.5	2.664+02	243.96	8.49	6.35	5.483-01	8.444-01
25.0	2.417+02	239.46	8.99	6.32	3.567-01	6.050-01
25.5	2.190+02	234.72	9.49	6.27	2.220-01	4.155-01
26.0	1.979+02	229.72	9.99	6.22	1.316-01	2.724-01
26.5	1.785+02	224.50	10.44	6.16	7.405-02	1.699-01
27.0	1.606+02	219.08	10.84	6.08	3.941-02	1.005-01
27.5	1.441+02	213.49	11.18	5.98	1.979-02	5.621-0?
28.0	1.289+02	207.76	11.46	5.86	9.331-03	2.963-0?
28.5	1.150+02	201.92	11.68	5.73	4.113-03	1.465-0?
29.0	1.022+02	195.99	11.86	5.59	1.682-03	6.738-0?
29.5	9.050+01	189.96	12.06	5.45	6.291-04	2.846-03
30.0	7.983+01	183.87	12.17	5.30	2.131-04	1.093-0?
30.5	7.011+01	177.73	12.28	5.13	6.408-05	3.741-04
31.0	6.130+01	171.55	12.37	4.97	1.662-05	1.110-04
31.5	5.334+01	165.32	12.46	4.80	3.564-06	2.736-05
32.0	4.615+01	159.05	12.54	4.63	5.949-07	5.276-0A
32.5	3.971+01	152.73	12.63	4.46	7.050-08	7.268-07
33.0	3.394+01	146.37	12.72	4.28	5.168-09	6.232-0A
33.5	2.882+01	139.97	12.80	4.10	1.896-10	2.693-09
34.0	2.427+01	133.53	12.88	3.93	2.506-12	4.226-11
34.5	2.028+01	127.05	12.96	3.74	7.144-15	1.442-13
35.0	1.678+01	120.53	13.04	3.56	1.955-18	4.771-17

TABLE 5

H_2O Ice Cloud Basic State Model of Venus Atmosphere

MODEL ATMOSPHERE FOR VENUS ICECLOUD

CONSTRUCTION PARAMETERS SCIENTIFIC UNITS DATE 3/18/70

SURFACE PRESSURE = 87370.00 MB
BASE OF EXOSPHERE = 1000.00(KM)
RADIUS OF VENUS = 6053.00(KM)
PERCENT OXYGEN = .000
PERCENT HYDROGEN = .000
PERCENT CO = .000

SURFACE TEMPERATURE = 735.20 K
MOLECULAR WEIGHT = 44.010
PERCENT NITROGEN = .000
PERCENT ARGON = .000
PERCENT HELIUM = .000
PERCENT SO2 = .000

SURFACE DENSITY = 6.29-02 GM/CC
SURFACE GRAVITY = 887.000 CM/SEC/SEC
PERCENT CO2 = 100.000
PERCENT NEON = .000
PERCENT WATER = .000

TEMPERATURE AND MOLECULAR WEIGHT DISTRIBUTION,

AT	55.00	GEOP KM	TEMPERATURE=	259.58 K	AND MOLECULAR WEIGHT=	44.01000
AT	65.00	GEOP KM	TEMPERATURE=	207.76 K	AND MOLECULAR WEIGHT=	44.01000
AT	115.00	GEOP KM	TEMPERATURE=	165.00 K	AND MOLECULAR WEIGHT=	44.01000
AT	125.00	GEOP KM	TEMPERATURE=	210.00 K	AND MOLECULAR WEIGHT=	44.01000
AT	135.00	GEOP KM	TEMPERATURE=	210.00 K	AND MOLECULAR WEIGHT=	44.01000
AT	145.00	GEOP KM	TEMPERATURE=	400.00 K	AND MOLECULAR WEIGHT=	44.01000
AT	195.00	GEOP KM	TEMPERATURE=	710.00 K	AND MOLECULAR WEIGHT=	42.00000
AT	250.00	GEOP KM	TEMPERATURE=	710.00 K	AND MOLECULAR WEIGHT=	24.00000
AT	1000.00	GEOM KM	TEMPERATURE=	710.00 K	AND MOLECULAR WEIGHT=	1.00000

CALCULATED QUANTITIES

HEIGHT (KM)	TEMP (K)	PRESSURE (MB)	DENSITY (GM/CC)	SPEED OF SOUND (M/SEC)	MOLECULAR WEIGHT	DENS SCALE (KM)	S.HTX RATIO (GM/KGM)	MEAN FREE PATH (M)	VIS- COSITY (E+5)	PRES SCALE (KM)	MEAN PARTICLE VELOCITY (M/SEC)	COLL FREQ (PER SEC)	COLUMNAR MASS
0	735.2	8.74+04	6.29-02	489.	44.0	19.19	0.00	1.67-09	3.16	15.66	595.	3.55+11	0.000
1	726.6	8.19+04	5.97-02	486.	44.0	18.98	0.00	1.76-09	3.13	15.48	591.	3.35+11	6.128+03
2	717.9	7.68+04	5.66-02	484.	44.0	18.76	0.00	1.86-09	3.11	15.30	588.	3.16+11	1.194+04
3	709.3	7.19+04	5.37-02	481.	44.0	18.54	0.00	1.96-09	3.08	15.12	584.	2.98+11	1.745+04
4	700.6	6.73+04	5.08-02	479.	44.0	18.32	0.00	2.07-09	3.06	14.94	581.	2.80+11	2.267+04
5	692.0	6.29+04	4.81-02	476.	44.0	18.10	0.00	2.19-09	3.02	14.76	577.	2.64+11	2.762+04
6	683.4	5.87+04	4.55-02	474.	44.0	17.88	0.00	2.31-09	2.99	14.58	573.	2.48+11	3.230+04
7	674.7	5.48+04	4.30-02	472.	44.0	17.66	0.00	2.45-09	2.96	14.40	570.	2.33+11	3.672+04
8	666.1	5.11+04	4.06-02	469.	44.0	17.44	0.00	2.59-09	2.93	14.22	566.	2.18+11	4.090+04
9	657.5	4.76+04	3.84-02	467.	44.0	17.22	0.00	2.75-09	2.90	14.05	562.	2.05+11	4.485+04
10	648.9	4.43+04	3.62-02	465.	44.0	17.00	0.00	2.91-09	2.87	13.87	559.	1.92+11	4.857+04
11	640.2	4.12+04	3.41-02	462.	44.0	16.78	0.00	3.09-09	2.84	13.69	555.	1.80+11	5.209+04
12	631.6	3.83+04	3.21-02	460.	44.0	16.56	0.00	3.28-09	2.81	13.51	551.	1.68+11	5.539+04
13	623.0	3.56+04	3.02-02	457.	44.0	16.34	0.00	3.49-09	2.78	13.33	547.	1.57+11	5.851+04
14	614.4	3.30+04	2.84-02	455.	44.0	16.12	0.00	3.71-09	2.75	13.15	544.	1.47+11	6.144+04
15	605.8	3.05+04	2.67-02	452.	44.0	15.89	0.00	3.95-09	2.72	12.97	540.	1.37+11	6.419+04
16	597.2	2.83+04	2.50-02	450.	44.0	15.67	0.00	4.20-09	2.69	12.79	536.	1.27+11	6.678+04
17	588.6	2.61+04	2.35-02	448.	44.0	15.45	0.00	4.48-09	2.66	12.61	532.	1.19+11	6.920+04
18	580.0	2.41+04	2.20-02	445.	44.0	15.23	0.00	4.79-09	2.63	12.43	528.	1.10+11	7.148+04
19	571.4	2.22+04	2.06-02	443.	44.0	15.01	0.00	5.11-09	2.61	12.25	524.	1.03+11	7.361+04
20	562.8	2.05+04	1.93-02	440.	44.0	14.79	0.00	5.47-09	2.58	12.07	520.	9.52+10	7.560+04
21	554.2	1.88+04	1.80-02	437.	44.0	14.57	0.00	5.85-09	2.55	11.89	516.	8.82+10	7.746+04
22	545.6	1.73+04	1.68-02	435.	44.0	14.35	0.00	6.27-09	2.52	11.71	512.	8.17+10	7.920+04
23	537.1	1.59+04	1.57-02	432.	44.0	14.13	0.00	6.73-09	2.49	11.53	508.	7.55+10	8.082+04
24	528.5	1.46+04	1.46-02	430.	44.0	13.91	0.00	7.23-09	2.46	11.35	504.	6.98+10	8.233+04

25	519.9	1.33+04	1.36-02	347.	44.0	13.69	0.00	7.77-09	2.43	11.16	500.	6.44+10	8.373+04
26	511.3	1.22+04	1.26-02	344.	44.0	13.46	0.00	8.36-09	2.40	10.98	496.	5.93+10	8.504+04
27	502.8	1.11+04	1.17-02	342.	44.0	13.24	0.00	9.01-09	2.37	10.80	492.	5.46+10	8.625+04
28	494.2	1.01+04	1.08-02	339.	44.0	13.02	0.00	9.73-09	2.34	10.62	488.	5.01+10	8.738+04
29	485.6	9.19+03	1.00-02	336.	44.0	12.80	0.00	1.05-08	2.30	10.44	483.	4.60+10	8.842+04
30	477.1	8.35+03	9.26-03	333.	44.0	12.58	0.00	1.14-08	2.27	10.26	479.	4.21+10	8.938+04
31	468.5	7.56+03	8.55-03	331.	44.0	12.36	0.00	1.23-08	2.23	10.08	475.	3.85+10	9.027+04
32	459.9	6.84+03	7.88-03	328.	44.0	12.14	0.00	1.34-08	2.19	9.90	470.	3.52+10	9.109+04
33	451.4	6.18+03	7.25-03	325.	44.0	11.91	0.00	1.45-08	2.16	9.72	466.	3.21+10	9.185+04
34	442.8	5.57+03	6.66-03	322.	44.0	11.69	0.00	1.58-08	2.12	9.54	462.	2.92+10	9.254+04
35	434.3	5.01+03	6.11-03	319.	44.0	11.47	0.00	1.72-08	2.09	9.36	457.	2.65+10	9.318+04
36	425.7	4.50+03	5.59-03	316.	44.0	11.25	0.00	1.88-08	2.05	9.18	453.	2.40+10	9.377+04
37	417.2	4.03+03	5.11-03	314.	44.0	11.03	0.00	2.06-08	2.02	8.99	448.	2.17+10	9.430+04
38	408.6	3.60+03	4.67-03	311.	44.0	10.80	3.05+03	2.26-08	1.99	8.81	443.	1.96+10	9.479+04
39	400.1	3.21+03	4.25-03	308.	44.0	10.58	1.35+03	2.48-08	1.95	8.63	439.	1.77+10	9.523+04
40	391.6	2.86+03	3.86-03	305.	44.0	10.36	7.97+02	2.73-08	1.91	8.45	434.	1.59+10	9.564+04
41	383.0	2.53+03	3.50-03	302.	44.0	10.14	5.27+02	3.01-08	1.87	8.27	429.	1.43+10	9.601+04
42	374.5	2.24+03	3.17-03	299.	44.0	9.91	3.69+02	3.32-08	1.82	8.09	424.	1.28+10	9.634+04
43	366.0	1.98+03	2.86-03	295.	44.0	9.69	2.66+02	3.68-08	1.78	7.91	420.	1.14+10	9.664+04
44	357.4	1.74+03	2.58-03	292.	44.0	9.47	1.95+02	4.08-08	1.74	7.72	415.	1.02+10	9.691+04
45	348.9	1.53+03	2.32-03	289.	44.0	9.25	1.44+02	4.54-08	1.70	7.54	410.	9.01+09	9.716+04
46	340.4	1.34+03	2.08-03	286.	44.0	9.02	1.07+02	5.07-08	1.66	7.36	405.	7.98+09	9.736+04
47	331.9	1.16+03	1.86-03	283.	44.0	8.80	7.88+01	5.67-08	1.62	7.18	400.	7.04+09	9.757+04
48	323.4	1.01+03	1.65-03	279.	44.0	8.58	5.80+01	6.36-08	1.58	7.00	394.	6.20+09	9.775+04
49	314.9	8.75+02	1.47-03	276.	44.0	8.35	4.19+01	7.16-08	1.55	6.82	389.	5.43+09	9.791+04
50	306.4	7.54+02	1.30-03	273.	44.0	8.13	2.98+01	8.09-08	1.51	6.63	384.	4.75+09	9.804+04
51	297.9	6.47+02	1.15-03	269.	44.0	7.91	2.07+01	9.16-08	1.47	6.45	379.	4.13+09	9.817+04
52	289.4	5.53+02	1.01-03	266.	44.0	7.68	1.41+01	1.04-07	1.43	6.27	373.	3.58+09	9.827+04
53	280.9	4.70+02	8.86-04	262.	44.0	7.46	9.37+00	1.19-07	1.38	6.09	368.	3.09+09	9.837+04
54	272.4	3.98+02	7.73-04	259.	44.0	7.24	6.02+00	1.36-07	1.34	5.90	362.	2.66+09	9.845+04
55	263.9	3.35+02	6.72-04	255.	44.0	7.01	3.74+00	1.57-07	1.30	5.72	356.	2.27+09	9.852+04
56	254.5	2.80+02	5.83-04	251.	44.0	6.92	2.07+00	1.81-07	1.26	5.52	350.	1.94+09	9.859+04
57	244.4	2.33+02	5.05-04	247.	44.0	6.81	1.00+00	2.09-07	1.21	5.30	343.	1.64+09	9.864+04
58	234.2	1.92+02	4.35-04	242.	44.0	6.52	4.49-01	2.42-07	1.17	5.08	336.	1.39+09	9.869+04
59	224.0	1.57+02	3.72-04	237.	44.0	6.24	1.83-01	2.83-07	1.12	4.86	328.	1.16+09	9.873+04
60	213.9	1.27+02	3.15-04	232.	44.0	5.96	6.67-02	3.34-07	1.08	4.65	321.	9.61+08	9.876+04
61	207.5	1.02+02	2.61-04	229.	44.0	5.24	3.58-02	4.03-07	1.05	4.51	316.	7.84+08	9.879+04
62	206.7	8.20+01	2.10-04	229.	44.0	4.57	4.03-02	5.01-07	1.05	4.49	315.	6.29+08	9.881+04
63	205.9	6.56+01	1.69-04	228.	44.0	4.55	4.53-02	6.24-07	1.05	4.48	315.	5.04+08	9.883+04
64	205.2	5.25+01	1.35-04	228.	44.0	4.54	5.10-02	7.78-07	1.04	4.46	314.	4.04+08	9.885+04
65	204.4	4.19+01	1.09-04	228.	44.0	4.52	5.74-02	9.70-07	1.04	4.45	314.	3.23+08	9.886+04
66	203.6	3.35+01	8.70-05	227.	44.0	4.51	6.45-02	1.21-06	1.04	4.43	313.	2.59+08	9.887+04
67	202.9	2.67+01	6.97-05	227.	44.0	4.49	7.26-02	1.51-06	1.03	4.42	312.	2.07+08	9.888+04
68	202.1	2.13+01	5.57-05	227.	44.0	4.48	8.16-02	1.89-06	1.03	4.40	312.	1.65+08	9.888+04
69	201.4	1.70+01	4.46-05	226.	44.0	4.46	9.17-02	2.36-06	1.03	4.39	311.	1.32+08	9.889+04
70	200.6	1.35+01	3.56-05	226.	44.0	4.45	1.03-01	2.96-06	1.02	4.37	311.	1.05+08	9.889+04
71	199.8	1.07+01	2.84-05	225.	44.0	4.43	1.16-01	3.71-06	1.02	4.36	310.	8.37+07	9.890+04
72	199.1	8.53+00	2.27-05	225.	44.0	4.41	1.30-01	4.65-06	1.01	4.34	309.	6.66+07	9.890+04
73	198.3	6.77+00	1.81-05	225.	44.0	4.40	1.46-01	5.83-06	1.01	4.33	309.	5.30+07	9.890+04
74	197.6	5.37+00	1.44-05	224.	44.0	4.38	1.64-01	7.32-06	1.00	4.31	308.	4.21+07	9.890+04
75	196.8	4.26+00	1.14-05	224.	44.0	4.37	1.84-01	9.20-06	1.00	4.30	308.	3.34+07	9.890+04
76	196.1	3.37+00	9.10-06	223.	44.0	4.35	2.06-01	1.16-05	.99	4.28	307.	2.65+07	9.890+04
77	195.3	2.67+00	7.23-06	223.	44.0	4.34	2.32-01	1.46-05	.99	4.27	307.	2.10+07	9.891+04
78	194.5	2.11+00	5.74-06	223.	44.0	4.32	2.60-01	1.84-05	.98	4.25	306.	1.67+07	9.891+04
79	193.8	1.67+00	4.55-06	222.	44.0	4.31	2.91-01	2.31-05	.97	4.24	305.	1.32+07	9.891+04
80	193.0	1.32+00	3.61-06	222.	44.0	4.29	3.26-01	2.92-05	.97	4.22	305.	1.04+07	9.891+04
81	192.3	1.04+00	2.86-06	221.	44.0	4.28	3.65-01	3.69-05	.96	4.21	304.	8.25+06	9.891+04
82	191.5	8.18-01	2.26-06	221.	44.0	4.26	4.09-01	4.66-05	.96	4.19	304.	6.51+06	9.891+04

83	190.8	6.44-01	1.79-06	221.	44.0	4.25	4.58-01	5.90-05	.95	4.17	303.	5.14+06	9.891+04
84	190.0	5.06-01	1.41-06	220.	44.0	4.23	5.12-01	7.47-05	.95	4.16	302.	4.05+06	9.891+04
85	189.2	3.98-01	1.11-06	220.	44.0	4.21	5.73-01	9.46-05	.94	4.14	302.	3.19+06	9.891+04
86	188.5	3.13-01	8.78-07	219.	44.0	4.20	6.40-01	1.20-04	.94	4.13	301.	2.51+06	9.891+04
87	187.7	2.45-01	6.91-07	219.	44.0	4.18	7.15-01	1.52-04	.93	4.11	301.	1.97+06	9.891+04
88	187.0	1.92-01	5.44-07	218.	44.0	4.17	7.99-01	1.94-04	.93	4.10	300.	1.55+06	9.891+04
89	186.2	1.51-01	4.28-07	218.	44.0	4.15	8.91-01	2.46-04	.92	4.08	299.	1.22+06	9.891+04
90	185.5	1.18-01	3.36-07	218.	44.0	4.14	9.94-01	3.13-04	.92	4.07	299.	9.53+05	9.891+04
91	184.7	9.21-02	2.64-07	217.	44.0	4.12	1.11+00	3.99-04	.91	4.05	298.	7.47+05	9.891+04
92	184.0	7.19-02	2.07-07	217.	44.0	4.11	1.23+00	5.09-04	.91	4.04	297.	5.84+05	9.891+04
93	183.2	5.61-02	1.62-07	216.	44.0	4.09	1.37+00	6.50-04	.90	4.02	297.	4.57+05	9.891+04
94	182.4	4.37-02	1.27-07	216.	44.0	4.07	1.53+00	8.30-04	.90	4.01	296.	3.57+05	9.891+04
95	181.7	3.41-02	9.92-08	216.	44.0	4.06	1.70+00	1.06-03	.89	3.99	296.	2.79+05	9.891+04
96	180.9	2.65-02	7.75-08	215.	44.0	4.04	1.89+00	1.36-03	.89	3.98	295.	2.17+05	9.891+04
97	180.2	2.06-02	6.05-08	215.	44.0	4.03	2.10+00	1.74-03	.88	3.96	294.	1.69+05	9.891+04
98	179.4	1.60-02	4.72-08	214.	44.0	4.01	2.33+00	2.23-03	.88	3.95	294.	1.32+05	9.891+04
99	178.7	1.24-02	3.68-08	214.	44.0	4.00	2.58+00	2.86-03	.87	3.93	293.	1.02+05	9.891+04
100	177.9	9.62-03	2.86-08	213.	44.0	3.98	2.86+00	3.68-03	.87	3.92	293.	7.95+04	9.891+04
105	174.2	2.65-03	8.05-09	211.	44.0	3.90	4.68+00	1.31-02	.84	3.84	289.	2.21+04	9.891+04
110	170.4	7.11-04	2.21-09	209.	44.0	3.83	7.47+00	4.77-02	.82	3.76	286.	6.00+03	9.891+04
115	166.7	1.86-04	5.90-10	207.	44.0	3.75	1.15+01	1.79-01	.80	3.69	283.	1.59+03	9.891+04
120	177.0	4.87-05	1.46-10	213.	44.0	3.58	0.00	7.24-01	.86	3.92	292.	4.03+02	9.891+04
125	198.6	1.46-05	3.90-11	225.	44.0	4.02	0.00	2.70+00	1.01	4.41	309.	1.14+02	9.891+04
130	210.0	4.92-06	1.24-11	230.	44.0	4.67	0.00	8.49+00	1.06	4.67	318.	3.75+01	9.891+04
135	210.0	1.69-06	4.25-12	230.	44.0	4.67	0.00	2.48+01	1.06	4.67	318.	1.28+01	9.891+04
140	244.9	5.98-07	1.29-12	247.	44.0	3.89	0.00	8.15+01	1.22	5.46	343.	4.21+00	9.891+04
145	335.5	2.75-07	4.33-13	284.	44.0	5.33	0.00	2.43+02	1.64	7.49	402.	1.65+00	9.891+04
150	408.5	1.52-07	1.96-13	311.	44.0	8.02	0.00	5.36+02	1.99	9.15	444.	8.27-01	9.891+04
155	438.0	8.96-08	1.08-13	322.	43.8	8.65	0.00	9.73+02	2.10	9.87	460.	4.73-01	9.891+04
160	467.5	5.49-08	6.16-14	332.	43.6	9.27	0.00	1.69+03	2.23	10.59	477.	2.82-01	9.891+04
165	496.9	3.48-08	3.66-14	342.	43.4	9.90	0.00	2.84+03	2.35	11.33	492.	1.73-01	9.891+04
170	526.2	2.27-08	2.24-14	352.	43.2	10.54	0.00	4.61+03	2.45	12.07	508.	1.10-01	9.891+04
175	555.5	1.52-08	1.41-14	362.	43.0	11.18	0.00	7.28+03	2.55	12.82	523.	7.19-02	9.891+04
180	584.8	1.04-08	9.16-15	372.	42.8	11.83	0.00	1.12+04	2.65	13.58	538.	4.81-02	9.891+04
185	614.0	7.27-09	6.07-15	381.	42.6	12.48	0.00	1.68+04	2.75	14.34	552.	3.28-02	9.891+04
190	643.1	5.17-09	4.11-15	390.	42.4	13.14	0.00	2.47+04	2.85	15.11	566.	2.29-02	9.891+04
195	672.3	3.75-09	2.83-15	399.	42.2	13.80	0.00	3.57+04	2.95	15.89	580.	1.63-02	9.891+04
200	701.3	2.76-09	1.99-15	408.	42.1	14.47	0.00	5.06+04	3.06	16.68	594.	1.17-02	9.891+04
210	710.0	1.55-09	1.03-15	424.	39.4	15.87	0.00	9.11+04	3.08	18.09	618.	6.78-03	9.891+04
220	710.0	9.12-10	5.62-16	442.	36.3	16.90	0.00	1.55+05	3.08	19.67	643.	4.15-03	9.891+04
230	710.0	5.61-10	3.16-16	461.	33.3	18.02	0.00	2.52+05	3.08	21.53	672.	2.67-03	9.891+04
240	710.0	3.60-10	1.85-16	484.	30.3	19.24	0.00	3.92+05	3.08	23.77	705.	1.80-03	9.891+04
250	710.0	2.42-10	1.12-16	510.	27.2	20.53	0.00	5.85+05	3.08	26.49	743.	1.27-03	9.891+04
260	710.0	1.69-10	6.95-17	541.	24.2	21.86	0.00	8.35+05	3.08	29.87	788.	9.44-04	9.891+04
270	710.0	1.22-10	4.89-17	547.	23.7	29.35	0.00	1.16+06	3.08	30.67	797.	6.87-04	9.891+04
280	710.0	8.82-11	3.49-17	551.	23.3	29.84	0.00	1.60+06	3.08	31.22	803.	5.01-04	9.891+04
290	710.0	6.42-11	2.50-17	555.	23.0	30.35	0.00	2.20+06	3.08	31.79	809.	3.67-04	9.891+04
300	710.0	4.70-11	1.80-17	560.	22.6	30.86	0.00	3.01+06	3.08	32.37	815.	2.71-04	9.891+04
310	710.0	3.46-11	1.31-17	564.	22.3	31.39	0.00	4.08+06	3.08	32.98	821.	2.01-04	9.891+04
320	710.0	2.56-11	9.53-18	568.	22.0	31.93	0.00	5.51+06	3.08	33.59	827.	1.50-04	9.891+04
330	710.0	1.91-11	6.99-18	573.	21.6	32.48	0.00	7.40+06	3.08	34.23	834.	1.13-04	9.891+04
340	710.0	1.43-11	5.15-18	577.	21.3	33.05	0.00	9.89+06	3.08	34.89	840.	8.50-05	9.891+04
350	710.0	1.08-11	3.82-18	582.	20.9	33.63	0.00	1.31+07	3.08	35.56	847.	6.45-05	9.891+04
360	710.0	8.14-12	2.84-18	587.	20.6	34.23	0.00	1.74+07	3.08	36.26	854.	4.92-05	9.891+04
370	710.0	6.19-12	2.13-18	592.	20.3	34.84	0.00	2.28+07	3.08	36.97	861.	3.78-05	9.891+04
380	710.0	4.74-12	1.60-18	597.	19.9	35.47	0.00	2.98+07	3.08	37.71	868.	2.91-05	9.891+04
390	710.0	3.65-12	1.21-18	602.	19.6	36.11	0.00	3.88+07	3.08	38.47	876.	2.26-05	9.891+04
400	710.0	2.82-12	9.20-19	607.	19.3	36.77	0.00	5.01+07	3.08	39.26	883.	1.76-05	9.891+04

TABLE 6

Dust Cloud Basic State Model of Venus Atmosphere

MODEL ATMOSPHERE FOR VENUS DUST

CONSTRUCTION PARAMETERS SCIENTIFIC UNITS DATE 3/18/70

SURFACE PRESSURE = 87370.00 MB
BASE OF EXOSPHERE = 1000.00(KM)
RADIUS OF VENUS = 6053.00(KM)
PERCENT OXYGEN = .000
PERCENT HYDROGEN = .000
PERCENT CO = .000

SURFACE TEMPERATURE = 735.20 K
MOLECULAR WEIGHT = 44.010
PERCENT NITROGEN = .000
PERCENT ARGON = .000
PERCENT HELIUM = .000
PERCENT SO2 = .000

SURFACE DENSITY = 6.29-02 GM/CC
SURFACE GRAVITY = 887.000 CM/SEC/SEC
PERCENT CO2 = 100.000
PERCENT NEON = .000
PERCENT WATER = .000

TEMPERATURE AND MOLECULAR WEIGHT DISTRIBUTION,

AT	52.00	GEOP KM	TEMPERATURE=	286.40 K	AND MOLECULAR	WEIGHT=	44.01000
AT	115.00	GEOP KM	TEMPERATURE=	165.00 K	AND MOLECULAR	WEIGHT=	44.01000
AT	125.00	GEOP KM	TEMPERATURE=	210.00 K	AND MOLECULAR	WEIGHT=	44.01000
AT	135.00	GEOP KM	TEMPERATURE=	210.00 K	AND MOLECULAR	WEIGHT=	44.01000
AT	145.00	GEOP KM	TEMPERATURE=	400.00 K	AND MOLECULAR	WEIGHT=	44.01000
AT	195.00	GEOP KM	TEMPERATURE=	710.00 K	AND MOLECULAR	WEIGHT=	42.00000
AT	250.00	GEOP KM	TEMPERATURE=	710.00 K	AND MOLECULAR	WEIGHT=	24.00000
AT	1000.00	GEOM KM	TEMPERATURE=	710.00 K	AND MOLECULAR	WEIGHT=	1.00000

CALCULATED QUANTITIES

HEIGHT (KM)	TEMP (K)	PRESSURE (MB)	DENSITY (GM/CC)	SPEED OF SOUND (M/SEC)	MOLECULAR WEIGHT	DENS SCALE (KM)	S.MIX RATIO (GM/KGM)	MEAN FREE PATH (M)	VIS-COSITY (E+5)	PRES SCALE (KM)	MEAN PARTICLE VELOCITY (M/SEC)	COLL FREQ (PER SEC)	COLUMNAR MASS
0	735.2	8.74+04	6.29-02	409.	44.0	19.18	0.00	1.67-09	3.16	15.66	595.	3.55+11	0.000
1	726.6	8.19+04	5.97-02	406.	44.0	18.97	0.00	1.76-09	3.13	15.48	591.	3.35+11	6.128+03
2	717.9	7.68+04	5.66-02	404.	44.0	18.75	0.00	1.86-09	3.11	15.30	588.	3.16+11	1.194+04
3	709.3	7.19+04	5.37-02	401.	44.0	18.53	0.00	1.96-09	3.08	15.12	584.	2.98+11	1.745+04
4	700.7	6.73+04	5.08-02	399.	44.0	18.31	0.00	2.07-09	3.06	14.94	581.	2.80+11	2.267+04
5	692.1	6.29+04	4.81-02	396.	44.0	18.09	0.00	2.19-09	3.02	14.76	577.	2.64+11	2.762+04
6	683.5	5.87+04	4.55-02	394.	44.0	17.87	0.00	2.31-09	2.99	14.59	573.	2.48+11	3.230+04
7	674.9	5.48+04	4.30-02	392.	44.0	17.65	0.00	2.45-09	2.96	14.41	570.	2.33+11	3.672+04
8	666.2	5.11+04	4.06-02	389.	44.0	17.43	0.00	2.59-09	2.93	14.23	566.	2.18+11	4.090+04
9	657.6	4.76+04	3.83-02	387.	44.0	17.21	0.00	2.75-09	2.90	14.05	562.	2.05+11	4.485+04
10	649.0	4.43+04	3.62-02	385.	44.0	16.99	0.00	2.91-09	2.87	13.87	559.	1.92+11	4.857+04
11	640.4	4.12+04	3.41-02	382.	44.0	16.77	0.00	3.09-09	2.84	13.69	555.	1.80+11	5.208+04
12	631.8	3.83+04	3.21-02	380.	44.0	16.55	0.00	3.28-09	2.81	13.51	551.	1.68+11	5.539+04
13	623.2	3.56+04	3.02-02	377.	44.0	16.33	0.00	3.49-09	2.78	13.33	548.	1.57+11	5.850+04
14	614.6	3.30+04	2.84-02	375.	44.0	16.11	0.00	3.71-09	2.75	13.15	544.	1.47+11	6.143+04
15	606.1	3.05+04	2.67-02	373.	44.0	15.89	0.00	3.95-09	2.72	12.97	540.	1.37+11	6.418+04
16	597.5	2.83+04	2.50-02	370.	44.0	15.67	0.00	4.21-09	2.69	12.79	536.	1.27+11	6.677+04
17	588.9	2.61+04	2.35-02	368.	44.0	15.45	0.00	4.48-09	2.66	12.61	532.	1.19+11	6.919+04
18	580.3	2.41+04	2.20-02	365.	44.0	15.23	0.00	4.79-09	2.64	12.43	528.	1.10+11	7.147+04
19	571.7	2.22+04	2.06-02	363.	44.0	15.01	0.00	5.11-09	2.61	12.25	524.	1.03+11	7.360+04
20	563.2	2.05+04	1.93-02	360.	44.0	14.79	0.00	5.47-09	2.58	12.07	521.	9.52+10	7.559+04
21	554.6	1.88+04	1.80-02	358.	44.0	14.57	0.00	5.85-09	2.55	11.89	517.	8.82+10	7.745+04
22	546.0	1.73+04	1.68-02	355.	44.0	14.35	0.00	6.27-09	2.52	11.71	513.	8.17+10	7.919+04
23	537.4	1.59+04	1.57-02	352.	44.0	14.13	0.00	6.73-09	2.49	11.53	508.	7.56+10	8.081+04
24	528.9	1.46+04	1.46-02	350.	44.0	13.91	0.00	7.23-09	2.46	11.35	504.	6.98+10	8.232+04
25	520.3	1.33+04	1.36-02	347.	44.0	13.69	0.00	7.77-09	2.43	11.17	500.	6.44+10	8.372+04

26	511.8	1.22+04	1.26-02	344.	44.0	13.47	0.00	8.36-09	2.40	10.99	496.	5.93+10	8.503+04
27	503.2	1.11+04	1.17-02	342.	44.0	13.25	0.00	9.01-09	2.37	10.81	492.	5.46+10	8.624+04
28	494.7	1.01+04	1.08-02	339.	44.0	13.03	0.00	9.73-09	2.34	10.63	488.	5.01+10	8.737+04
29	486.1	9.20+03	1.00-02	336.	44.0	12.81	0.00	1.05-08	2.30	10.45	484.	4.60+10	8.841+04
30	477.6	8.36+03	9.26-03	334.	44.0	12.59	0.00	1.14-08	2.27	10.27	479.	4.21+10	8.937+04
31	469.0	7.57+03	8.55-03	331.	44.0	12.37	0.00	1.23-08	2.23	10.09	475.	3.86+10	9.026+04
32	460.5	6.85+03	7.88-03	328.	44.0	12.14	0.00	1.34-08	2.20	9.91	471.	3.52+10	9.108+04
33	451.9	6.19+03	7.25-03	325.	44.0	11.92	0.00	1.45-08	2.16	9.73	466.	3.21+10	9.184+04
34	443.4	5.58+03	6.66-03	322.	44.0	11.70	0.00	1.58-08	2.13	9.55	462.	2.92+10	9.253+04
35	434.9	5.02+03	6.11-03	320.	44.0	11.48	0.00	1.72-08	2.09	9.37	457.	2.65+10	9.317+04
36	426.3	4.51+03	5.60-03	317.	44.0	11.26	0.00	1.88-08	2.06	9.19	453.	2.41+10	9.376+04
37	417.8	4.04+03	5.12-03	314.	44.0	11.04	0.00	2.06-08	2.02	9.01	448.	2.18+10	9.429+04
38	409.3	3.61+03	4.67-03	311.	44.0	10.82	3.53+03	2.26-08	1.99	8.83	444.	1.97+10	9.478+04
39	400.8	3.22+03	4.25-03	308.	44.0	10.59	1.46+03	2.48-08	1.96	8.65	439.	1.77+10	9.523+04
40	392.2	2.86+03	3.87-03	305.	44.0	10.37	8.43+02	2.72-08	1.91	8.46	434.	1.59+10	9.563+04
41	383.7	2.54+03	3.51-03	302.	44.0	10.15	5.52+02	3.00-08	1.87	8.28	430.	1.43+10	9.600+04
42	375.2	2.25+03	3.17-03	299.	44.0	9.93	3.84+02	3.32-08	1.83	8.10	425.	1.28+10	9.633+04
43	366.7	1.99+03	2.87-03	296.	44.0	9.71	2.77+02	3.67-08	1.79	7.92	420.	1.14+10	9.663+04
44	358.2	1.75+03	2.58-03	293.	44.0	9.48	2.03+02	4.08-08	1.74	7.74	415.	1.02+10	9.691+04
45	349.7	1.53+03	2.32-03	289.	44.0	9.26	1.50+02	4.54-08	1.70	7.56	410.	9.04+09	9.715+04
46	341.2	1.34+03	2.08-03	286.	44.0	9.04	1.11+02	5.06-08	1.66	7.38	405.	8.00+09	9.737+04
47	332.7	1.17+03	1.86-03	283.	44.0	8.82	8.19+01	5.66-08	1.63	7.20	400.	7.07+09	9.757+04
48	324.2	1.02+03	1.66-03	280.	44.0	8.59	6.04+01	6.35-08	1.59	7.01	395.	6.22+09	9.774+04
49	315.7	8.79+02	1.47-03	276.	44.0	8.37	4.37+01	7.14-08	1.55	6.83	390.	5.45+09	9.790+04
50	307.2	7.58+02	1.31-03	273.	44.0	8.15	3.11+01	8.06-08	1.51	6.65	384.	4.77+09	9.804+04
51	298.7	6.51+02	1.15-03	270.	44.0	7.93	2.17+01	9.13-08	1.48	6.47	379.	4.15+09	9.816+04
52	290.2	5.56+02	1.01-03	266.	44.0	7.70	1.49+01	1.04-07	1.43	6.29	374.	3.60+09	9.827+04
53	285.4	4.74+02	8.79-04	264.	44.0	6.91	1.27+01	1.20-07	1.41	6.18	371.	3.09+09	9.836+04
54	283.5	4.03+02	7.53-04	263.	44.0	6.41	1.32+01	1.40-07	1.40	6.15	369.	2.64+09	9.845+04
55	281.6	3.42+02	6.43-04	263.	44.0	6.37	1.37+01	1.64-07	1.39	6.11	368.	2.25+09	9.852+04
56	279.7	2.90+02	5.50-04	262.	44.0	6.33	1.42+01	1.92-07	1.38	6.07	367.	1.91+09	9.857+04
57	277.8	2.46+02	4.69-04	261.	44.0	6.29	1.47+01	2.25-07	1.37	6.03	366.	1.63+09	9.863+04
58	275.9	2.08+02	4.00-04	260.	44.0	6.25	1.52+01	2.63-07	1.36	5.99	364.	1.38+09	9.867+04
59	274.0	1.76+02	3.41-04	259.	44.0	6.21	1.57+01	3.09-07	1.35	5.95	363.	1.17+09	9.871+04
60	272.1	1.49+02	2.90-04	259.	44.0	6.16	1.62+01	3.64-07	1.34	5.91	362.	9.95+08	9.874+04
61	270.2	1.26+02	2.46-04	258.	44.0	6.12	1.67+01	4.28-07	1.33	5.87	361.	8.43+08	9.876+04
62	268.3	1.06+02	2.09-04	257.	44.0	6.08	1.72+01	5.04-07	1.32	5.83	359.	7.13+08	9.879+04
63	266.5	8.92+01	1.77-04	256.	44.0	6.04	1.77+01	5.94-07	1.32	5.79	358.	6.02+08	9.881+04
64	264.6	7.50+01	1.50-04	255.	44.0	6.00	1.82+01	7.02-07	1.31	5.75	357.	5.08+08	9.882+04
65	262.7	6.30+01	1.27-04	255.	44.0	5.96	1.87+01	8.29-07	1.30	5.72	355.	4.29+08	9.884+04
66	260.8	5.29+01	1.07-04	254.	44.0	5.92	1.92+01	9.82-07	1.29	5.68	354.	3.61+08	9.885+04
67	258.9	4.43+01	9.06-05	253.	44.0	5.88	1.97+01	1.16-06	1.28	5.64	353.	3.03+08	9.886+04
68	257.0	3.71+01	7.64-05	252.	44.0	5.84	2.02+01	1.38-06	1.27	5.60	352.	2.55+08	9.887+04
69	255.1	3.10+01	6.43-05	251.	44.0	5.80	2.06+01	1.64-06	1.26	5.56	350.	2.14+08	9.887+04
70	253.3	2.59+01	5.41-05	251.	44.0	5.76	2.10+01	1.95-06	1.25	5.52	349.	1.79+08	9.888+04
71	251.4	2.16+01	4.54-05	250.	44.0	5.71	2.14+01	2.32-06	1.24	5.48	348.	1.50+08	9.888+04
72	249.5	1.80+01	3.81-05	249.	44.0	5.67	2.18+01	2.76-06	1.24	5.44	346.	1.25+08	9.889+04
73	247.6	1.49+01	3.19-05	248.	44.0	5.63	2.22+01	3.30-06	1.23	5.40	345.	1.05+08	9.889+04
74	245.7	1.24+01	2.67-05	247.	44.0	5.59	2.25+01	3.94-06	1.22	5.36	344.	8.72+07	9.889+04
75	243.8	1.03+01	2.23-05	246.	44.0	5.55	2.28+01	4.72-06	1.21	5.32	343.	7.26+07	9.890+04
76	242.0	8.52+00	1.86-05	246.	44.0	5.51	2.31+01	5.65-06	1.20	5.28	341.	6.04+07	9.890+04
77	240.1	7.04+00	1.55-05	245.	44.0	5.47	2.33+01	6.78-06	1.19	5.24	340.	5.01+07	9.890+04
78	238.2	5.82+00	1.29-05	244.	44.0	5.43	2.35+01	8.15-06	1.19	5.21	339.	4.15+07	9.890+04
79	236.3	4.80+00	1.07-05	243.	44.0	5.39	2.36+01	9.80-06	1.18	5.17	337.	3.44+07	9.890+04
80	234.5	3.95+00	8.92-06	242.	44.0	5.35	2.37+01	1.18-05	1.17	5.13	336.	2.84+07	9.890+04
81	232.6	3.25+00	7.39-06	241.	44.0	5.30	2.37+01	1.43-05	1.16	5.09	334.	2.35+07	9.890+04
82	230.7	2.67+00	6.12-06	240.	44.0	5.26	2.37+01	1.72-05	1.15	5.05	333.	1.93+07	9.891+04
83	228.8	2.19+00	5.05-06	239.	44.0	5.22	2.37+01	2.08-05	1.14	5.01	332.	1.59+07	9.891+04

84	227.0	1.79+00	4.17-06	239.	44.0	5.18	2.36+01	2.53-05	1.14	4.97	330.	1.31+07	9.891+04
85	225.1	1.46+00	3.44-06	238.	44.0	5.14	2.34+01	3.07-05	1.13	4.93	329.	1.07+07	9.891+04
86	223.2	1.19+00	2.83-06	237.	44.0	5.10	2.32+01	3.73-05	1.12	4.89	328.	8.79+06	9.891+04
87	221.3	9.71-01	2.32-06	236.	44.0	5.06	2.29+01	4.54-05	1.11	4.85	326.	7.19+06	9.891+04
88	219.5	7.89-01	1.90-06	235.	44.0	5.02	2.26+01	5.53-05	1.10	4.81	325.	5.87+06	9.891+04
89	217.6	6.40-01	1.56-06	234.	44.0	4.98	2.22+01	6.76-05	1.10	4.77	324.	4.79+06	9.891+04
90	215.7	5.19-01	1.27-06	233.	44.0	4.93	2.17+01	8.27-05	1.09	4.73	322.	3.89+06	9.891+04
91	213.8	4.20-01	1.04-06	232.	44.0	4.89	2.12+01	1.01-04	1.08	4.69	321.	3.16+06	9.891+04
92	212.0	3.39-01	8.46-07	231.	44.0	4.85	2.07+01	1.24-04	1.07	4.65	319.	2.57+06	9.891+04
93	210.1	2.73-01	6.88-07	231.	44.0	4.81	2.01+01	1.53-04	1.06	4.61	318.	2.08+06	9.891+04
94	208.2	2.20-01	5.58-07	230.	44.0	4.77	1.94+01	1.89-04	1.06	4.57	317.	1.68+06	9.891+04
95	206.4	1.76-01	4.52-07	229.	44.0	4.73	1.87+01	2.33-04	1.05	4.53	315.	1.35+06	9.891+04
96	204.5	1.41-01	3.66-07	228.	44.0	4.69	1.80+01	2.88-04	1.04	4.49	314.	1.09+06	9.891+04
97	202.6	1.13-01	2.95-07	227.	44.0	4.65	1.72+01	3.57-04	1.03	4.46	312.	8.75+05	9.891+04
98	200.8	9.02-02	2.38-07	226.	44.0	4.60	1.64+01	4.43-04	1.02	4.42	311.	7.02+05	9.891+04
99	198.9	7.18-02	1.91-07	225.	44.0	4.56	1.56+01	5.51-04	1.01	4.38	309.	5.62+05	9.891+04
100	197.0	5.71-02	1.53-07	224.	44.0	4.52	1.47+01	6.87-04	1.00	4.34	308.	4.48+05	9.891+04
105	187.7	1.75-02	4.95-08	219.	44.0	4.32	1.02+01	2.13-03	.93	4.14	301.	1.41+05	9.891+04
110	178.4	5.09-03	1.51-08	214.	44.0	4.11	6.02+00	6.98-03	.87	3.94	293.	4.20+04	9.891+04
115	169.1	1.38-03	4.33-09	208.	44.0	3.90	2.79+00	2.43-02	.81	3.74	285.	1.17+04	9.891+04
120	177.0	3.64-04	1.09-09	213.	44.0	3.58	7.29+01	9.67-02	.86	3.92	292.	3.02+03	9.891+04
125	198.6	1.09-04	2.92-10	225.	44.0	4.02	0.00	3.61-01	1.01	4.41	309.	8.56+02	9.891+04
130	210.0	3.68-05	9.29-11	230.	44.0	4.67	0.00	1.13+00	1.06	4.67	318.	2.80+02	9.891+04
135	210.0	1.26-05	3.18-11	230.	44.0	4.67	0.00	3.31+00	1.06	4.67	318.	9.61+01	9.891+04
140	244.9	4.48-06	9.68-12	247.	44.0	3.89	0.00	1.09+01	1.22	5.46	343.	3.15+01	9.891+04
145	335.5	2.05-06	3.24-12	284.	44.0	5.33	0.00	3.25+01	1.64	7.49	402.	1.24+01	9.891+04
150	408.5	1.13-06	1.47-12	311.	44.0	8.02	0.00	7.16+01	1.99	9.15	444.	6.19+00	9.891+04
155	438.0	6.70-07	8.06-13	322.	43.8	8.65	0.00	1.30+02	2.10	9.87	460.	3.54+00	9.891+04
160	467.5	4.11-07	4.61-13	332.	43.6	9.27	0.00	2.26+02	2.23	10.59	477.	2.11+00	9.891+04
165	496.9	2.61-07	2.74-13	342.	43.4	9.90	0.00	3.80+02	2.35	11.33	492.	1.30+00	9.891+04
170	526.2	1.70-07	1.68-13	352.	43.2	10.54	0.00	6.16+02	2.45	12.07	508.	8.24-01	9.891+04
175	555.5	1.14-07	1.06-13	362.	43.0	11.18	0.00	9.73+02	2.55	12.82	523.	5.38-01	9.891+04
180	584.8	7.78-08	6.85-14	372.	42.8	11.83	0.00	1.50+03	2.65	13.58	538.	3.60-01	9.891+04
185	614.0	5.44-08	4.54-14	381.	42.6	12.48	0.00	2.25+03	2.75	14.34	552.	2.46-01	9.891+04
190	643.1	3.87-08	3.07-14	390.	42.4	13.14	0.00	3.31+03	2.85	15.11	566.	1.71-01	9.891+04
195	672.3	2.80-08	2.12-14	399.	42.2	13.80	0.00	4.77+03	2.95	15.89	580.	1.22-01	9.891+04
200	701.3	2.06-08	1.49-14	408.	42.1	14.47	0.00	6.77+03	3.06	16.68	594.	8.78-02	9.891+04
210	710.0	1.16-08	7.74-15	424.	39.4	15.87	0.00	1.22+04	3.08	18.09	618.	5.07-02	9.891+04
220	710.0	6.82-09	4.20-15	442.	36.3	16.90	0.00	2.07+04	3.08	19.67	643.	3.11-02	9.891+04
230	710.0	4.20-09	2.37-15	461.	33.3	18.02	0.00	3.37+04	3.08	21.53	672.	2.00-02	9.891+04
240	710.0	2.70-09	1.38-15	484.	30.3	19.24	0.00	5.24+04	3.08	23.77	705.	1.34-02	9.891+04
250	710.0	1.81-09	8.35-16	510.	27.2	20.53	0.00	7.81+04	3.08	26.49	743.	9.51-03	9.891+04
260	710.0	1.27-09	5.20-16	541.	24.2	21.86	0.00	1.12+05	3.08	29.87	788.	7.06-03	9.891+04
270	710.0	9.11-10	3.66-16	547.	23.7	29.35	0.00	1.55+05	3.08	30.67	797.	5.14-03	9.891+04
280	710.0	6.60-10	2.61-16	551.	23.3	29.84	0.00	2.14+05	3.08	31.22	803.	3.75-03	9.891+04
290	710.0	4.80-10	1.87-16	555.	23.0	30.35	0.00	2.94+05	3.08	31.79	809.	2.75-03	9.891+04
300	710.0	3.52-10	1.35-16	560.	22.6	30.86	0.00	4.02+05	3.08	32.37	815.	2.03-03	9.891+04
310	710.0	2.59-10	9.78-17	564.	22.3	31.39	0.00	5.46+05	3.08	32.98	821.	1.50-03	9.891+04
320	710.0	1.92-10	7.13-17	568.	22.0	31.93	0.00	7.37+05	3.08	33.59	827.	1.12-03	9.891+04
330	710.0	1.43-10	5.23-17	573.	21.6	32.48	0.00	9.90+05	3.08	34.23	834.	8.43-04	9.891+04
340	710.0	1.07-10	3.85-17	577.	21.3	33.05	0.00	1.32+06	3.08	34.89	840.	6.36-04	9.891+04
350	710.0	8.05-11	2.85-17	582.	20.9	33.63	0.00	1.76+06	3.08	35.56	847.	4.83-04	9.891+04
360	710.0	6.09-11	2.13-17	587.	20.6	34.23	0.00	2.32+06	3.08	36.26	854.	3.68-04	9.891+04
370	710.0	4.64-11	1.59-17	592.	20.3	34.84	0.00	3.05+06	3.08	36.97	861.	2.83-04	9.891+04
380	710.0	3.55-11	1.20-17	597.	19.9	35.47	0.00	3.98+06	3.08	37.71	868.	2.18-04	9.891+04
390	710.0	2.73-11	9.06-18	602.	19.6	36.11	0.00	5.18+06	3.08	38.47	876.	1.69-04	9.891+04
400	710.0	2.11-11	6.88-18	607.	19.3	36.77	0.00	6.70+06	3.08	39.26	883.	1.32-04	9.891+04
410	710.0	1.64-11	5.26-18	612.	18.9	37.45	0.00	8.62+06	3.08	40.07	891.	1.03-04	9.891+04

TABLE 7

CIRCULATION MODEL COMPUTER PROGRAM

```
C TWO DIMENSIONAL
C RETURN TO DAVID F PITTS BLDG 343 ELLINGTON BOX 105
      DIMENSION RHOBAR(30),TBAR(30),HBAR(30),A1(30),G(30)
     1,XJ(10),JJ2(10),II2(10),A2(10,10),B2(10,10),C2(10,10)
     1,UBAR1(30)
      DOUBLE PRECISION A2,B2,C2,XJ
     1,RHOBAR,B,C,Z,DX,DH,G,XNU,CP,A1,HBAR,XNUH,XK,XKH,R,XM,RO,RHO,P,T,#
     2,U,TBAR,S11,S12,S13,S14,S15,S21,S22,S23,S24,S25,S31,S32,S33,S34,
     3S41,S42,S43,S44,S51,S52,S53,CONV,DUM1,DUM2,DUM3,DUM4,DUM5,S45
     4,UBAR1
      COMMON ANS(36),P(30,30),RHO(30,30),U(30,30),W(30,30),T(30,30)
      DATA RO/8.31432D+07/,R/8.31432D+07/,XM/44.011D+00/,PI/3.14159/
      CTEST3=6HVARBLT
      DO 203 I=1,10
      DO 203 J=1,10
      A2(I,J)=0.0
      B2(I,J)=0.0
  203 C2(I,J)=0.0
 1970 ANS(1)=-1.0
      CALL MODATM(-1.0,PP,4HGEOM,.6)
   42 READ (5,1) ZMAX,XX,XN,XNU1,XNUH1,PRNDTL,CONV1,B1,C1,CTEST1,CTEST2
    1 FORMAT (F4.0,2F5.0,2E9.2,4F6.0,A6,A6)
      C1=C1/100.0
      WRITE (6,505)
  505 FORMAT (1H0,'ZMAX   XX   XN     XNU1          XNUH1  PRNDTL CONV B1
     1       C1   CTEST1 CTEST2 CTEST3',//)
      WRITE (6,506) ZMAX,XX,XN,XNU1,XNUH1,PRNDTL,CONV1,B1,C1,CTEST1,CTES
     1T2,CTEST3
  506 FORMAT (1X,F4.0,2F5.0,1P2E12.3,0P2F5.2,F5.1,1PE12.3,3A6,///)
      XK=XNU1/PRNDTL
      XKH=XNUH1/PRNDTL
      XNU=XNU1
      XNUH=XNUH1
      B=B1
      C=C1
      CONV=CONV1
      DH=(ZMAX/XN)*1.0E+05
      DX=(    PI*6053.0*1.0E+05)/XX
      CP=1.00E+07
      N=XN+1
      K=XN
C XN IS NUMBER OF LEVELS IN VERTICAL
C N IS THE NUMBER OF LEVEL INTERFACES IN VERTICAL
      KJ=XX+1.0
      NJ=XX+2.0
C KJ= NUMBER OF DIVISIONS IN HORIZONTAL
C NJ= NUMBER OF INTERFACES IN HORIZONTAL
      DO 201 I=1,N
      DO 201 J=1,NJ
      CALL BOUND (I,J,0.0)
  201 CONTINUE
      WRITE (6,523)
  523 FORMAT (1X,/,'      Z            PBAR        RHOBAR        TBAR
     1   G           DT/DZ        HBAR         UBAR')
```

TABLE 7 (continued)

```
      Z=-DH
      DO 2 L=1,N
      Z=Z+DH
      ZX=Z
      CALL MODATM(ZX/100000.0,PP,4HGEOM,.6)
      RHOBAR(L)=ANS(3)
      TBAR(L)=ANS(2)
      G(L)=ANS(5)
      A1(L)=ANS(25)/100.0
      IF (CTEST1.EQ.6HADIABA) A1(L)=-G(I)/CP
      HBAR(L)=ANS(16)*1.0E+05
      IF (CTEST2.EQ.4HBOUSSI)  HBAR(L)=1.0D+100
      UBAR1(L)=B+C*Z
      WRITE (6,100) Z,ANS(1),RHOBAR(L),TBAR(L),G(L),A1(L),HBAR(L),UBAR1(
     1L)
  100 FORMAT (1X,1PD12.3,1PE12.3,1P6D12.3)
    2 CONTINUE
      DO 40 LQ=1,100
      DO 400 J=2,KJ
      DUM1=COS((J-2)     *PI/(KJ-2))
      IF (DUM1.LT.0.0)  DUM1=0.0
      U(N,J)=U(K,J)
      T(N,J)=(-XK*RHOBAR(N)*CP*(A1(N)+G(N)/CP-T(N-1,J)/DH)-5.6699D-05*TB
     1AR(N)**4
     1+.23     *2.667D+06*DUM1)/(XK*RHOBAR(N)*CP/DH+4.0*TBAR(N)**3*
     1(5.6699D-05))
      T(1,J)=T(2,J)+DH*(G(1)/CP+A1(1))
      P(N,J)=P(K,J)+(-RHO(K,J)*G(K)+RHOBAR(K)*XNU*(W(N,J)-2.0*W(K,J)+
     1W(K-1,J))/(DH**2)) *DH
      RHO(N,J)=XM/(TBAR(N)*R)*(P(N,J)-R/XM*RHOBAR(N)*T(N,J) )
      P(1,J)=P(2,J)+(RHO(2,J)*G(2)-RHOBAR(2)*XNU*(W(3,J)-2.0*W(2,J)
     1+W(1,J))/(DH**2))*DH
  400 CONTINUE
      DO 4 I=2,K
      Z=(I-1)*DH
      DO 4 J=2,KJ
      IF (I.EQ.K.AND.CTEST3.EQ.6H GOODBY) GO TO 511
      GO TO 512
  511 T(N,J)=0.0
      DUM1=COS((J-2)*PI/(KJ-2))
      IF (DUM1.LT.0.0)DUM1=0.0
      T(K,J)=(-1.6D-05*(3.14159*DUM1-1.0)/(XK*RHOBAR(K)*CP)+A1(K))*DH
  512 DO 205 KLL=1,5
      DO 205 LLL=1,5
  205 A2(KLL,LLL)=0.0
      S11=RHOBAR(I)*(B+C*Z)*(W(I,J+1)-W(I,J  ))/(    DX)
      S12=(P(I+1,J)-P(I  ,J))/(    DH)
      S13=RHO(I,J)*G(I)
      S14=-RHOBAR(I)*XNU*(W(I+1,J)-2.0*W(I,J)+W(I-1,J))/(DH**2)
      S15=-RHOBAR(I)*XNUH*(W(I,J+1)-2.0*W(I,J)+W(I,J-1))/(DX**2)
      S21=RHOBAR(I)*(B+C*Z)*(U(I,J+1)-U(I,J  ))/(    DX)
      S22=RHOBAR(I)*W(I,J)*C
      S23=(P(I,J+1)-P(I,J  ))/(    DX)
      S24=-RHOBAR(I)*XNU*(U(I+1,J)-2.0*U(I,J)+U(I-1,J))/(DH**2)
      S25=-RHOBAR(I)*XNUH        *(U(I,J+1)-2.0*U(I,J)+U(I,J-1))/(DX**2)
      S31=(U(I,J+1)-U(I,J  ))/(    DX)
      S32=(W(I+1,J)-W(I  ,J))/(    DH)
      S33=-W(I,J)/RHOBAR(I)
```

TABLE 7 (continued)

```
      S34=(B+C*Z)*(RHO(I,J+1)-RHO(I,J  ))/(    DX*RHOBAR(I))
      IF (CTEST3.EQ.6H GOODY) S34=0.0
      S41=(B+C*Z)*(T(I,J+1)-T(I,J  ))/(    DX)
      S42=R(I,J)*(A1(I)+G(I)/CP)
      S43=-XK*(T(I+1,J)-2.0*T(I,J)+T(I-1,J))/(DH**2)
      S44=-AKH       *(T(I,J+1)-2.0*T(I,J)+T(I,J-1))/(DX**2)
      S45=-(P(I,J+1)-P(I,J  ))*(B+C*Z)/(RHOBAR(I)*CP*    DX)
      S51=0.0
      S52=-R/XM*(RHOBAR(I)*T(I,J))
      S53=-R/XM*(RHO(I,J)*TBAR(I))
      IF (LQ.EQ.100)
     1WRITE (6,252) S11,S12,S13,S14,S15,S21,S22,S23,S24,S25,
     1S31,S32,S33,S34,S41,S42,S43,S44,S45,S51,S52,S53
252   FORMAT (1H0,1P5D12.2,5X,1P5D12.2,/,1P4D12.2,17X,1PD12.2,//,
     11P3D12.2)
      C2(1,1)=S11+S12+S13+S14+S15
      C2(2,1)=S21+S22+S23+S24+S25
      C2(3,1)=S31+S32+S33+S34
      C2(4,1)=S41+S42+S43+S44+S45
      C2(5,1)=S51+S52+S53
      IF (I.EQ.3.AND.J.EQ.5)
     1WRITE (6,251) I,J,C2(1,1),C2(2,1),C2(3,1),C2(4,1),C2(5,1)
251   FORMAT (20X,2I3,1P5D12.2)
      A2(1,1)=G(I)
      A2(1,2)=-1.0/DH
      A2(1,4)=-RHOBAR(I)*(B+C*Z)/DX
     1+2.0*RHOBAR(I)*XNU/(DH**2)+2.0*RHOBAR(I)*XNUH/(DX**2)
      A2(2,2)=-1.0/DX
      A2(2,3)=-RHOBAR(I)*(B+C*Z)/DX+2.0*RHOBAR(I)*XNU/(DH**2)
     1+2.0*RHOBAR(I)*XNUH        /(DX**2)
      A2(2,4)=RHOBAR(I)*C
      A2(3,1)=-(B+C*Z)/(RHOBAR(I)*DX)
      IF (CTEST3.EQ.6H GOODY) A2(3,1)=0.0
      A2(3,3)=-1.0/DX
      A2(3,4)=-1.0/DH-1.0/HBAR(I)
      A2(4,2)=1.0/(RHOBAR(I)*CP*DX)*(B+C*Z)
      A2(4,4)=(A1(I)+G(I)/CP)
      A2(4,5)=-(B+C*Z)/DX+2.0*XK/(DH**2)+2.0*XKH        /(DX**2)
      A2(5,1)=-R0/XM*TBAR(I)
      A2(5,5)=-R0*RHOBAR(I)/XM
      CALL MINVDP(A2,5,.1D-10,$9,IN,XJ,JJ2,II2)
      CALL XMA(A2,C2,B2,5,5,1)
      DUM1=B2(1,1)
      DUM2=B2(2,1)
      DUM3=B2(3,1)
      DUM4=B2(4,1)
      DUM5=B2(5,1)
      RHO(I,J)=RHO(I,J)-CONV*DUM1
      P(I,J)=P(I,J)-CONV*DUM2
      U(I,J)=U(I,J)-CONV*DUM3
      W(I,J)=W(I,J)-CONV*DUM4
      T(I,J)=T(I,J)-CONV*DUM5
    4 CONTINUE
   40 CONTINUE
      GO TO 5
    9 WRITE (6,1983)
1983  FORMAT (1X,'MATRIX SINGULAR OR ILLCONDITIONED')
    5 WRITE (6,300)
```

TABLE 7 (continued)

```
  300 FORMAT (1H1,'RHO')
      WRITE (6,505)
      WRITE (6,506) ZMAX,XX,XN,XNU1,XNUH1,PRNDTL,CONV1,B1,C1,CTEST1,CTES
     1T2,CTEST3
      WRITE (6,250) ((RHO(I,J),J=1,NJ),I=1,N)
      WRITE (6,302)
  302 FORMAT (1H1,'U')
      WRITE (6,505)
      WRITE (6,506) ZMAX,XX,XN,XNU1,XNUH1,PRNDTL,CONV1,B1,C1,CTEST1,CTES
     1T2,CTEST3
      WRITE (6,250) ((  U(I,J),J=1,NJ),I=1,N)
      WRITE (6,301)
  301 FORMAT (1H1,'W')
      WRITE (6,505)
      WRITE (6,506) ZMAX,XX,XN,XNU1,XNUH1,PRNDTL,CONV1,B1,C1,CTEST1,CTES
     1T2,CTEST3
      WRITE (6,250) ((  W(I,J),J=1,NJ),I=1,N)
      WRITE (6,507)
  507 FORMAT (1H1,'UBAR1+U')
      DO 508 I=1,N
      DO 508 J=1,NJ
  508 U(I,J)=U(I,J)+UBAR1(I)
      WRITE (6,250) ((  U(I,J),J=1,NJ),I=1,N)
      WRITE (6,303)
  303 FORMAT (1H1,'T')
      WRITE (6,505)
      WRITE (6,506) ZMAX,XX,XN,XNU1,XNUH1,PRNDTL,CONV1,B1,C1,CTEST1,CTES
     1T2,CTEST3
      WRITE (6,250) ((  T(I,J),J=1,NJ),I=1,N)
      WRITE (6,304)
  304 FORMAT (1H1,'P')
      WRITE (6,250) ((  P(I,J),J=1,NJ),I=1,N)
  250 FORMAT (1H0,1P12D10.2,/)
      GO TO 1970
      END
```

```
F UNIVAC 1108 FORTRAN V COMPILATION.      0 *DIAGNOSTIC* MESSAGE(S)
```

```
      SUBROUTINE BOUND (I,J,SET)
      DOUBLE PRECISION P,RHO,U,W,T
      COMMON ANS(35),P(30,30),RHO(30,30),U(30,30),W(30,30),IL(30,30)
      P(I,J)=SET
      RHO(I,J)=SET
      U(I,J)=SET
      T(I,J)=SET
      W(I,J)=SET
      RETURN
      END
```

TABLE 7 (continued)

```
      DO 5 I=1,M
      DO 1 I3=1,L1
      IF(I-I2(I3))1,5,1
    1 CONTINUE
      DO 4 J=1,M
      DO 2 I3=1,L1
      IF(J-J2(I3))2,4,2
    2 CONTINUE
      IF(BIGA-DABS(A(I,J)))3,3,4
    3 BIGA=DABS(A(I,J))
      J1=J
      I1=I
    4 CONTINUE
    5 CONTINUE
C*    TAG THE ROW AND COLUMN FROM WHICH THE ELEMENT IS CHOSEN.
      J2(L)=J1
      I2(L)=I1
      DIV=A(I1,J1)
C*    TEST ELEMENT AGAINST ZERO CRITERION.
      IF(DABS(DIV)-E)221,221,6
C*    PERFORM THE COMPUTATIONS
    6 DO 7 J=1,M
      A(I1,J)=A(I1,J)/DIV
    7 CONTINUE
      A(I1,J1)=1.000/DIV
      DO 11 I=1,M
      IF(I-I1)8,11,8
    8 DO 10 J=1,M
      IF(J1-J)9,10,9
    9 A(I,J)=A(I,J)-A(I1,J)*A(I,J1)
   10 CONTINUE
   11 CONTINUE
      DO 14 I=1,M
      IF(I1-I) 13,14,13
   13 A(I,J1)=-A(I,J1)*A(I1,J1)
   14 CONTINUE
   15 CONTINUE
C*    COMPUTATION COMPLETE AT THIS POINT
C*    UNSCRAMBLE THE INVERSE
      DO 18 J=1,M
      DO 16 I=1,M
      I1=I2(I)
      J1=J2(I)
      X(J1)=A(I1,J)
   16 CONTINUE
      DO 17 I=1,M
      A(I,J)=X(I)
   17 CONTINUE
   18 CONTINUE
      DO 21 I=1,M
      DO 19 J=1,M
      I1=I2(J)
      J1=J2(J)
      X(I1)=A(I,J1)
   19 CONTINUE
      DO 20 J=1,M
      A(I,J)=X(J)
   20 CONTINUE
```

TABLE 7 (continued)

```
   21 CONTINUE
      RETURN
  241 K=1
      RETURN 4
      END

F UNIVAC 1108 FORTRAN V COMPILATION.      0 *DIAGNOSTIC* MESSAGE(S)
```

```
      SUBROUTINE XMA(A,B,C,M,N,IIP)
C
C
C THIS IS A MATRIX MULTIPLICATION ROUTINE IN WHICH AN (M*N) IS MULTIPLI
C     -ED BY AN (N*IIP)
C     IT MULTIPLIES AS FOLLOWS  (A,B=C)
C
C
      DIMENSION A(10,10),B(10,10),C(10,10)
      DOUBLE PRECISION A,B,C
      DO 4 IM=1,M
      DO 5 IP=1,IIP
      C(IM,IP)=0.0
      DO 3 J=1,N
    3 C(IM,IP)=A(IM,J)*B(J,IP)+C(IM,IP)
    5 CONTINUE
    4 CONTINUE
      RETURN
      END

F UNIVAC 1108 FORTRAN V COMPILATION.      0 *DIAGNOSTIC* MESSAGE(S)
```

TABLE 7 (continued)

```
      SUBROUTINE MINVDP(A,N,E,S,J8,X,J2,I2)
C*      MATRIX INVERSION ROUTINE-FORMULATED BY E. G. CLAYTON
C*      --- CALLING SEQUENCE ---
C***     CALL MINVDP(A,N,E,K)
C****   A--SQUARE ARRAY (DOUBLE PRECISION) CONTAINING ORIGINAL MATRIX
C****   N--ORDER OF ORIGINAL MATRIX
C****   E--TEST CRITERION FOR NEAR ZERO DIVISOR (DOUBLE PRECISION)
C***    K--LOCATION FOR SINGULARITY OR ILL-CONDITION INDICATOR
C**       K=0 =) MATRIX NONSINGULAR.
C*        K=1 =) MATRIX SINGULAR (OR ILL-CONDITIONED)
      DOUBLE PRECISION A,X,BIGA,DIV,E
      DIMENSION A(J8,J8),X(J8),J2(J8),I2(J8)
C*    INITIALIZATION
      M=N
      K=0
      I2(1)=0
      J2(1)=0
C*    BEGIN COMPUTATION OF THE INVERSE
      DO 15 L=1,M
      L1=L-1
      BIGA=0.0D0
C*    LOOK FOR THE ELEMENT OF GREATEST ABSOLUTE VALUE,CHOOSING
C*    ONE FROM A ROW AND COLUMN NOT PREVIOUSLY USED.
```

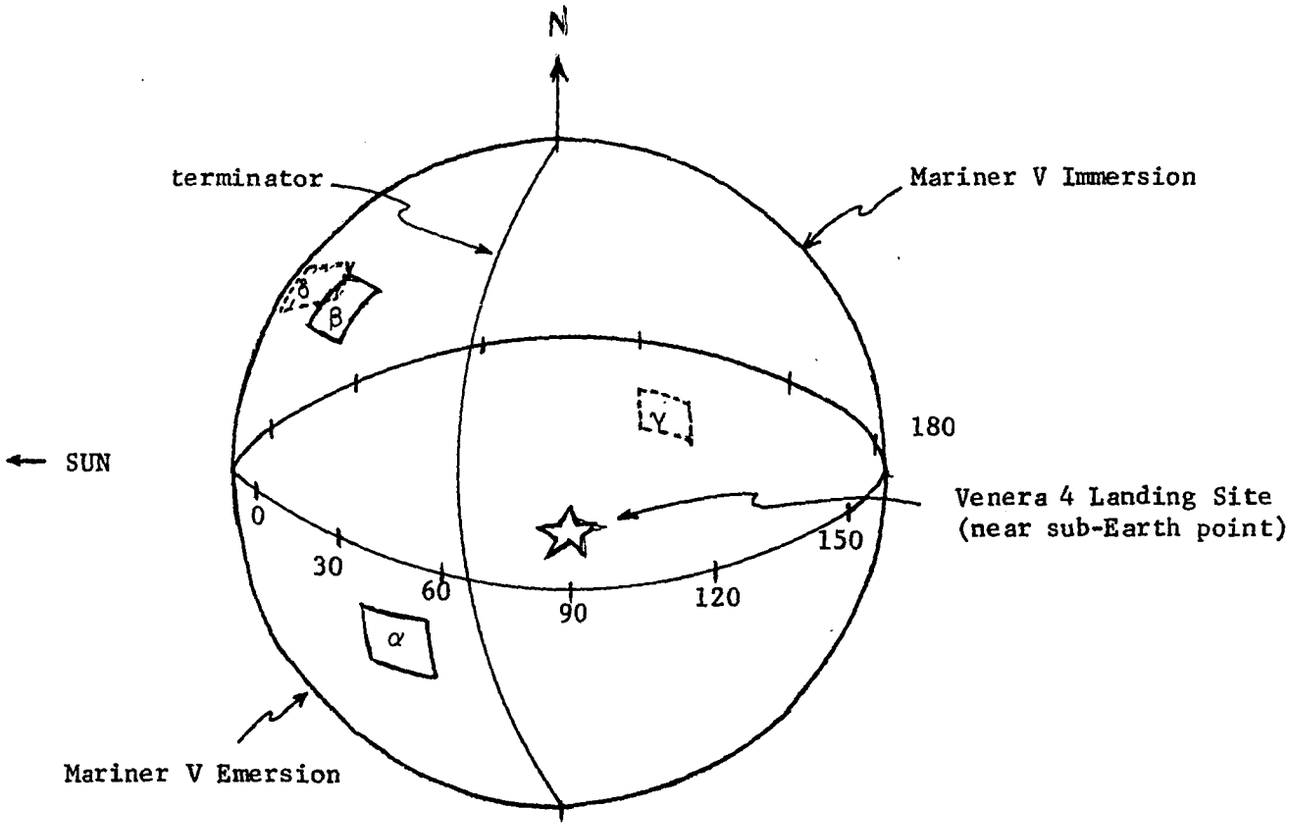

Figure 1 Venus Geometry at Mariner V- Venera 4 Encounter, after Anderson, et al (1968) and Von Eshleman, et al (1968). α, β, γ, and δ are strong radar scatters and could possibly be orographic highs.

Figure 2

TYPICAL ULTRAVIOLET PHOTOGRAPHS (λ3650 TO 4000)[1] TAKEN FROM 1927 TO 1948 DISPLAYING VARIATIONS IN THE CLOUD COVER ON VENUS

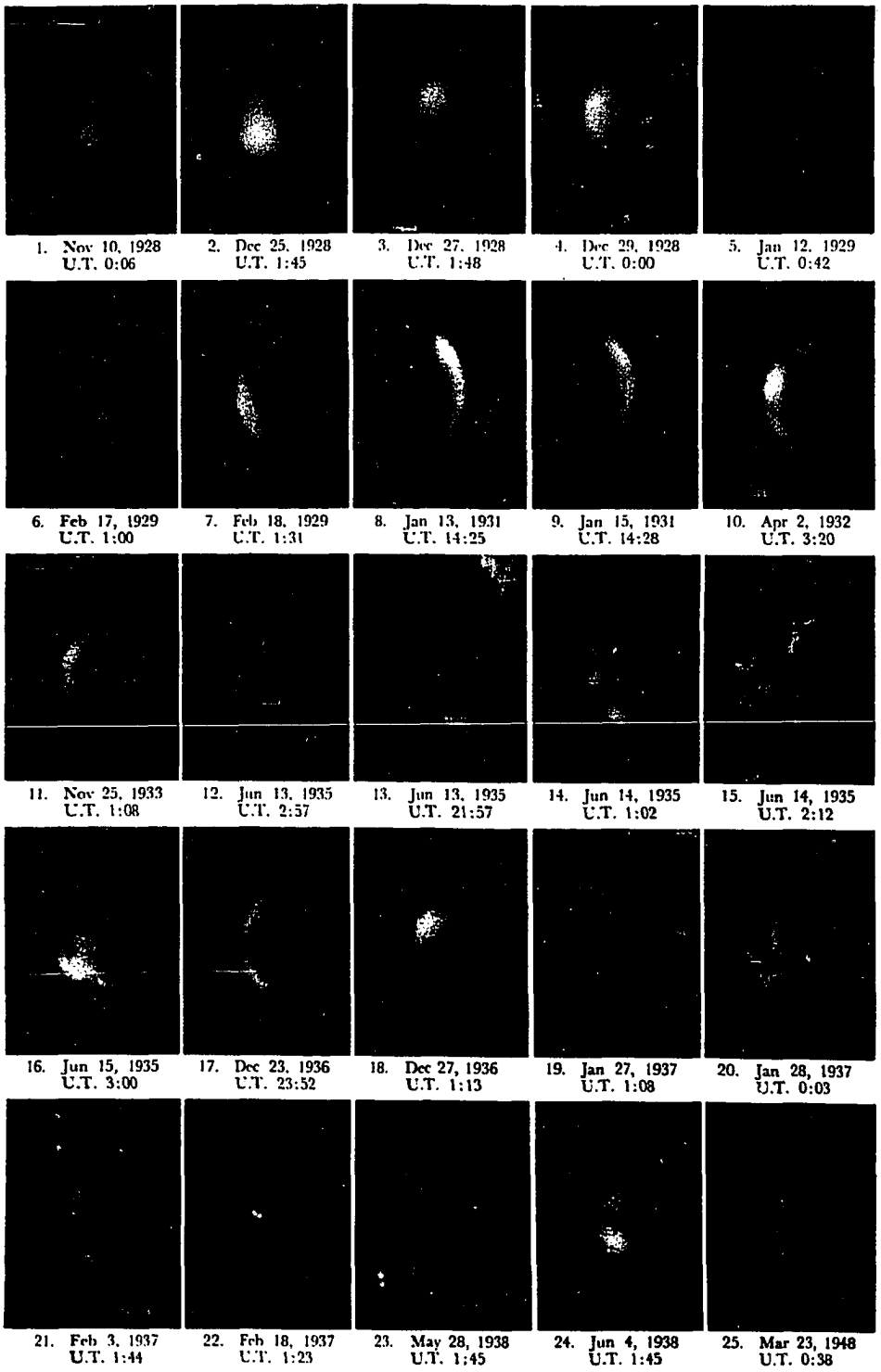

1. Nov 10, 1928 U.T. 0:06
2. Dec 25, 1928 U.T. 1:45
3. Dec 27, 1928 U.T. 1:48
4. Dec 29, 1928 U.T. 0:00
5. Jan 12, 1929 U.T. 0:42
6. Feb 17, 1929 U.T. 1:00
7. Feb 18, 1929 U.T. 1:31
8. Jan 13, 1931 U.T. 14:25
9. Jan 15, 1931 U.T. 14:28
10. Apr 2, 1932 U.T. 3:20
11. Nov 25, 1933 U.T. 1:08
12. Jun 13, 1935 U.T. 2:57
13. Jun 13, 1935 U.T. 21:57
14. Jun 14, 1935 U.T. 1:02
15. Jun 14, 1935 U.T. 2:12
16. Jun 15, 1935 U.T. 3:00
17. Dec 23, 1936 U.T. 23:52
18. Dec 27, 1936 U.T. 1:13
19. Jan 27, 1937 U.T. 1:08
20. Jan 28, 1937 U.T. 0:03
21. Feb 3, 1937 U.T. 1:44
22. Feb 18, 1937 U.T. 1:23
23. May 28, 1938 U.T. 1:45
24. Jun 4, 1938 U.T. 1:45
25. Mar 23, 1948 U.T. 0:38

LOWELL OBSERVATORY PHOTOGRAPHS

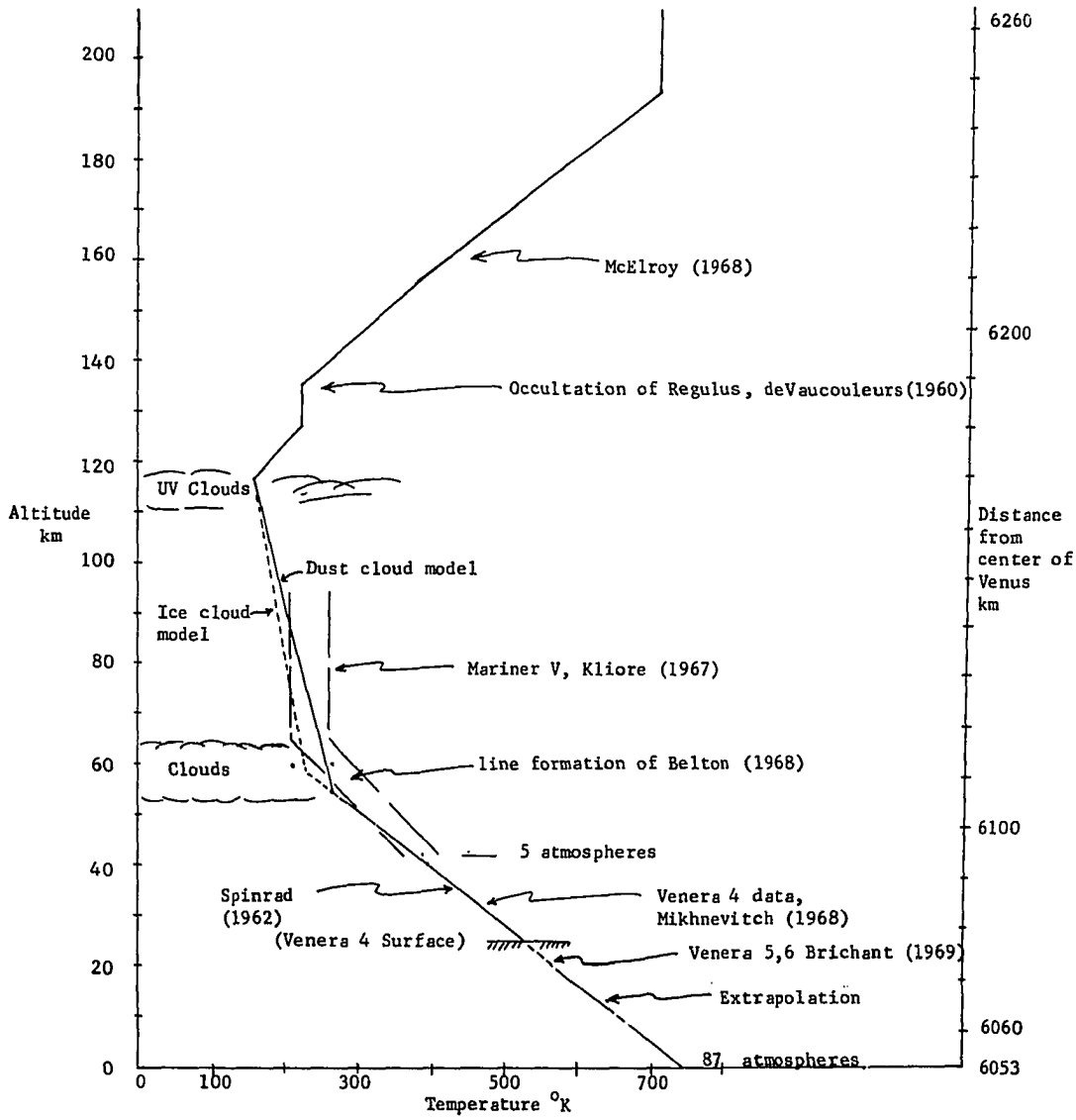

Figure 3. Structure of Two Possible Models of the Atmosphere of Venus.

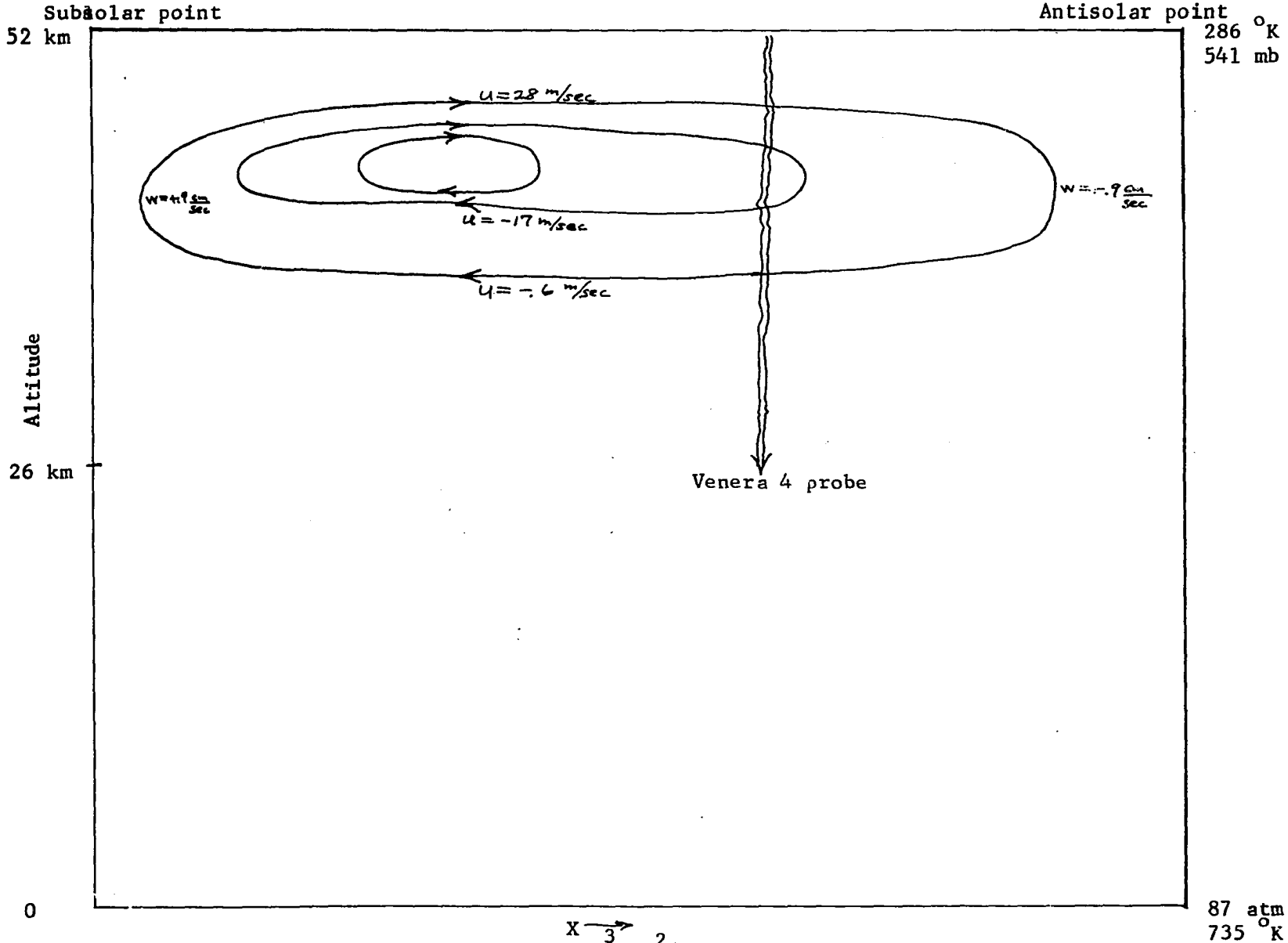

Figure 4. Compressible Dust Model, $\nu_2 = 10^3$ cm^2/sec , Pr = 1
Model 1

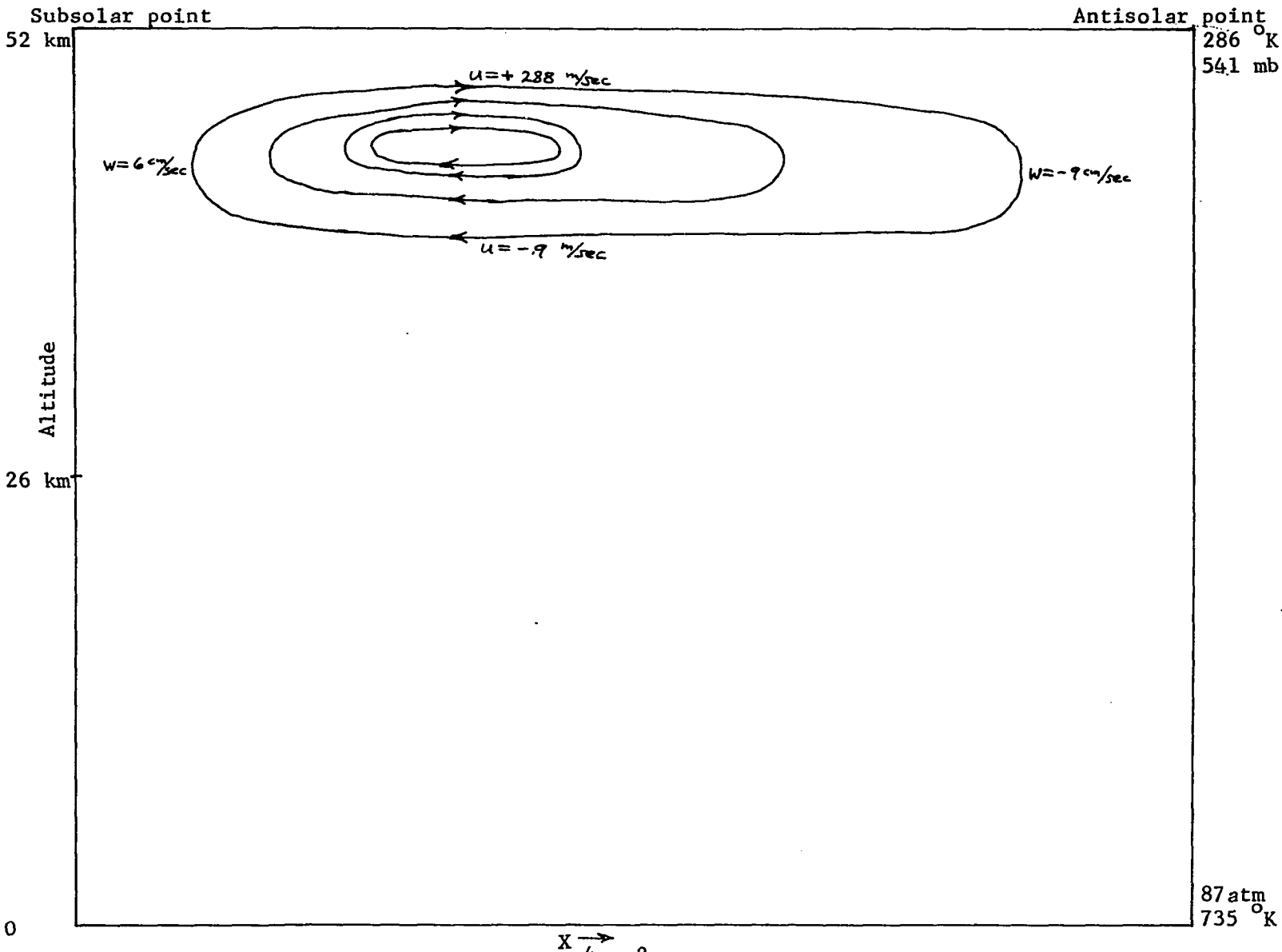

Figure 5. Compressible Dust Model, $\nu_s = 10^4$ cm^2/sec, Pr = 1
Model 2

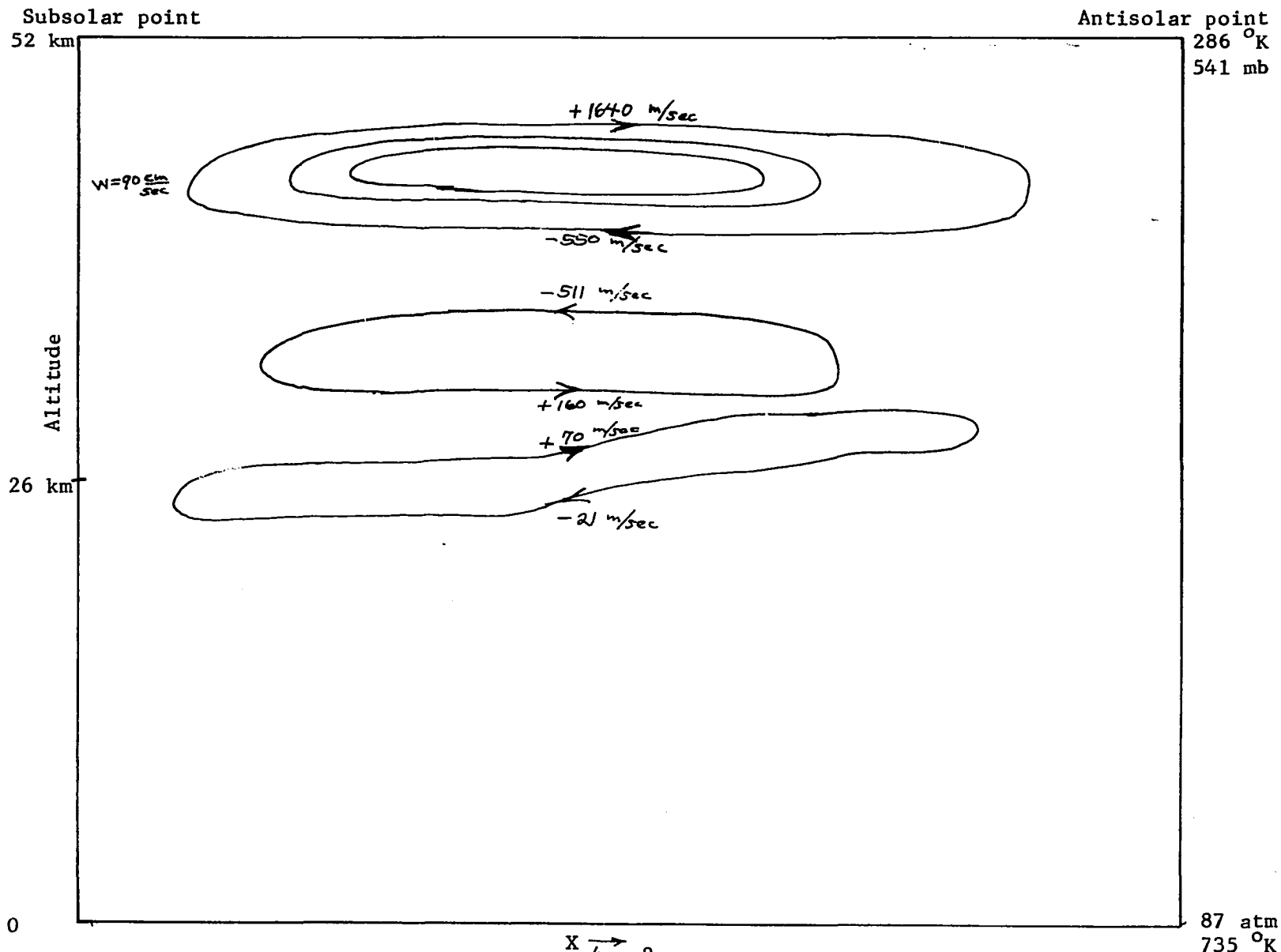

Figure 6. Compressible Dust Model, $\nu_2 = 10^4$ cm^2/sec, Pr = 0.1
Model 4

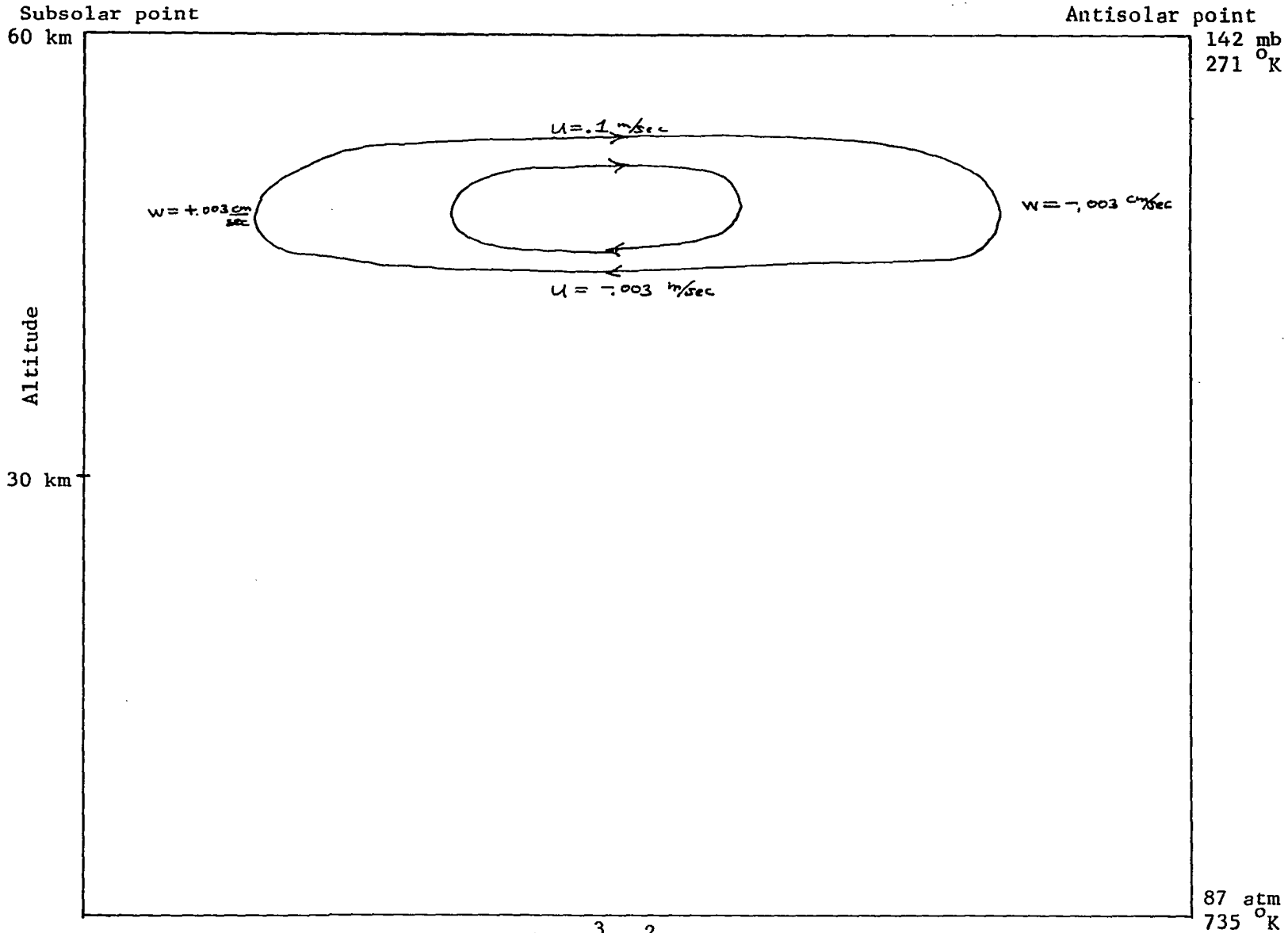

Figure 7. Compressible Dust Model, $\nu_2 = 10^3$ cm^2/sec, Pr = 1
Model 5

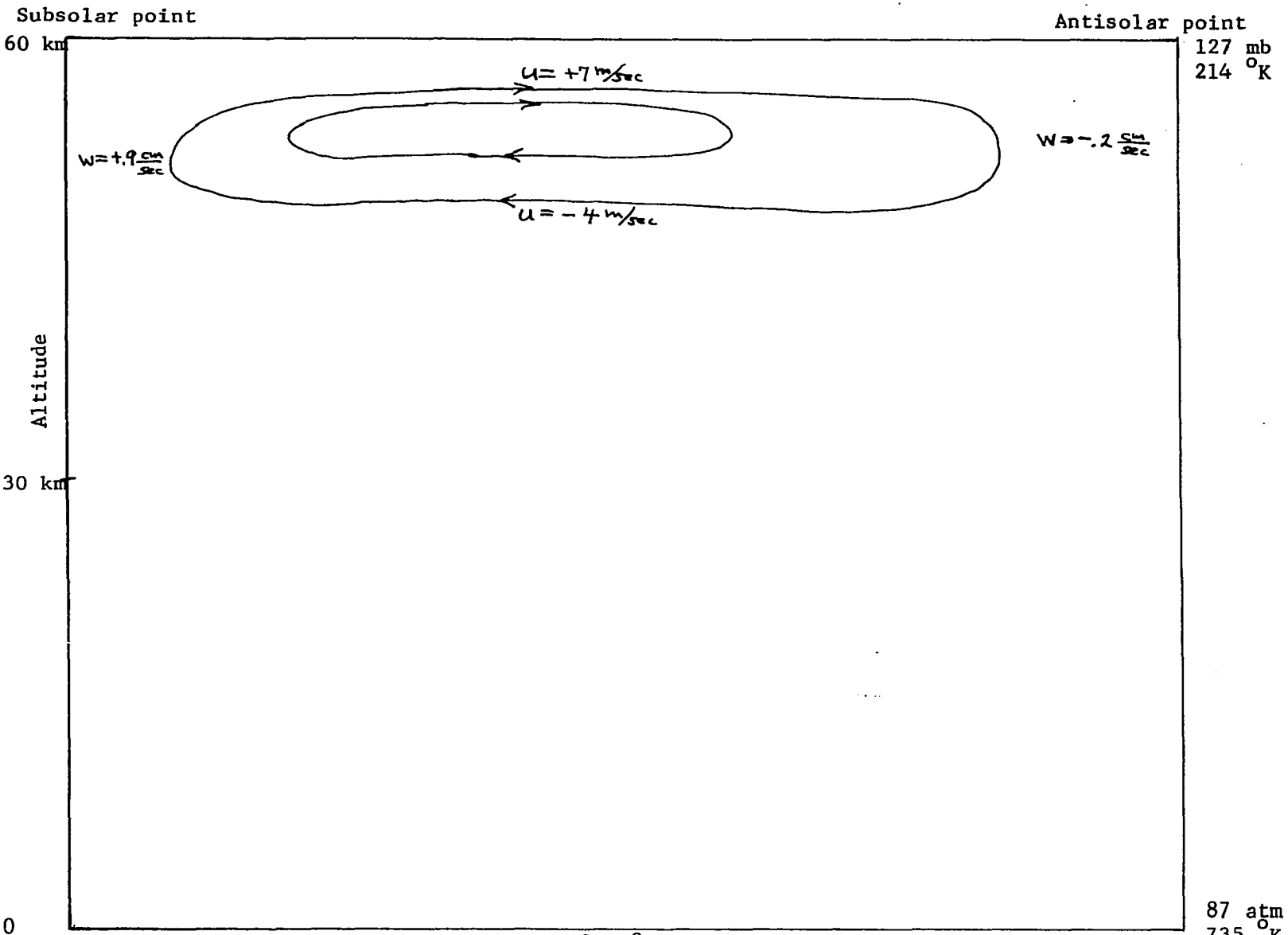

Figure 8 Water - Ice Cloud Model, $\nu_2 = 10^3$ cm^2/sec, Pr = 1
Model 6